FOSSIL ENERGY

DOE/BC/14942-12
(OSTI ID: 788818)

ADVANCED RESERVOIR CHARACTERIZATION AND EVALUATION OF CO_2 GRAVITY DRAINAGE IN THE NATURALLY FRACTURED SPRABERRY TREND AREA – CLASS III

Annual Report
September 1, 2000-August 31, 2001

By:
Harold Vance, Texas A&M University
Bill Knight, Pioneer Natural Resources
Davis S. Schechter, Texas A&M University

Date Published: November 2001

Work Performed Under Contract No. DE-FC22-95BC14942

Pioneer Natural Resources
Irving, Texas

National Energy Technology Laboratory
National Petroleum Technology Office
U.S. DEPARTMENT OF ENERGY
Tulsa, Oklahoma

DOE/BC/14942-12
Distribution Category UC-122

Advanced Reservoir Characterization and Evaluation of CO_2 Gravity Drainage in the Naturally Fractured Spraberry Trend Area – Class III

By
Harold Vance, Texas A&M University
Bill Knight, Pioneer Natural Resources
Davis S. Schechter, Texas A&M University

November 2001

Work Performed Under DE-FC22-95BC14942

Prepared for
U.S. Department of Energy
Assistant Secretary for Fossil Energy

Dan Ferguson, Project Manager
National Petroleum Technology Office
P.O. Box 3628
Tulsa, OK 74101

Prepared by
Pioneer Natural Resources
Suite 1400
5205 N. O'Connor Blvd.
Irving, TX 75039-3746

TABLE OF CONTENTS

LIST OF TABLES

TECHNICAL PROGRESS

FIELD DEMOSTRATION STATUS

LIST OF FIGURES

TECHNICAL PROGRESS

FIELD DEMOSTRATION STATUS

ABSTRACT

The goal of this project is to assess the economic feasibility of CO_2 flooding the naturally fractured Spraberry Trend Area in west Texas. This objective is being accomplished through research in four areas: 1) extensive characterization of the reservoirs, 2) experimental studies of crude oil/brine/rock (COBR) interactions in the reservoirs, 3) reservoir performance analysis, and 4) experimental investigations on CO_2 gravity drainage in Spraberry whole cores. The four areas have been completed and reported in the previous annual reports. This report provides the results of the final year of the project including two SPE papers (SPE 71605 and SPE 71635) presented in the 2001 SPE Annual Meeting in New Orleans, two simulation works, analysis of logging observation wells (LOW) and progress of CO_2 injection.

The first paper (SPE 71605) addresses the field activities to develop a 15 well, 60-acre CO_2 pilot in the Spraberry Trend Area in west Texas. We reviewd the old pilot performed in this area and demonstrated that an unexpected response to water injection may alter conventional wisdom.

The second SPE paper discusses the development of a composite fracture model for the Spraberry. We have integrated the information obtained over seven years from interference, step rate, inter-well tracer, salt tracer, buildup tests, fall-off tests, horizontal core, discrete fracture modeling, outcrop analyses, fracture logs, production tests and profile logging data to show the nature of the Spraberry fracture system.

We continued working on the Humble pilot simulation in order to derive necessary parameters used for simulating waterflood and CO_2 injections in the E.T O'Daniel pilot. We found that the dramatic increase in the center well of the Humble pilot was not because of water injection response alone, but because of the installation of larger pumping unit during the water injection as well. The installation of pumping unit during the water injection clearly obscures the waterflood interpretation. Because of this reason, water injection response on the center production well cannot be used as our interpretation. Meanwhile, the observation wells located on a northeast-southwest trend received good responses while wells located perpendicular to this trend demonstrated no response to water injection. We also found that there is not much interference between the producing wells. As a result, we decided to simulate one injector and one producer located in the on-trend direction (northeast southwest) that demonstrated a good response to water injection. From this study we determined the on trend and off trend fracture permeability and recommended where to place the production wells relative to the fracture trend to have a fast and good waterflood response.

We performed another simulation study to analyze the response of surrounding wells on tracer injection in the E.T O'Daniel pilot. The objective of this study is to determine the fracture orientation and fracture permeability by matching the tracer response (breakthrough time and peak concentration) collected from producing wells. Six water phase inter-well tracers were injected into the six ring fence wells of the E. T. O'Daniel

lease in the middle of August 2000. The collected water samples were analyzed from the twenty-nine producing wells in the O'Daniel tracer program. The analysis shows only four tracer concentrations near or exceeding 100,000 ppt in producing wells due to tracer injection. The remaining wells have only shown weak tracer response or the tracer wave is just beginning to arrive at the well. In the three wells with high peak tracer concentration, tracer shows up in a few days after tracer injection. Tracer breakthrough in this short time is usually indicative of fast communication in the reservoir via isolated natural fractures or extremely high permeability and thin intervals. The results of the tracer simulation confirm fracture permeability is extremely high and highly anisotropy. In addition, the fracture orientation obtained from the tracer study is similar with the average orientation obtained from natural fracture counts in horizontal core acquired in a near-by well.

In the last part of this report, we discuss the progress of the CO_2 pilot project through the interpretation of logs from the observation wells in the E.T O'Daniel CO_2 flood pilot. The purpose is to monitor the movement of CO_2 and saturation changes of oil, water and gas in the upper Spraberry interval of E.T O'Daniel wells. The preliminary interpretation from the two observation wells shows a contrary result in describing the movement of CO_2 at the Upper Spraberry zone. More investigation will be carried out to draw a firm conclusion.

Finally, the field activity during CO_2 injection in the E.T. O'Daniel Pilot is reported in the field demonstration section.

ACKNOWLEDGMENTS

This work has been financially supported by the United States Department of Energy's National Petroleum Technology Office and the following consortium of companies; Chevron, Marathon Oil Co., Mobil Research and Development Corp., Mobil E&P USA, Pioneer Natural Resources (formerly Parker and Parsley Petroleum Co.), Petroglyph Operating Co., Texaco E&P Technology Dept., The Wiser Oil Co. and Union Pacific Resources. This support is gratefully acknowledged. Geographix Inc. donated software used in reservoir characterization. GeoQuest donated ECLIPSE software used in reservoir simulation. I greatly appreciate diligent efforts from the following individuals who contributed to this project: Erwinsyah Putra, Tanvir Chowdhury and Gokul Laskman of Texas A&M University, R.O. Baker and Rupam Bora of Epic Consulting Ltd., Paul McDonald, William H. Knight, Paul Leonard and Carl Rounding of Pioneer Natural Resources (USA) Inc.

The authors would like to show our appreciation to the Spraberry CO_2 pilot team for their enthusiasm and lively discussions. Richard Baker, President of Epic Consulting Ltd., Paul M^{c}Donald, William H. Knight and Tracy Heckman of Pioneer Natural Resources and Steve Melzer continue to lead the team. Other acknowledgments go to Eric Denbina of Epic Consulting, Paul Leonard of Pioneer and Loren Stiles. In addition we recognize the contributions and spirit of Lincoln Elkins in pioneering many of the practical techniques used today in naturally fractured reservoirs.

David S. Schechter
Texas A&M University
September 2001

I. INTRODUCTION

The goal of this project is to determine the technical and economic feasibility of CO_2 injection in the naturally fractured Spraberry Trend Area in the West Texas. Currently, CO_2 flooding in the E.T O'Daniel Pilot is being implemented. The E.T O'Daniel Pilot is located in Section 4 T2S Block 37 of the E.T. O'Daniel lease in Midland County, Texas. The pilot area was selected due to high oil recovery that occurred from primary and secondary operations in this particular area. The pilot has been completed with four CO_2 injection wells, the central production wells and two logging observation wells. The well pattern is oriented along the major trend with the three producers forming a line parallel to the primary fracture trend. The producers are flanked by four CO_2 injectors surrounded by six water injections in an approximately regular hexagonal pattern. The overall area confined by six water injectors is sixty-seven acres while the area enclosed by the four CO_2 injectors is twenty acres. Such configuration is believed to provide an adequate confinement in most directions although some on trend CO_2 losses in a NE-SW direction could occur.

This report addresses the field activities to develop a 15 well, 60-acre CO_2 pilot in the Spraberry Trend Area in west Texas. Two SPE papers, SPE 71605 and 71635, have been published in this particular subject. The first paper compares performance of documented waterflood projects in the Spraberry Trend Area in order to reach stage of development practices that could eventually unlock the key to successful water injection. The results of water injection in the current CO_2 pilot are reviewed in order to use this information for the development of widespread waterflooding throughout the Spraberry Trend Area. The second paper illustrate how a representative Spraberry fractured model was constructed by ***integrating*** the static geological data (core, fracture log and outcrop) with the dynamic engineering data (tracer test, production and pressure transient data). The simulation studies to analyze the response of waterflooding and tracer were performed to confirm our previous findings of fracture permeability and fracture orientations. The waterflood and tracer responses were matched using similar value parameters obtained from horizontal core analysis and humble pilot simulation study. The interpretation of logs from the observation wells in the E.T O'Daniel was carried out to monitor the movement of CO_2 and saturation changes. Finally, we also report the progress of CO_2 injection in the pilot along with the production database. To date there is still no immediate oil response observed in the observation wells even though the CO_2 has broken through. However, the large volumes of CO_2 are being retained in the reservoir and a relatively small volume of CO_2 has been injected on a HCPV basis warrants continuation of CO_2 injection. To monitor the progress and development of this pilot and also to manage the abundant data on each well, the production database was created and can be found in the last chapter of this report.

II. TECHNICAL PROGRESS

1. Review of Water Injection Performance in the Naturally Fractured Spraberry Trend Area, West Texas

1.1 Introduction

The Spraberry Trend Area in west Texas was discovered in 1949 and continues to produce 60 Mbopd from more than 7,500 wells from an eight county area encompassing over 2,500 square miles. Spraberry reservoirs originally contained some 10 Bbbls OOIP of which less than 10% has been recovered.

The Spraberry Trend Area has proven to be elusive to engineers since discovery. Half a century later, the reservoir has maintained the status of one of the more complicated naturally fractured reservoirs to understand or forecast. There are three sets of highly permeable fractures distributed among the two pay intervals in the Upper Spraberry, the 1U and 5U sand (there is the lower Spraberry that is not discussed here). The fractures are stress-sensitive and the fracturing pressure of shales zones are very near fracturing pressure for Spraberry oil sands. Oil recovery is dominated by the imbibition mechanism, however Spraberry sands are weakly water-wet and the matrix permeability is very low. Waterflooding has not been widely applied in the Spraberry Trend Area. In the past, water injection wells were aligned parallel to the major NE-SW fracture trend and perpendicular to a line of production wells (line-drive). Line-drive pattern configuration in anisotropic reservoirs is commonplace as is shown in Fig. 1.1 However, aligning injectors along the same fracture trend with producers was viewed as unwise since the fractures would rapidly conduct injected water to the production well.

The general idea was to build interference between injectors along the fracture trend and force injected fluid to a line of producing wells, also aligned along the primary fracture trend. We believe this de facto approach to water injection in Spraberry has been the primary reason this tremendous resource is so underutilized. The fractures are highly anisotropic[1], and the matrix permeability is very low[2,3] thus requiring high rate fluid injection to force fluids to a line of production wells. The injection rate required to achieve this communication probably creates hydraulic fractures with variable orientation. The small difference in stress anisotropy between adjacent sand and shale layers (as measured in a mini-frac test) and the unquestionable stress sensitivity of the fracture system may result in preferential channeling in non-pay resulting in poor sweep efficiency.

The tremendous size of the reservoir, large number of active and plugged wells, lack of historical production/injection data, and fluid migration across lease boundaries have hampered assessment of water injection over the years. This has resulted in a lack of confidence in the application of water injection in Spraberry reservoirs.

In this paper, we will review the five most documented water injection tests in order to reach stage of development practices that could eventually unlock the key to successful water injection. We will review the results of water injection in the current CO_2 pilot area in order to use this information for development of widespread waterflooding throughout the Spraberry Trend Area. The documented waterflood projects in Spraberry are listed below:

1) Atlantic Richfield Pilot (1952)
2) Humble Pilot (1955)
3) Mobil O'Daniel Co-op Flood (1959)
4) SOHIO Driver Unit Waterflood Expansion (1960)
5) Pioneer Natural Resources O'Daniel DOE/NPTO project (1995)

1.2 Atlantic Richfield Pilot (1952)

Figure 1.2 shows locations of unitized areas waterflooded in the 60's and location of the current water/CO_2 pilot. In 1952 Atlantic Richfield Pilot developed an 80-acre pilot based on imbibition experiments that indicated spontaneous imbibition could recover oil in strongly water-wet rock.[4] The pilot area consisted of 3 injection wells on an 80-acre pattern. The debut of waterflooding in Spraberry demonstrated that wells would respond along the perceived fracture orientation of N50°E.

Figure 1.3 shows that wells along this orientation responded by a significant decrease in GOR's from 10,000 down to 2,000 scf/bbl accompanied by a modest increase in oil production in the range of 10 – 30 bopd per well. A good example was the Magnolia Bowles #2 in Tract 40 directly southeast of the Schrock #5 injection well as shown in Fig. 1.3. In the 2½ months from the middle of September to the first of December of 1952, production from this well was averaging 29 bopd. Production increased erratically but steadily from the first of December on. By the first of February 1954, production had increased to 78 bopd and GOR dropped from 2,400 to 400 scf/bbl.
Since much of the Spraberry was still being produced under primary depletion in 1952, few major operators were interested in pursuing waterflooding for the modest increases noted in production, especially with more water to process. Explanations were provided for the "poor" performance of this pilot, usually related to the unconfined nature of the pilot since only 3 injection wells were utilized.

Figure 1.3 demonstrates positive response from water injection outside the pilot area. However, it should be noted that the primary observation well, the Atlantic Schrock #7, observed a decrease in GOR yet there was almost no production response. The following is taken verbatim from May 17th, 1954 edition of the Oil and Gas Journal.[5]
"Through an unexplained quirk, Atlantic #7 W.M. Schrock, located on the base of the triangle equidistant from each injection well and pre-selected as the observation well for the experiment, showed absolutely no evidence of injected water or increase in oil production... If a fourth injection well were in place, the Atlantic #7 W.M. Schrock would have been the central production well in a classic 80-acre 5-spot pattern."

1.3 Humble Pilot (1955)

Humble Oil Co. embarked upon another 80-acre pilot[6] beginning in 1955 in the Midkiff Spraberry Unit (Fig. 1.4). At this point there were over 2,000 producing wells and pressure/production in the Spraberry Trend Area had declined significantly.
Once again, the idea of the pilot waterflood was to inject into wells aligned along the primary fracture trend, build interference and force water perpendicular to the primary fracture trend to a center production well. The Humble 80-acre pilot was completely confined with four injection wells as opposed to the Atlantic pilot where only 3 injection wells were utilized. This difference in confinement for the two pilots would eventually result in many sources believing that confinement made the difference between the results of the Humble pilot and the unsuccessful Atlantic pilot. This observation added more ambiguity to the question of water injection in Spraberry.

Twelve surrounding wells were monitored for fluid production and reservoir pressure as is shown in Fig. 1.4. The numbers above the well symbol indicate production of oil (barrels) before and after injection of water. The numbers below the well symbol represent the reservoir pressure (psi) before and after the initiation of water injection.
Unlike the center well in the Atlantic pilot, the center production well in the Humble pilot, the Shackelford #9, demonstrated a sharp increase in oil production. A summary of injection and production data for the Humble pilot is shown in Fig. 1.5. A sharp oil bank is seen to arrive at the central production well and as is noted in Fig. 1.4. Production in the center well increased from 70 to 250 barrels of oil per day. The response of this single well (Shackelford #9) in the Humble pilot dictated future development of waterflood patterns. As we shall demonstrate in this report, basing field-wide waterflood development on the results of this single well may have created erroneous expectations for future water injection projects.

There are many explanations and hypotheses why this center production well performed far above previous and future waterflood producers. It should be noted however, the important difference that existed between the Humble pilot and all other Spraberry waterflood projects. The center well was a newly completed well flowing at 80 bopd. A flowing Spraberry well implies the reservoir was still under primary depletion. After initiation of water injection, the well was converted to a pumping well. During the time that a sharp increase in oil production was observed, as noted in Fig. 1.5 (August 1955), a larger pumping unit was installed. This information was not reported in Barfield and Jordan's paper[6] but was retrieved from internal company memorandum. [7] The fact that the well was still on primary and a larger pumping unit was installed during water injection obscures the interpretation since the dramatic increase in oil rate is not a result of water injection alone.

Since the center well responded in a dramatic fashion, the surrounding wells were ignored however as one can see from Fig. 1.4, all wells oriented along the NE-SW direction demonstrated an increase in oil production and/or pressure as the result of water injection.

1.4 Mobil O'Daniel Co-op Flood (1959)

In 1959, Mobil Oil Co. injected water in the E.T. O'Daniel cooperative waterflood (Fig. 1.6). This was a "dump flood" where water from the Santa Rosa Sand, at about 1,000 feet of depth was injected by gravity into the Spraberry sands at 7,000 feet. Initial injection rates were measured close to 1,500 bwpd and declined to 400 bwpd as the Santa Rosa aquifer was depleted. Guidroz[7] published a paper demonstrating a "successful Spraberry waterflood as measured by a significant increase in oil production in the O'Daniel Unit Co-op flood." It is known that the O'Daniel Unit waterflood far out-performed other waterfloods in Spraberry, especially the large-scale Driver Unit waterflood. Upon closer inspection, it appears that the O'Daniel Unit performed very similar to the Atlantic and Humble pilots. Wells outside the area of confinement yet along the dominant fracture trend responded favorably.

Figure 1.6 shows that several injection wells were aligned along the N50°E line in the adjacent Floyd, Powell and Leach leases, south of the O'Daniel Unit. The N50°E orientation was the generally accepted orientation of the fracture system by this point in the development of the reservoir, however, this was the result of pressure transient testing[8]. No verification of this orientation was pursued prior to injection in the co-op flood. This line of injectors terminated with the injection well E.T. O'Daniel #14.

Fifty five percent of the oil recovered as a result of water injection in the O'Daniel pilot came from wells in section four. [8] As is shown in Fig. 1.6, Section 4 was essentially parallel to the line of injection wells to the south of the O'Daniel lease, yet still within the co-op area. The injection/production profile shown in Fig. 1.7 shows a substantial increase in oil production near the end of 1959 and throughout 1960. Guidroz stated in his paper, "The greatest pressure increases were noted in wells 1 and 16. Correspondingly, the increase in oil production from Nov. 1959, through Dec. 1960 is due largely to waterflood response in wells 1, 2 and 16." As is shown in Fig. 1.6, the wells that Guidroz describes were outside an area of significant injection well density and generally along an orientation of N32°E, shown as a series of parallel lines drawn through water injectors in Fig. 1.6. One may presume that much of the rapid increase in oil production and incremental waterflood recovery described by Guidroz was a result of injection south of the O'Daniel lease and rapid movement of injected fluids in a northeasterly direction towards the lease line wells in Section 4 of the O'Daniel Unit.

Other company records reported that outside the co-op area the best performing section was the Powell lease to the south of Section 4 of the O'Daniel Unit. Fig. 1.6 demonstrates this is consistent with on-trend production as opposed to building interference between injection wells and forcing fluid to a line of production wells. Results from the early O'Daniel waterflood provides strong evidence that on-trend injection wells aligned with production wells are capable of producing significant improvements in well productivity.

1.5 SOHIO Driver Unit Waterflood Expansion (1960)

The dramatic increase from 70 to 250 bopd in the Humble pilot resulted in a new fervor of activity in the Spraberry Trend in the late 50's and early 60's. The immediate result of the Humble Midkiff pilot was development of a 9-section test of wide-scale waterflooding by Sohio in the Driver Unit of the Spraberry Trend Area shown in Fig. 1.8. This was and still remains the largest unitized area in the Spraberry Trend comprising approximately 60,000 acres.

Injection wells were aligned along the main fracture trend as determined by interference tests[9] (N50°E) and production wells were aligned along the same orientation as previously described and shown in Fig. 1.1. The alignment of injection wells in a line drive configuration was a result of the Humble pilot with the belief that large production increases would be noted in the line of injection wells, as was the case in the Humble pilot. Figure 1.8 shows the configuration of wells in the Driver Unit. There is little data in the public domain describing well-to-well response in the Driver Unit flood so it is difficult to discern any patterns of wells that responded to water injection. It is known that there was no "flush production" of oil in the line of production wells perpendicular to the line of injection wells, unlike the central production well in the Humble pilot. There was a clear increase in oil production due to injection of water in the Unit as a whole[10], but the lack of "flush" production dampened enthusiasm for water injection in Spraberry sands.

Elkins did mention that Area 3 performed better than Area 2 although the geological conditions are not as favorable in Area 3. Furthermore, there was about half the injection wells in Area 3 as opposed to Area 2 yet Area 3 performed better under water injection. Once again, it may be possible that there were insufficient production wells oriented along the fracture trend with injection wells to provide a rapid increase in production that may have instilled a level of confidence in early waterflood trials. A secondary hypothesis is the good response seen in Area 3 was a result of more injection wells located in Area 1 that mobilized oil into Area 3.

The injection wells were oriented along the N50°E line as shown in Fig. 1.8. Earvin[11] later reported that an N32°E fracture orientation was a possibility. His evidence was based on the response of wells 376, 385, 389, 394 and 398 that are aligned an N32°E orientation with injection wells. It remains undocumented whether the "possible trend" described by Earvin was a result of pressure or production data. As is often the case in Spraberry, reconstruction of historical data is a crucial constraint to developing waterflood reserves.

1.6 Results of Water Injection in the E.T. O'Daniel Pilot Project (1995)

The E.T. O'Daniel Pilot is located in Section 4 T2S Block 37 of the E.T. O'Daniel lease in Midland County, Texas (Fig. 1.2). This site was selected due to the high oil recovery that occurred from primary and secondary operations in this particular area.

The pilot configuration is shown in Fig. 1.9. 15 wells have been completed with four CO_2 injection wells, three central production wells and two logging observation wells. The well pattern is oriented along the major trend with the three producers forming a line parallel to the primary fracture trend. The producers are flanked by four CO_2 injectors and surrounded by six water injections in an approximate regular hexagonal pattern. The overall area confined by six water injectors is sixty-seven acres while the area enclosed by the four CO_2 injectors is twenty acres. Such a configuration is believed to provide an adequate confinement in most directions although some on trend CO_2 losses in a NE-SW direction could occur.

Stable water injection was initiated in October of 1999 in order to increase the reservoir pressure above the minimum miscible pressure (MMP). Also, another goal was establishment of a waterflood baseline decline so that all produced oil as a result of CO_2 injection can be quantified. Since this is a 40-year-old waterflood area, it was assumed the area was at residual oil saturation and there would be minimal response from water injection. Production has been recorded in 37 wells in and around the pilot area as shown by the green dashed curve in Fig. 1.9. We have divided oil production into 23 off-trend and 7 on-trend wells. The 7 on-trend wells are located along the NE-SW natural fracture orientation as determined by horizontal core. [12]

The three central production wells 38, 39, and 40 have shown small incremental oil production after initiation of water injection. However, wells oriented parallel to the primary fracture trend responded with a significant increase in oil production. Some of the wells over one mile from the injection wells have responded whereas wells oriented perpendicular to injection wells at a fraction of distance from injection wells have shown little response, similar to that observed in the tracer survey. It is possible that off-trend wells will respond in the future but the unexpected increase in production wells along the fracture trend clearly indicate the presence of un-swept oil even though the area has been previously waterflooded.

The composite performance of the "expanded" pilot area shows that oil production has steadily increased from 200 bopd before water injection to a current level near 400 bopd with an additional cumulative production of > 75,000 bbls after 1.5 years of water injection (Fig. 1.10). Thus, the seven on-trend wells are responsible for 150-200 barrels of incremental oil per day. This represents an incremental gain of 20-30 barrels for each seven on-trend wells. The results also dispel the notion that on-trend injection wells will channel via the fractures and rapidly water-out production wells without producing incremental oil via the imbibition mechanism.

1.7 Conclusions

1. Even though waterflooding in Spraberry Area has been documented as a poor recovery mechanism, recent results of low rate water injection has revealed that waterflooding can dramatically increase oil production.
2. On-trend well responded favorably in almost all waterflood pilots in the Spraberry Trend Area. The results oppose previously held notions that production wells aligned

on-trend with injection wells will experience rapid channeling via fractures, thereby watering-out production wells with no incremental oil production.

3. High water injection rates were able to restore pressure in the O'Daniel Pilot area from about 1000 psia to pressure levels between the Minimum Miscible Pressure (MMP) of 1550 psia and Formation Parting Pressure (FPP) of 2730 psia.
4. The imbibition mechanism coupled with high permeability anisotropy and heterogeneity in the fracture system facilitated the increase oil production rate observed in the on-trend wells during steady, low rate water injection. This unexpected result implies that water is contacting unswept rock in an area that has been previous waterflooded.

1.8 References

1. "Radioactive Gas Tracer Survey Aids Waterflood Planning," World Oil (Feb. 1961).
2. Dyes, A.B. and Johnston, O.C.: "Spraberry Permeability from Build-Up Curve Analyses," Trans., *AIME* (1953) 198, 135-138.
3. Christie, R.S., and Blackwood, J.C.: "Production Performance in Spraberry," *OGC* (April 7, 1952) 107-15.
4. Brownscombe, E.R. and Dyes, A.B.: "Water-Imbibition Displacement...Can It Release Reluctant Spraberry Oil?" *OGC* (Nov.17, 1952) 264-265 & 377-378.
5. Enright, R.J., "Imbibition – Newest Producing Technique" OGC (May 17, 1954) 104 – 107.
6. Barfield, E.C., Jordan, J.K. and Moore, W.D.: "An Analysis of Large-Scale Flooding in the Fractured Spraberry Trend Area Reservoir," *JPT* (April 1959) 15-19.
7. "Waterflood Possibilities Spraberry Trend Area Field," Sohio Production Company Internal Report, (Sep. 1957).
8. Guidroz, G.M.: "E.T. O'Daniel Project- A Successful Spraberry Flood," *JPT* (September 1967) 1137 – 1140.
9. Elkins, L.F. and Skov, A.M.: "Determination of Fracture Orientation from Pressure Interference," Trans., *AIME* (1960) **219**.
10. Elkins, L.F.: "Cyclic Water Flooding the Spraberry Utilizes 'End Effect' to Increase Oil Production Rate," *JPT* (August 1963) 877-884.
11. Earvin, S. "Waterflood Performance in Spraberry" Internal Memorandum, Spraberry Database, Harold Vance Dept. PE, Texas A&M University (1988).
12. McDonald, P., Lorenz, J. C., Sizemore, C., Schechter, D.S., and Sheffield, T.: "Fracture Characterization Based on Oriented Horizontal Core From the Spraberry Trend Reservoir: A Case Study" paper SPE 38664 presented at the 1997 Annual Technical Conference and Exhibition, San Antonio, Tx, 5-8 October.

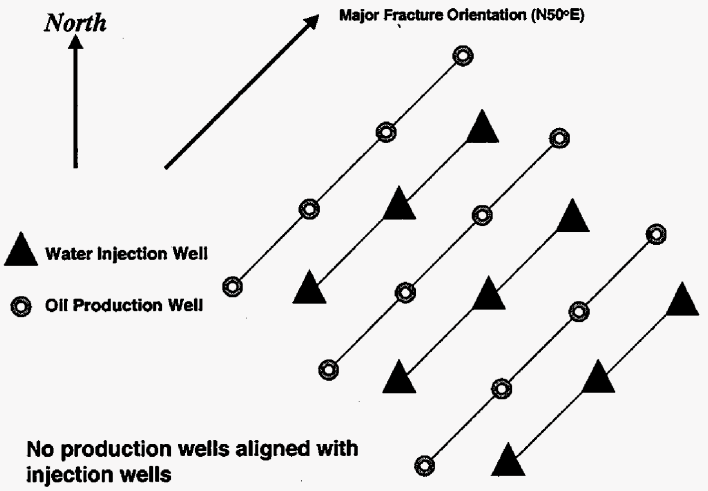

Fig. 1.1 - Line-drive pattern configuration in anisotropic reservoirs.

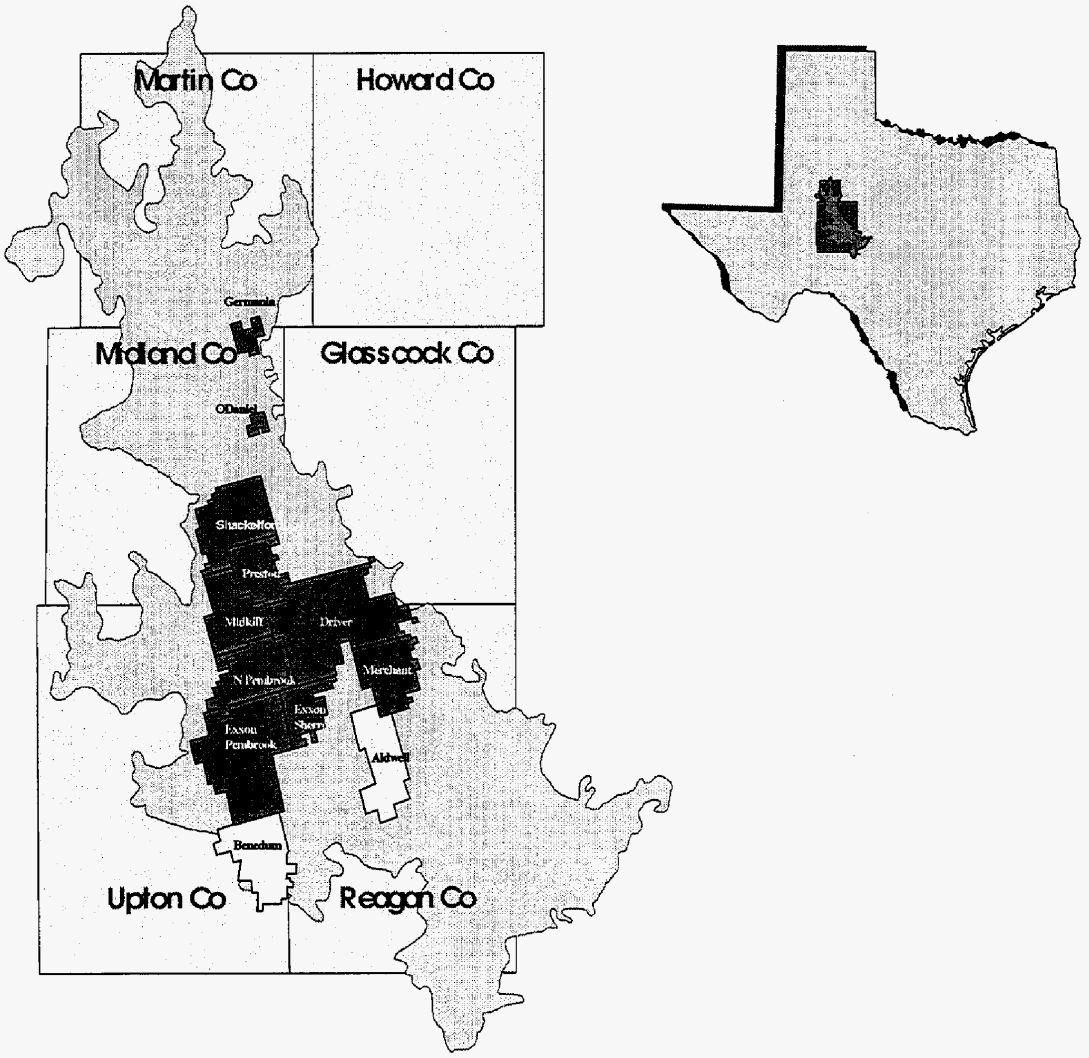

Fig. 1.2 – Units and reservoir extent in the Spraberry Trend Area.

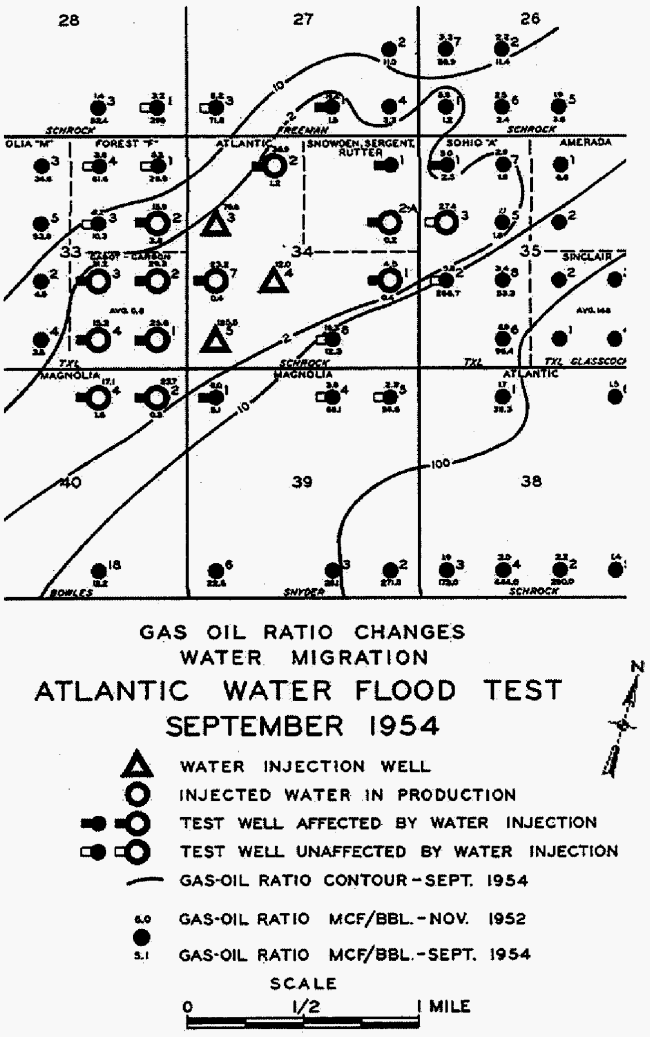

Fig. 1.3 - Atlantic Richfield waterflood pilot 1952.

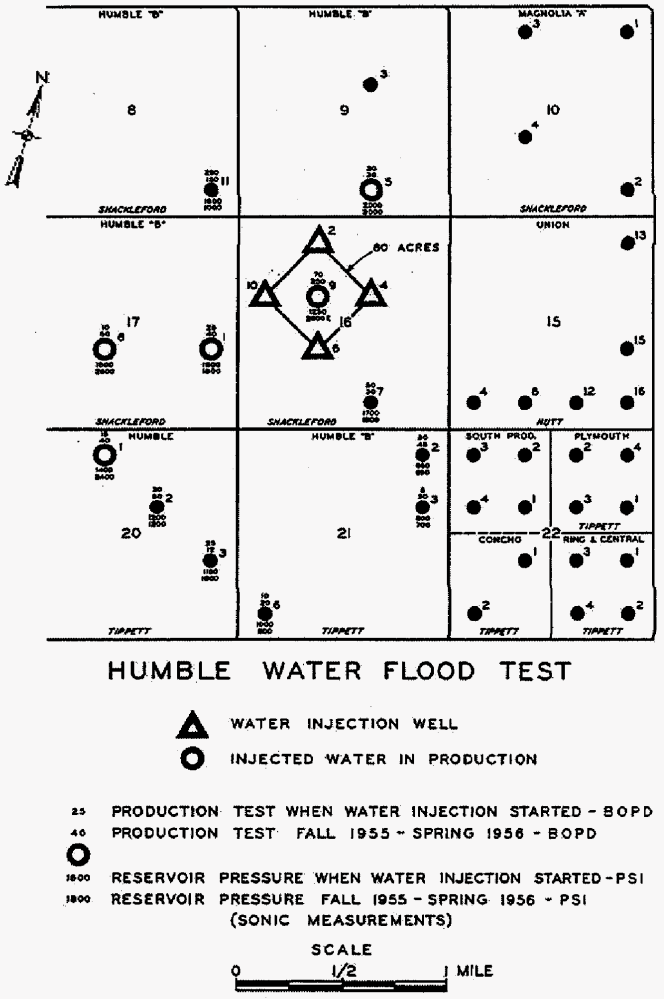

Fig. 1.4 – Humble water injection pilot in the Spraberry Midkiff Unit 1955.

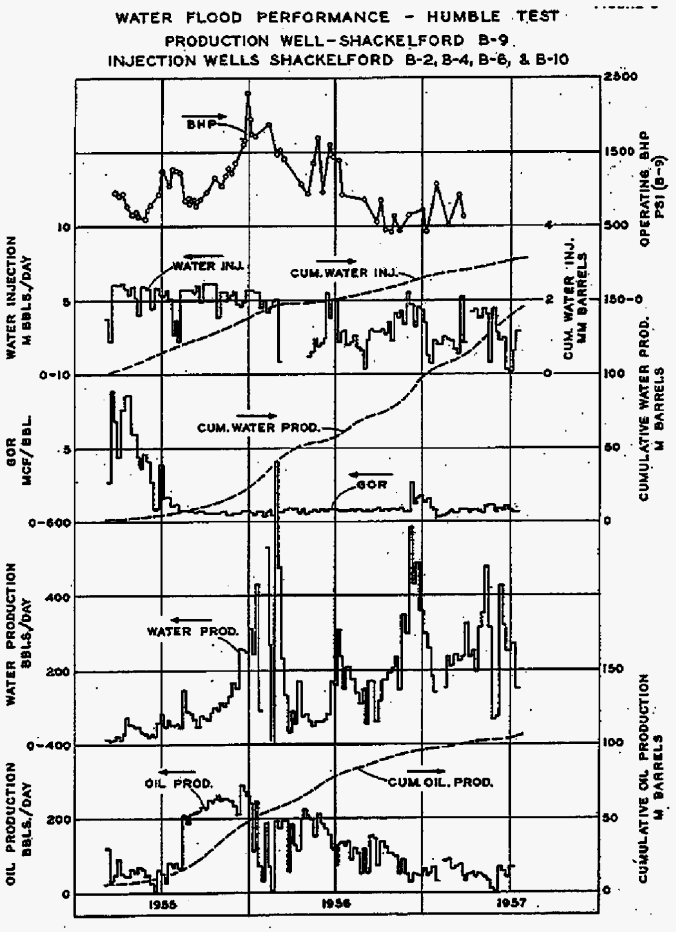

Fig. 1.5 - Production and injection data for the Humble pilot.

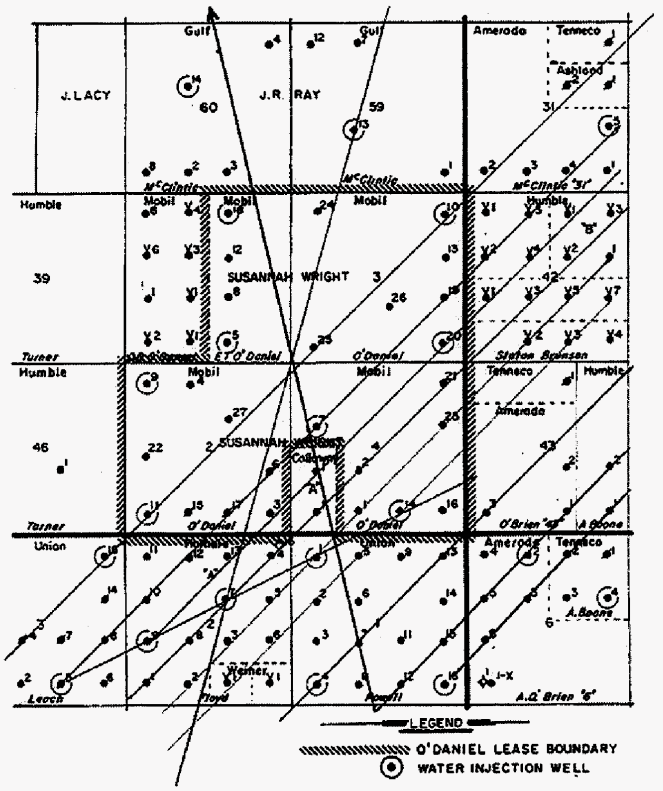

Fig. 1.6 - Waterflood Map, O'Daniel Unit Co-op Flood 1959: Injection wells originally aligned N50°E, series of lines indicates current fracture orientation as determined by waterflood response (approximately N32°E).

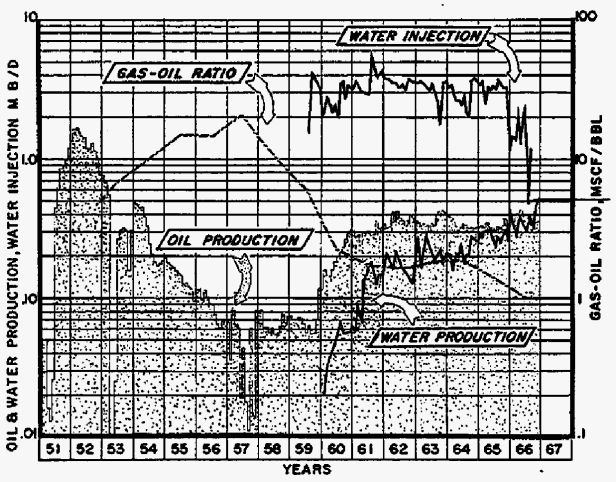

Fig. 1.7 – Performance of O'Daniel Unit co-op waterflood.

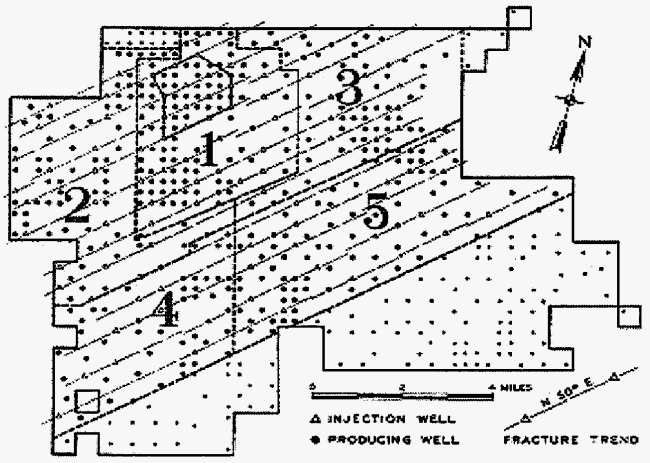

Fig. 1.8 - Areas developed for waterflood expansion in Spraberry Driver Unit, 1960.

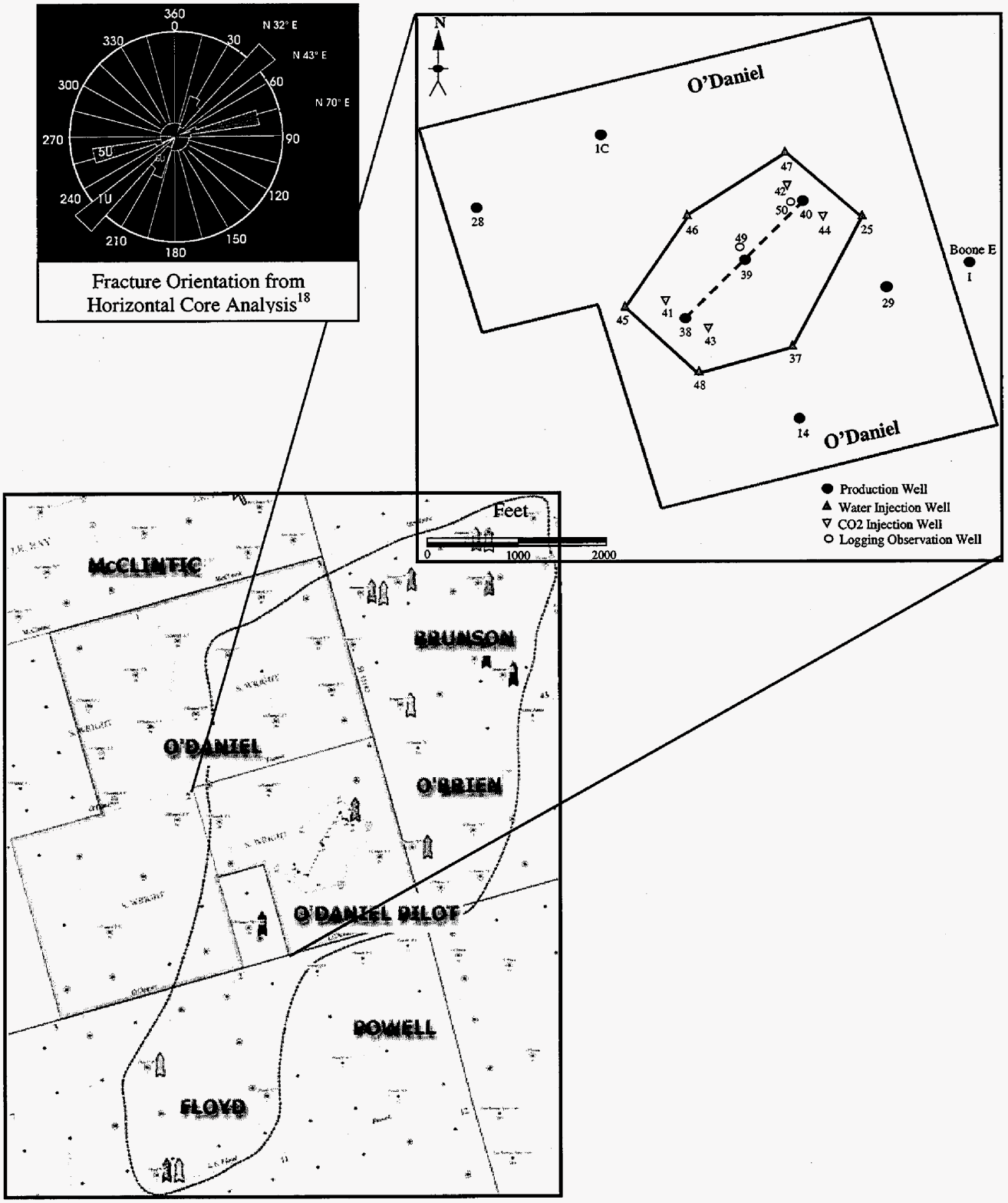

Fig. 1.9 – Map of O'Daniel pilot area and pilot well configuration.

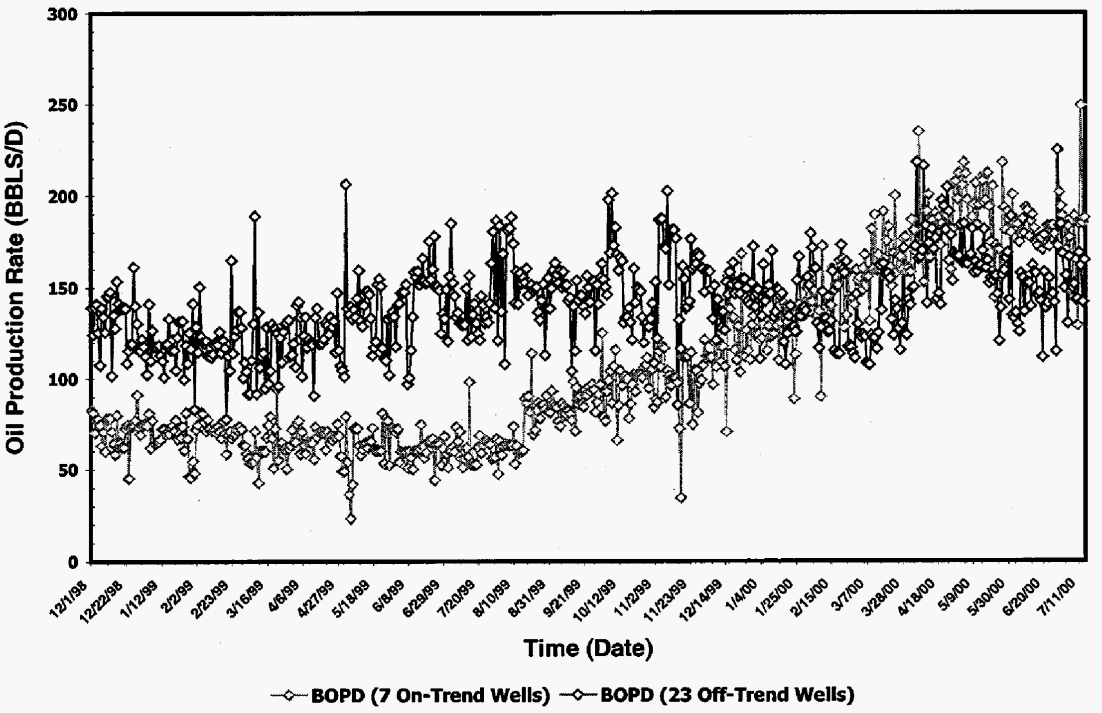

Fig. 1.10 - Response to water injection for 7 on-trend and 23 off-trend wells outside the pilot area.

2. Development of a Fracture Model for Spraberry Field, Texas USA

2.1 Introduction

At the time of its discovery in 1949 the Spraberry Trend (Fig. 2.1) was considered the largest oil field in the World. The original primary recovery factor was anticipated to be less than 10%. In an effort to increase recovery, several areas of Spraberry were placed on waterflood beginning in the late 1950's. Waterflooding, for the most part, has been only moderately successful. The noted exception to this is the waterflood performance on the E.T. O'Daniel lease. The waterflood recovery in this lease has exceeded 25% of the original oil in place. Failure of waterflooding in Spraberry has been attributed to the low matrix permeability and extensive fracturing [1]. Many studies have been conducted to understand the Spraberry fracture characteristics[2-21]. However, the characteristics of the fracture network and its interaction with the supporting matrix framework remains poorly understood.

Over the last seven years, interference, step rate, inter-well tracer, salt tracer, buildup tests, fall-off tests, horizontal core, discrete fracture modeling, outcrop studies, fracture logs, production tests and profile logging data have been integrated to improve understanding of the Spraberry fracture system.

2.2 Geology

The Spraberry formation was deposited during Permian age in the Midland Basin, a geological province of the Permian Basin. The formation is comprised of submarine fans and basin plane deposits with a complex stratigraphy composed of sandstone, shale, siltstone and limestone interbedding. Core analyses and well logs show that the reservoir is characterized by both low porosity and low matrix permeability. Matrix permeabilities are in the order of 0.05 md or less with porosities ranging from 6 to 14 percent. The effective permeability of the reservoir, as determined from pressure buildup tests, step rate tests or advanced decline analysis, ranges from 1 to 200 md. We interpret that the primary contribution to the effective permeability is from the fracture systems, as opposed to the matrix. The formation has been subdivided into three principal intervals including the Lower, Middle and Upper Spraberry formations with average depths of about 7,200, 7,400 and 8,000 feet, respectively. These principal intervals have been further subdivided to different units (Fig. 2.2). Of these, only two units in the Upper Spraberry (1U and 5U) have been identified as containing reservoir quality rock capable of making significant production contributions.

Objectives

The overall objective of this report is to illustrate how a representative reservoir model was constructed by ***integrating*** the static geological data (core, fracture log and outcrop) with the dynamic engineering data (tracer test, production and pressure transient data).

2.3 Fracture Characterization

Effectively, the Spraberry trend can be characterized as a "triple component" system. The first component is the long, well-connected fractures, the second is a combination of matrix and smaller, more discontinuous fractures with some micro fracturing, and finally, the third component is comprised of the low permeability matrix. A schematic view of the discontinuous fracture system is shown in Fig. 2.3. Figure 2.3 shows a diagram of more discontinuous fractures. The spacing of set 1 continuous fractures is not known.

The first component, the long fracture systems, or fracture clusters, are stress sensitive and greater than ~1000 feet in length. A secondary 'background' network of much shorter, partially connected (set 2) fractures, have an inter-fracture spacing in the two to four foot range.

The system of long, well-connected fractures initially controls flow in the reservoir and dictates which areas are invaded by injected fluids. In any short-term transport test (< 1 month), this component totally dominates the response, provided the wellbore area is not already pressure depleted. For example, if an individual producer intersects a well-connected fracture cluster, then that producer will have high initial fluid productivity, providing the reservoir is not depleted. The first component of the fracture system, although important initially, transports a relatively small proportion (<5%) of the flow over the well's total productive life.

The longer-term production response is controlled by both fracture sets and matrix crossflow. As water injection continues, water invades into the secondary, more discontinuous fracture system. The average fracture spacing, imbibition rate and matrix permeability then plays a more important role in controlling the production profile and recovery factors.

2.4 Data Types and Information

As is the case with a large number of naturally fractured reservoirs, there is limited direct fracture observation data available for the Spraberry trend. There is, however, plenty dynamic data that gives us some guidance for constructing a representative fracture model. The following is a review of this data.

2.4.1 Data from Direct Observation

1. Vertical core data show vertical fractures with fracture heights of one to four feet. Typically, vertical cores in Spraberry show NE-SW or East-West directionality[5, 9,20] as shown in Fig. 2.4. Fractures usually terminate against the shale barriers at the top or base of undisturbed geological events.
2. Recently, a horizontal core was acquired to better characterize the fracture system[14]. A lateral core was taken in each Upper Spraberry unit (1U and 5U). Figure 2.3 shows a schematic diagram of the Spraberry fracture distribution and orientation.
3. The Humble Unit Midkiff, deviated well [2,7] data shows that fractures are predominantly in the sand and not the shale, as shown in Fig. 2.5. From a mechanical strength perspective, this makes sense considering the ductility of shales whereas the sands are more brittle. As the fraction of shale content increases, fracture intensity

decreases because the rock is more ductile, decreasing the brittle strain. Shale content in some reservoirs can therefore strongly control fracture intensity.

4. Study on an outcrop of an "analogous" reservoir[13] yielded information on fracture lengths, stress sensitivity, and orientation. A comparison of three analogous outcrops showed large variations in fracture characteristics. Figures 2.6 and 2.7 show the fracture images, fracture maps and average fracture lengths, for these outcrops. Fracture clustering and some fracture branching are observed in some outcrops but not in others. What is interesting about the outcrop is that ***most fractures are short (< 30ft).***

2.4.2 Indirect Hydraulic Data

5. A large volume of production /injection data is available for many of the Spraberry Units. Portions of the field have been flooded, intermittently, since 1951. The waterflood behavior (i.e., water breakthrough timing) indicates an average N50°E fracture trend. However it is expected that there is some overall variability of this trend [5,9]. The production and injection data show a variation in fracture orientation as shown in Table 2.1.
6. Constant pressure tests (and advanced decline analyses) indicated an effective permeability to oil in the range of k_{oe} = 0.4 to 0.9 md[18]. Note that the effective matrix permeability, based on core analysis, is less than 0.05md. The effective permeability, within the well drainage area, is therefore greatly enhanced by the second component fractures. These tests (and pressure buildup tests) can be interpreted as wells producing from a single hydraulic fracture in a low permeability reservoir. The data for these constant pressure tests were collected over a ten-year period and therefore represent a large radius of investigation.
7. A multi-well interference test, run during the year 2000 (Fig. 2.8) confirmed pressure communication existed between wells within the CO_2 pilot area as shown in Fig. 2.9. These tests have been analyzed using both single porosity and dual porosity methods. Regardless of how these test were analyzed the effective permeability was determined to be in the 10md range. These tests, performed within a 67-acre pilot area, confirmed the presence of heterogeneous fracture permeability.
8. Multi-well interference tests were run in the 1960's, at varying water injection rates in the Midkiff Unit. Rates were varied as shown in Fig. 2.10. The test results showed a stress sensitivity of fracture permeability to injection pressures. The test results also showed that a strong NE-SW fracture trend as well as East-West and NNE-SW trends prevailed. An interesting observation to note is that tests with higher injection rates yielded higher values of permeability.
9. Early build up tests (prior to 1960) yielded higher initial effective permeability values, in the 2 md to 200 md range[4] when reservoir pressure was near original pressures.
10. Approximately ten single-well pressure transient tests (falloff & buildup tests) were run[18]. In recent years, these tests have been analyzed using both single porosity and dual porosity models. Each of the evaluated wells had been stimulated with hydraulic fractures. All single well tests show negative skins and linear flow periods. The more recent buildup tests typically show low permeability (<1 md) whereas falloff tests yield a much higher permeability (>1 md), again confirming the probable stress

sensitivity of the effective permeability (i.e., particularly of the fracture system). The falloff tests measure higher permeability because these tests are conducted in water injectors with higher 'reservoir' pressures.

11. Mini-frac and step rate tests have shown that hydraulic fracturing occurs at relatively low pressures (i.e., close to a hydrostatic pressure gradient).
12. Average fracture spacing was derived from decline analyses and laboratory imbibition data. From this data it was determined that the average effective fracture spacing was 3.1 feet[16]. This agreed very well with the direct sample from the horizontal core on fracture spacing.
13. An interwell tracer test was conducted in late 2000 where six injectors had six tracers injected into them[25] and 37 offset wells were sampled. These tests showed NE-SW, NNE-SW and E-W rapid communication paths. Many wells experienced tracer breakthrough within a week of injection.
14. Numerous simulation models and waterflood analyses completed for the O'Daniel Unit, indicated East-West and NE-SW communication paths.
15. Salt-water tracer tests confirm communication in the NE-SW direction from the pilot area. Salt-water tracer tests at wells 28 and O'Daniel C1 also show that very poor communication exists in the north-westerly direction from the pilot area.
16. Production logging tests (PLTs) were run on three water injectors (Wells 45, 47 and 48 of the O'Daniel Unit). A figure of the profile log for Well 45 is presented in Fig. 2.11. The results show a relatively uniform distribution of flow within the 1U and 5U sands.

Some of the dynamic data seems to suggest the presence of a single fracture system, comprised of long fractures (points 6, 10 and 13). The dynamic data also emphasizes that the effective permeability in the reservoir, at any distance away from the wellbore, is higher than the matrix permeability (points 6, 7, 8, 9, 10 and 12). The shorter semi-continuous fractures enhance the 'matrix' permeability and are a major contributor to flow. Evidence of the stress sensitivity of both on-trend and off-trend fractures is shown by points 7,8, 10 and 11.

2.4.3 Fracture Length and Lateral Connectivity

Outcrop data and buildup/interference test data tend to indicate that the majority of fractures are short and not well connected. ***Individual*** fracture lengths appear to be short, in their natural state, as observed from outcrop data. Later stage buildup data also supports the concept of laterally semi-disconnected fractures in the reservoir. Most late stage buildup tests and constant pressure tests, yield a low effective permeability (k_{eff} < 1md). Even then, however, the permeability is higher than matrix permeability observed from core data.

It must be realized that the majority (i.e., >80%) of the fractures are probably not in hydraulic communication. The numerous small, disconnected fractures probably don't contribute that much to the effective permeability[22]. The small proportion of hydraulically connected fractures has been noted in numerous mining and ground water flow studies[23, 24].

On the other hand, some of the hydraulic data, such as tracer and production data, supports the theory of a well-connected fracture system. Well-connected fracture systems (extending > 1000 feet) were evident in both the on-trend (N50°E) direction and off-trend direction (N30°E and N70°E), in the tracer tests and fall off test studies. Falloff tests on the well 47 and well 25 water injectors strongly suggest that the tests are dominated by linear flow as exhibited by the long duration linear flow periods (> 3 weeks).

These effective fracture system lengths are longer when water is injected. However it is believed that fractures close somewhat during depressurization of the reservoir. The systems of fractures are stress sensitive. Moderate water injection rates/pressures easily aggravate these systems. This observation made by comparing the falloff test results (permeability and fracture length) with build-up test results. The fracture lengths and permeabilities, determined from the falloff tests[18], are much greater.

Recent inter-well tracer tests conducted in the CO_2 pilot area, in the ET O'Daniel Unit, exhibit rapid water breakthrough times ranging from 1 to 99 days, corresponding to tracer velocities of 12,137 ft/day to 59 ft/day, respectively[25]. Six tracers were used in six injectors and sampling from 37 producing wells was done over a 100 day period. This implies that the waterflood tracer response was dominated by fracture flow and the first component (set 1) of the fracture system. However, the tracer recoveries during these tests were low, with maximum produced tracer concentrations of ~0.10 percent of injected tracer concentration, indicating low volumes of the highly connected fractures (set 1). Because of the high retention of tracer, it is believed that the bulk of the tracer is moving through the more tortuous pathways (set 2 fractures and matrix network). An example of fracture pathways inferred from tracer injection in Wells 46 and 47 is presented in Fig. 2.12. Figure 2.13 shows the tracer production response in well Brunson D-1. From tracers injected at well #46 and well #47, it was observed that tracer production declines sharply after breakthrough (peak concentration) and then gradually tapers off. The lag time and similar response pattern between injectors 46 and 47 is noteworthy. This echo of tracer response from injectors 46 and 47 suggest tracers are flowing in similar pathways

The results of salt tracer tests are summarized in Fig. 2.14. The salt tracer was sampled over a one-year period with 37 wells being sampled. Because of the earlier breakthrough of injected water, before salt-water tracer sampling, most wells do not show a marked change in sulfate concentration with time. Fig. 2.14 gives an estimation of the fraction of water produced by the well that comes directly from water injection. It **assumes** a background sulfate reading of zero. Clearly, on trend (NE-SW) producers such as Floyd "D1" and Brunson "D1" are strongly affected by the water injection.

Comparing results from the three interference tests, the salt-water tracer tests and the inter-well tracer tests, give insight into the nature of the long fracture systems. The Midkiff Unit interference test revealed a NE-SW as well as an East-West permeability trend. The O'Daniel interference test, within the 67-acre pilot area, showed that there was heterogeneous behavior. The O'Daniel tracer tests confirm all three trends: NNE-SSW,

NE-SE and East-West (confirming once again the prevailing reservoir heterogeneity). Tracer breakthrough was observed from Well 47 to O'Brien 10, in a NW-SE direction. With the exception of this observation, all other pressure and tracer measurements confirm a fracture orientation that is in excellent agreement with fractures observed in the core data.

2.4.4 Fracture Porosity, Aperture and Fracture Volume

The volume of these fracture systems is in the order of 1 to 1000 Bbls or 25 - 50 Bbls/acre. These volumes are based primarily on the Midkiff Tracer Test and water breakthrough response[6]. This results in a fracture porosity of 0.04 to 0.08%.

Measured fracture apertures are expected to have a large range due to the stress (i.e., pressure) sensitivity of fractures. Measured apertures in un-stressed raw core averages ~50 microns, with a range of 10 to 320 microns. Near the injection wells, fracture aperture is likely to be wider compared to the regions near producers due to the injection of high-pressure water that opens and extends some of the pre-existing fractures.

2.4.5 Discussion of Fracture Height

The height of the fractures as seen in the vertical core is limited (1-4 ft). However, the number of vertical cores is also limited. Therefore sample totals are small. As mentioned earlier, fractures generally terminate at shale barriers (see Fig. 2.5). Injection logging data on water injectors show a relatively uniform distribution of flow within 1U and 5U sands. The profiles taken to date do not show that there is any single fracture taking a very high proportion of flow, as shown in Fig. 2.11. However, despite termination of natural fractures at shale boundaries, temperature logs suggest that fracturing out of the pay zone is likely. Note that Fig. 2.11 shows lower temperatures well above the perforation interval confirming the presence of cooler, injected water. The water likely migrated to this position via fractures, propagating out of zone. Note, this water injector was not intentionally hydraulically fractured.

2.5 Discrete Fracture Network (DFN) Modeling

A discrete fracture network (DFN) model was developed for the E.T. O'Daniel Unit using commercial software[26]. This DFN model was developed to improve the understanding of the Spraberry fracture network and to better integrate the results obtained from various sources, such as core, logs, outcrop, tracer tests, pressure transient data and multi-well interference tests. The DFN model developed in this study is based on data from outcrop studies[13] and core data [9,14]. The steps involved in development of a DFN model for the E.T. O'Daniel lease is outlined in Fig. 2.15. The modeling approach is to assume a permeability and anisotropy ratio (roughly known) and investigate combinations of fracture parameters that would agree with these assumptions.

Different sensitivities were carried out by using different fracture aperture and average fracture lengths. Results for some of the runs are presented in Table 2.2. An example of directional permeability, calculated using fracture orientation from the Spraberry 5U

Unit, is illustrated in Fig. 2.16. Assuming that the measured fracture spacing and orientation is correct, the following observations can be made from DFN modeling:

- Fracture length has tremendous impact on effective fracture permeability
- Fracture length must be greater than 10 ft (as there is no connectivity with smaller length fractures)
- Fracture height has a relatively moderate impact on horizontal permeability, at least when the fracture length/connectivity is low
- Fracture height has significant impact on vertical permeability
- Fracture height varies between 2 ft and 5 ft (i.e. fractures do not extend through the entire pay thickness)
- With long or moderate fractures (~ 100 ft), fracture aperture (or transmissivity) strongly controls permeability
- Given the observed 'cross-fracturing', the anisotropy ratio (k_{max}/k_{min}) is low (~ 10 or less)

Modeling Spraberry fractures indicates that these fractures are not well connected. These set 2 fractures can be considered as "stochastic fractures". The set 1 fractures are classified as "deterministic fractures".

2.6 Fracture Flow Mechanics

Creating a viscous pressure drop across the fracture will be important in both waterfloods and CO2 flooding. However, large pressure gradients in either the on-trend or off-trend direction will not be possible because of the "check valve" or "pressure relief valve" effect that the fractures have (especially in the off-trend fracture sets). Fluids injected at high pressure will enhance fracture connectivity thus increasing both the on-trend and off-trend fracture permeability of the system.

Any short-term hydraulic (pressure or rate) response is likely to be dominated by the large-scale fractures if they are reasonably close to the observation or signal wells. For these wells, the high lateral-connectivity fractures will control flow direction and thus pressure and rate response (water breakthrough or pressure pulse response).

However, ultimate waterflood recovery factors and production are controlled by the average fractures spacing between both the short fractures and by the long fracture system pathways. The long fracture system establishes where water is initially distributed (initial volumetric sweep) but with time, and increasing injected water volumes, many of the small and more discontinuous fracture systems become invaded by water. At this time imbibition rate, fracture spacing and matrix permeability control waterflood production response.

2.7 Conclusions

We have proposed a fracture model that seems to fit all available data, consistently. Initially the longer fractures dominate production performance of individual wells or areas. Some fracture systems determine initial well deliverability (flush production). Fracture connectivity of long fracture systems determine initial water/tracer breakthrough in waterfloods. However, with continued production and injection the importance of shorter, less connected fracture systems and the matrix, are felt. At later stages of waterflooding, average fracture spacing, average effective permeability and imbibition processes dictate recovery profiles. For solution gas drive scenarios, the long term deliverability is largely controlled by effective permeability.

2.8 References

1. Guidroz, G.M.: "E.T. O'Daniel Project – A Successful Spraberry Flood," JPT, September 1967, pp. 1137-40.
2. Carlson, R.F.: "Special Directional Drilling in West Texas," Oil and Gas Journal, September 1 1952, pp. 99-101.
3. Brownscombe, E.R. and Dyes, A.B.: "Water Imbibition Displacement – Can It Release Reluctant Spraberry Oil?" Oil and Gas Journal, November, 1952.
4. Dyes, A.B. and Johnston, O.C.: "Spraberry Permeability from Build up Curve Analyses," AIME Vol. 198, 1953.
5. Elkins, L.F. and Skov, A.M.: "Determination of Fracture Orientation from Pressure Interference," *Trans*, AIME (1960). **219,** 301.
6. Elkins, L.F. and Skov, A.M.: "Cyclic Water Flooding the Spraberry Utilizes End Effects to Increase Oil Production Rate," *JPT*, August 1963.
7. "Midkiff Pulse Testing – Results of Spraberry Final Pulse Testing Experiments July 1 August 6, 1963," Humble Oil Internal Memo, PRRC Spraberry Database, September 1963.
8. Epic Consulting Services Ltd.: "Parker & Parsley Waterflood Surveillance E.T. O'Daniel Unit," correspondence with Parker & Parsley (now Pioneer Natural Resources USA, Inc.), February 1996.
9. Schechter, D.S. et al.: "Reservoir Characterization and CO_2 Pilot Design in Naturally Fractured Spraberry Trend Area," paper SPE 35469 presented at the 1996 SPE Permian Basin Oil and Gas Recovery Conference held in Midland, Texas, 27-29 March.
10. Schechter, D.S.: "Advanced Reservoir Characterization and Evaluation of CO_2 Gravity Drainage in the Naturally Fractured Spraberry Trend Area," First Annual Technical Progress Report to DOE under Contract No. DE-FC22-95BC14942, PRRC Report 96-42, Dec. 17, 1996.
11. Baker, R.O. and Spenceley, N.K.: "Pre and Post Hydraulic Fracture Buildup tests on E.T. O'Daniel #37," correspondence with Parker & Parsley (now Pioneer Natural Resources USA, Inc.), December, 1996.
12. Guo, B. and Schechter, D.S.: "An Integrated Study of Imbibition Waterflooding in the Naturally Fractured Spraberry Trend Area Reservoirs," paper SPE 39801

presented at the 1997 SPE Permian Basin Oil and Gas Recovery Conference held in Midland, Texas, 25-27 March.
13. Malmanger, E.M., Statistical Analysis and Simulation of Stress Sensitive Natural Fracture Networks, M.S. Thesis, New Mexico Institute of Mining and Technology, Socorro, NM, March 1997.
14. McDonald, P., Lorenz, J.C., Sizemore, C., Schechter, D.S. and Sheffield, T.: "Fracture Characterization Based on Oriented Horizontal Core From the Spraberry Trend Reservoir: A Case Study," paper SPE 38664, presented at the SPE Annual Technical Conference and Exhibition held in San Antonio, Texas, 5-8 October, 1997.
15. Schechter, D. et al.: "An Integrated Investigation for Design of a CO_2 Pilot in Naturally Fractured Spraberry Trend, West Texas," paper SPE 39881 presented at the SPE International Conference and Exhibition held in Villa Hermosa, Mexico, March 3-5, 1997.
16. Baker, R.O. et al.: "Using An Analytical Decline Model to Characterize Naturally Fractured Reservoirs," paper SPE 39623 presented at the 1998 SPE/DOE Improved Oil Recovery Symposium held in Tulsa, OK, 19-22 April.
17. Putra, E. et al.: "Use of Experimental and Simulation Results for Estimating Critical and Optimum Water Injection Rates in Naturally Fractured Reservoir," paper SPE 56431 presented at the 1999 SPE Annual Technical Conference and Exhibition held in Houston, Texas, 3-6 October.
18. Baker, R.O. et al.: "Characterization of the Dynamic Fracture Transport Properties in a Naturally Fractured Reservoir," paper SPE 59690 presented at the 2000 SPE Permian Basin Oil and Gas Recovery Conference held in Midland, Texas, 21-23 March.
19. Baker, R.O. et al.: "Reservoir Characterization of Naturally Fractured Reservoir," paper SPE 63286 presented at the SPE Annual Technical Conference and Exhibition held in Dallas, Texas, 1-4 October, 2000.
20. Wilkinson, W.M.: "Fracturing in Spraberry Reservoir, West Texas, Bulletin of the AAPG, Vol. 37, No. 2, February 1953, pp. 250-65.
21. Tyler, N. and Gholston, J.C.: "Heterogeneous Deep-Sea Fan Reservoir, Shackelford and Preston Waterflood Units, Spraberry Trend, West Texas," Report of Investigation No. 171, Bureau of Economic Geology, The University of Texas, Austin, 1988.
22. Baker, R.O. et al.: "An Integrated Fracture Characterization of a Heavy Oil Naturally Fractured Carbonate Reservoir," paper CIM 2001-13 presented Petroleum Society's Canadian International Petroleum Conference held in Calgary, June 12-14, 2001.
23. Olsson, O. et al: "Site Characterization and Validation, Stage 2 – Preliminary Predictions," Swedish Geological Co., Report ID No. 88.
24. Long, J.C.: "Construction of Equivalent Discontinuum Models for Fracture Hydrology," Lawrence Berkley Laboratory, Berkley, CA.
25. Epic Consulting Services Ltd.: "Analysis of E.T. O'Daniel Tracer Study: Spraberry Formation," correspondence with Pioneer Natural Resources USA, Inc., April 2001.
26. User Documentation, FracWorks/95, Discrete Fracture Network Simulator, Version 1.3, Golder Associates Inc., 1999.

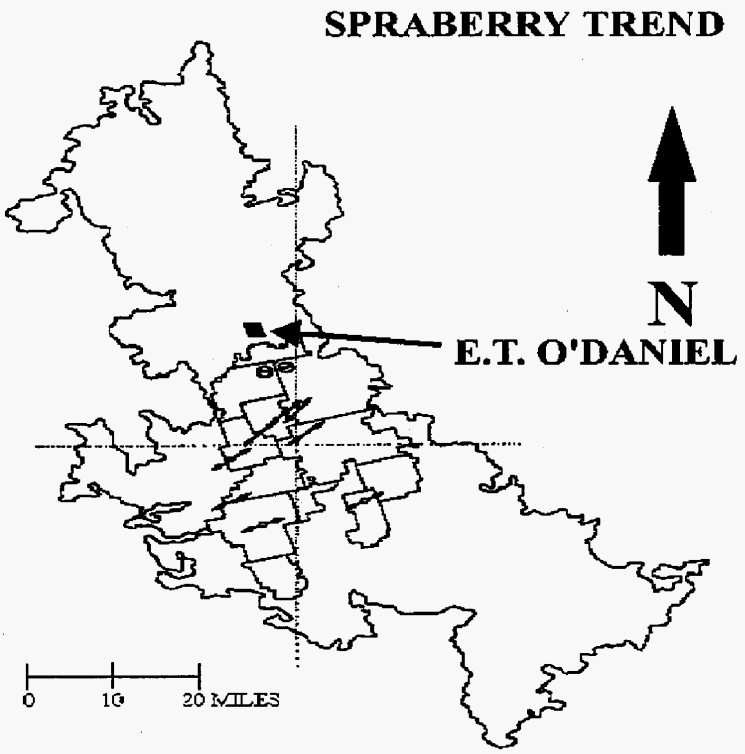

Fig. 2.1 – Map of Spraberry Trend illustrating location of the E.T. O'Daniel lease

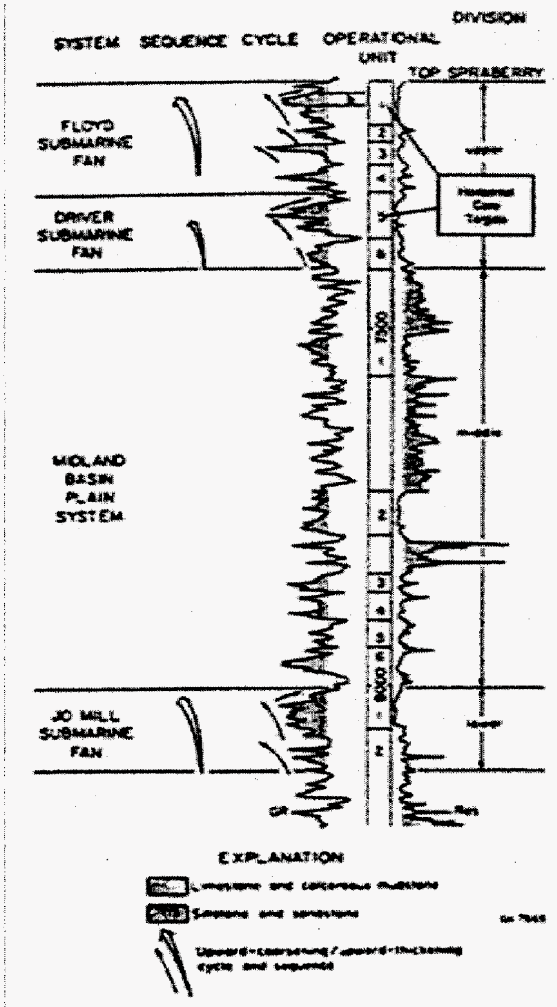

Fig. 2.2 – Division of Spraberry Formation in the central trend area, TXL Fee "B" No. 1 Well

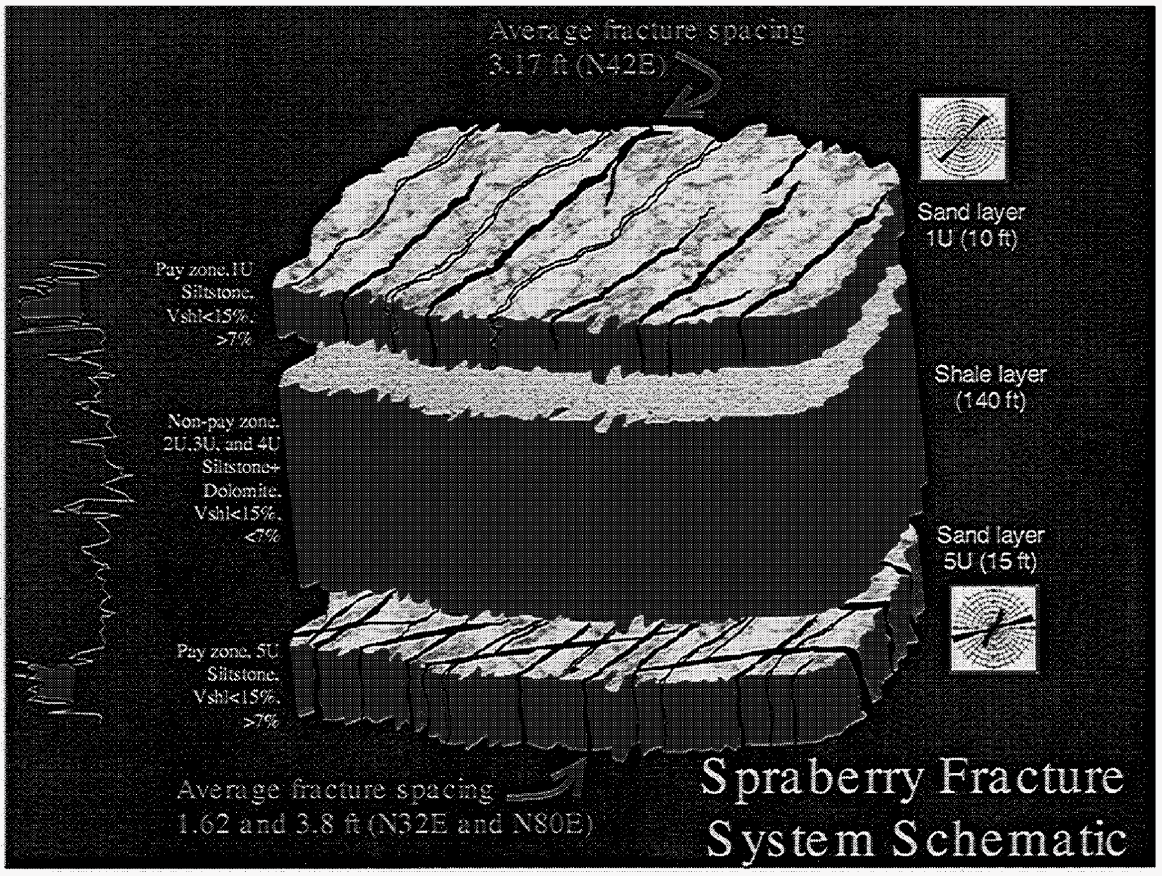

Fig. 2.3 – Schematic diagram of Spraberry fracture system.

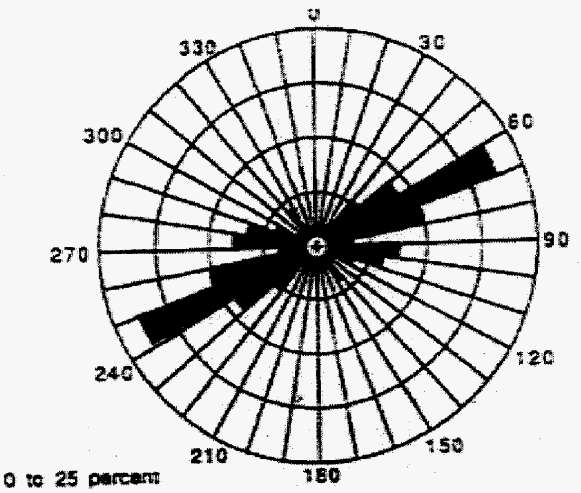

Fig. 2.4 – Azimuth of FMS Anomalies from Judkins A#5 and Preston #37 wells. This rose diagram indicates a conjugate fracture direction in the East-West direction.

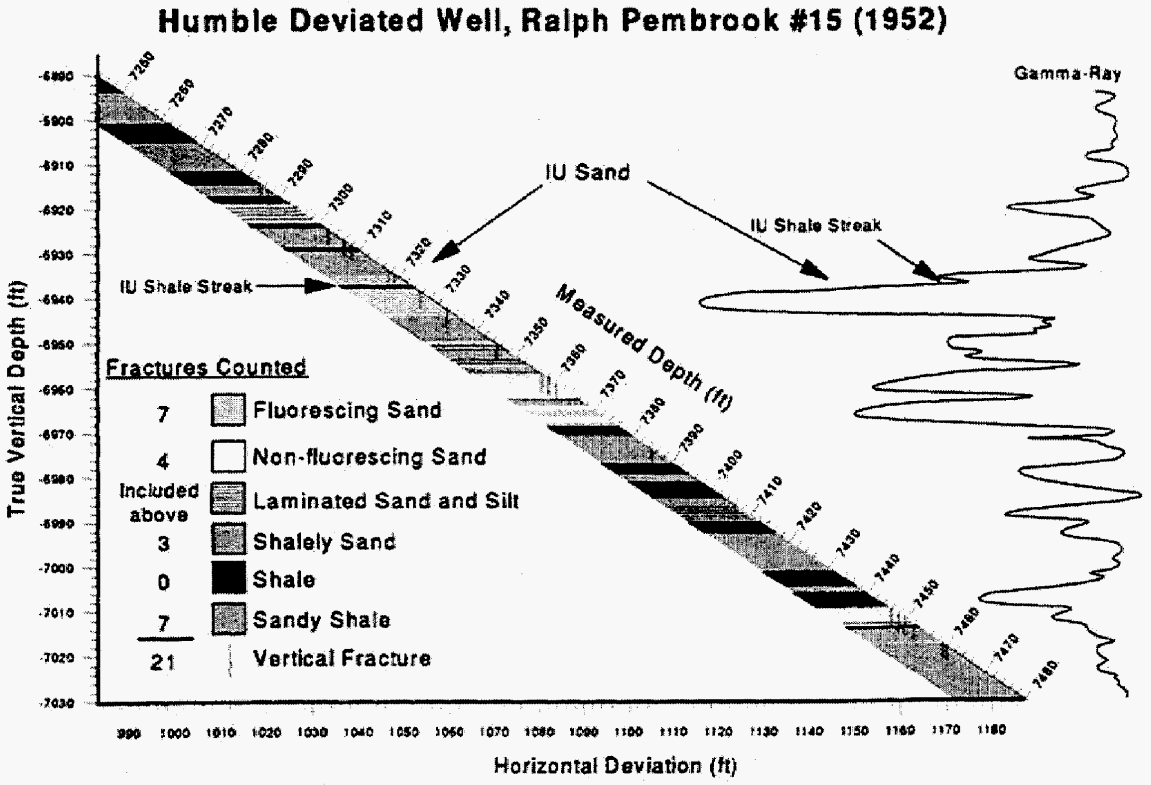

Fig. 2.5 – Humble deviated well showing fracture behavior and pattern.

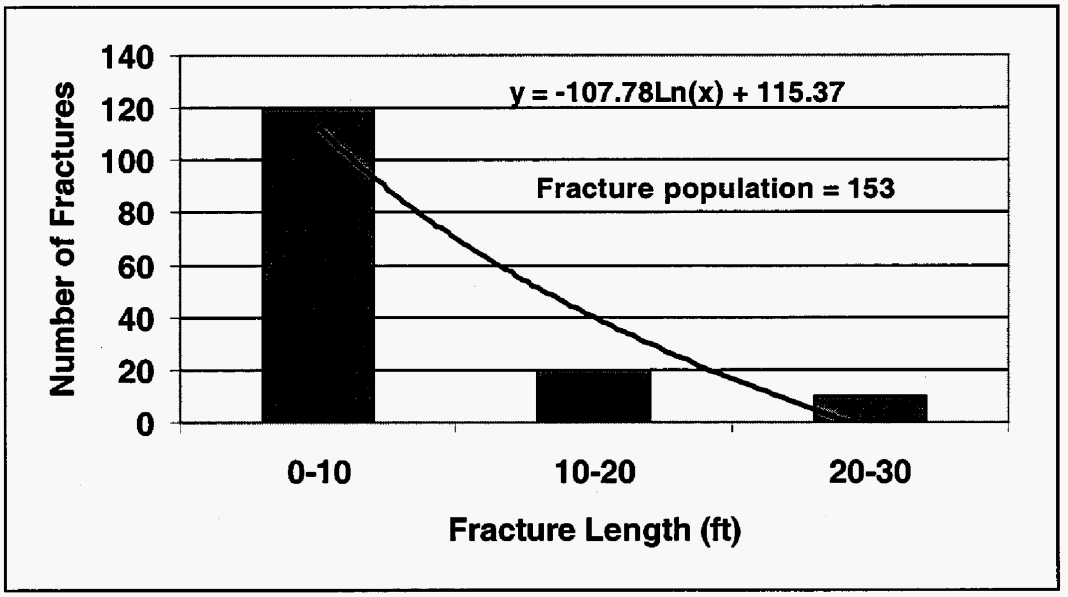

Fig. 2.6 – Fracture length frequency of Delaware outcrop data, West Texas

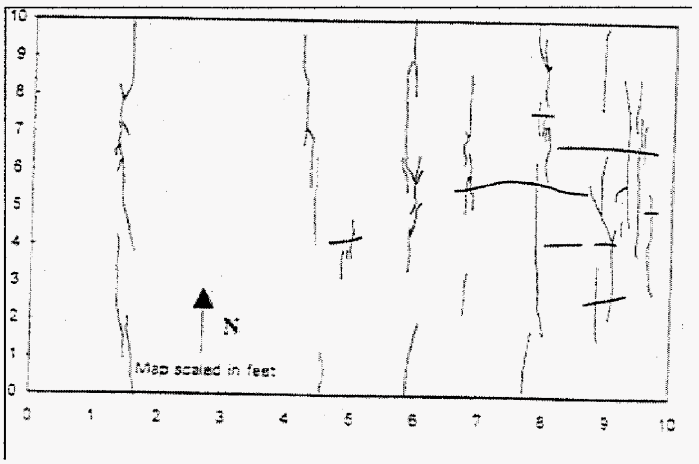

Fig. 2.7 – Fracture map of the Delaware outcrop data, West Texas.

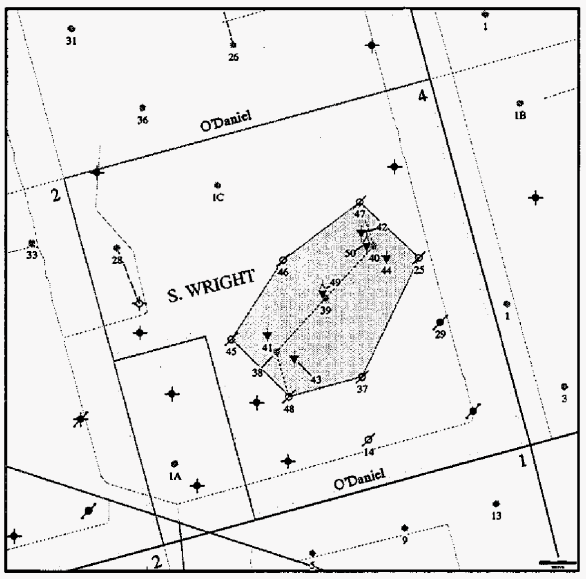

Fig. 2.8 – O'Daniel Interference Test; Wells 47,48,45 and 24 were injected into at high rates (2000 bbl/d) and wells 38,39,40,45 were observation wells; shaded pilot area is 67 acres in area

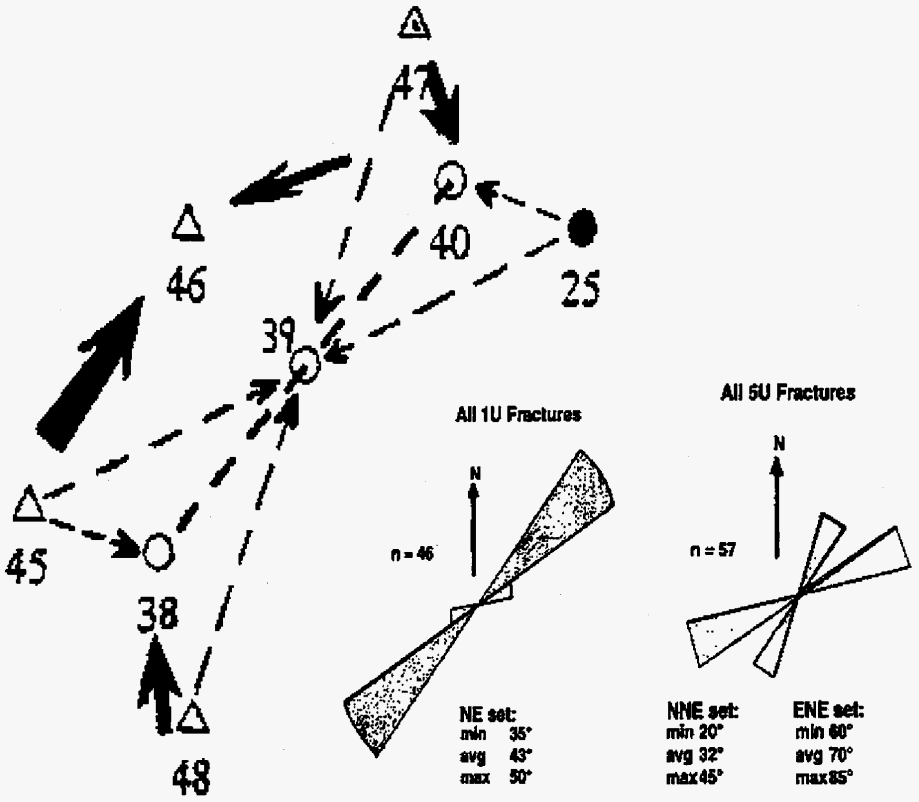

Fig. 2.9 – O'Daniel interference test map with arrows noting the strength of the response and horizontal well fracture (Rose Diagram)

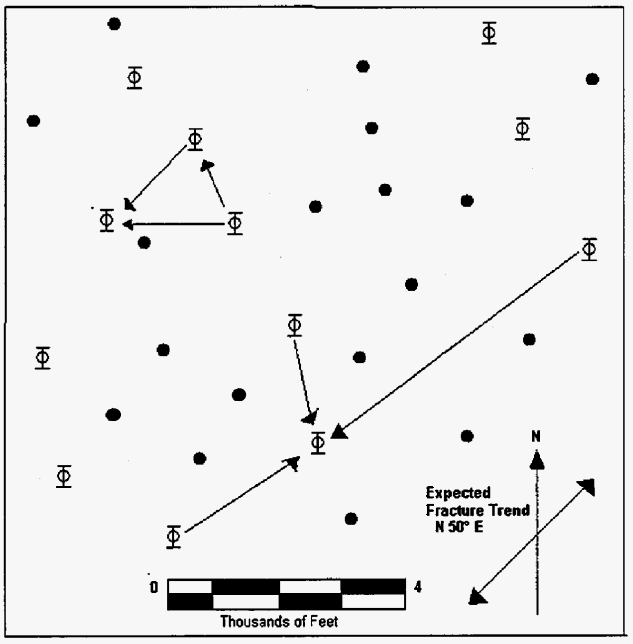

Fig. 2.10 – Humble interference test in Midkiff unit demonstrating the variability in direction of main fracture trend (NE and E-W) arrow indicate communication.

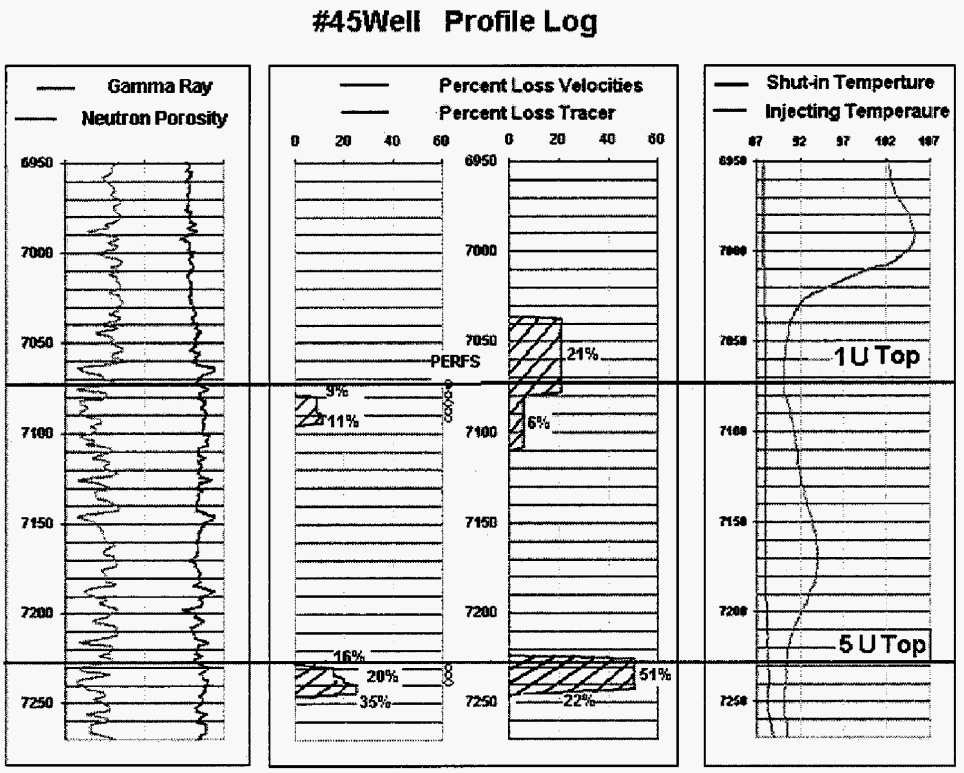

Fig. 2.11 – Injection profile log on Well 45.

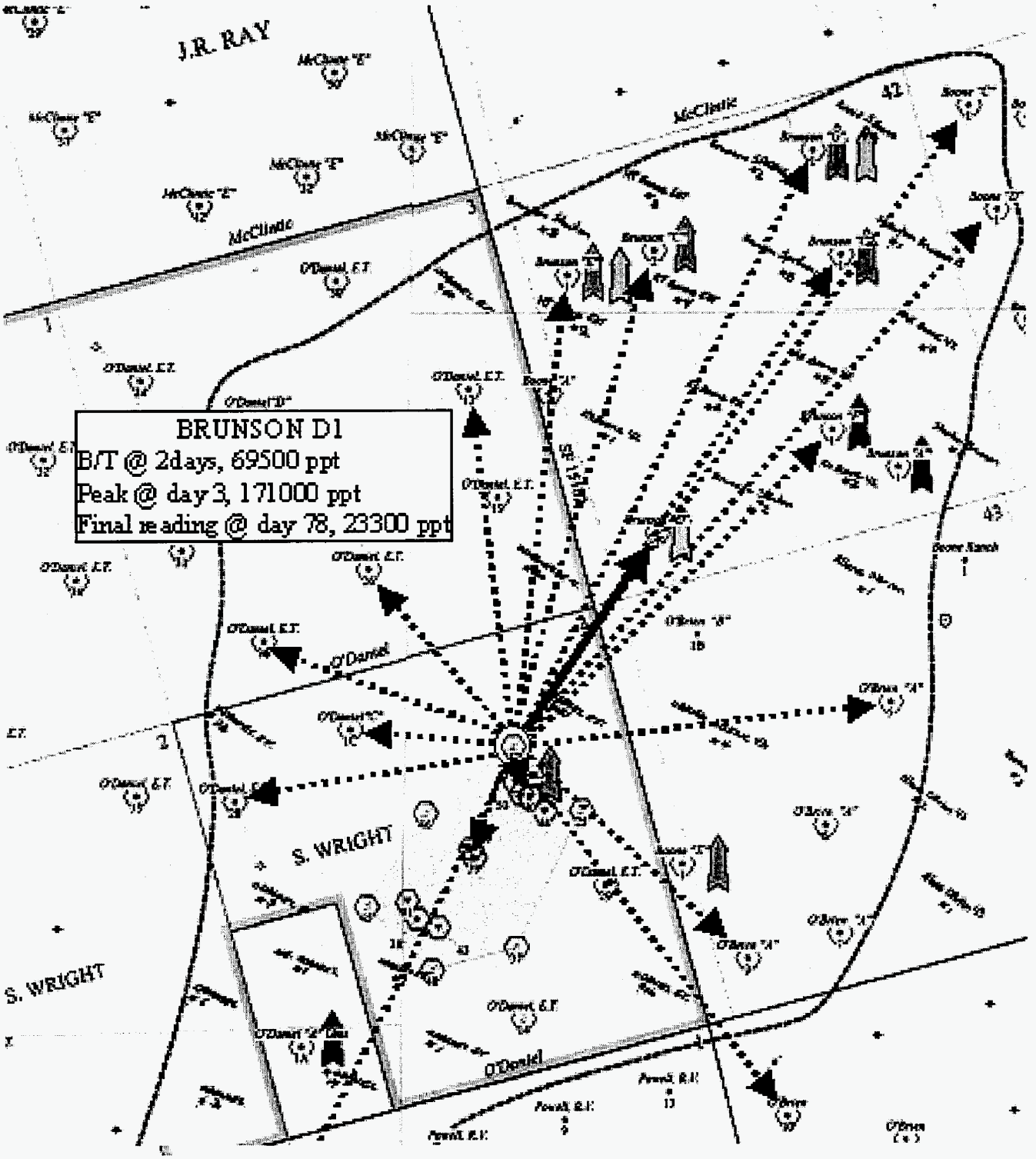

Fig. 2.12 – Fracture Pathways Inferred From Tracer Tests.

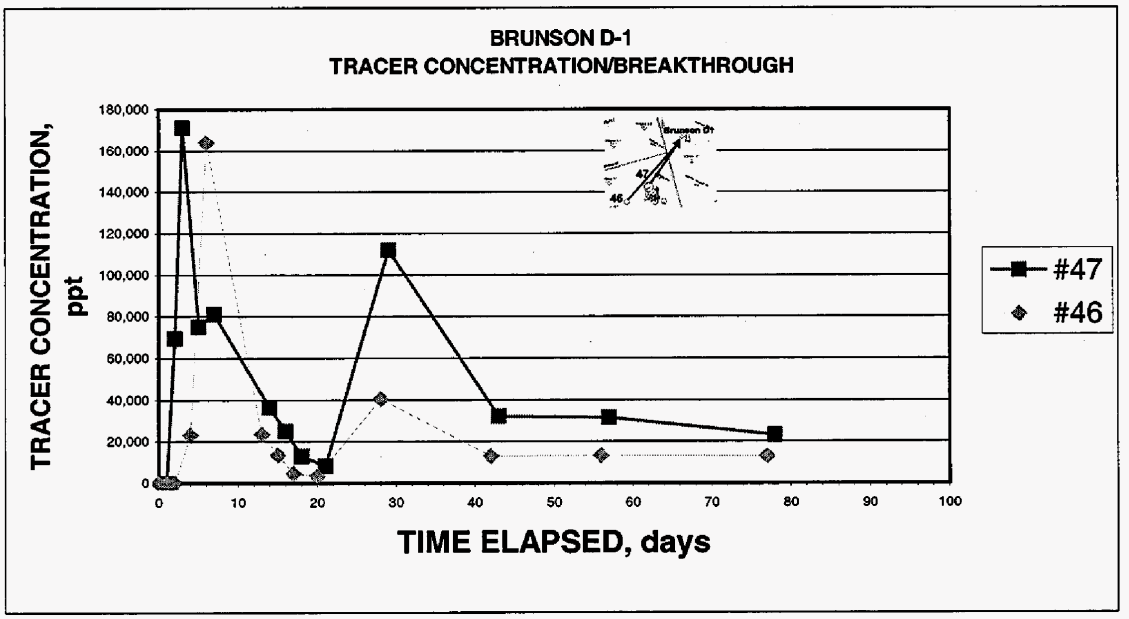

Fig. 2.13 – Brunson D1 tracer produced vs. time.

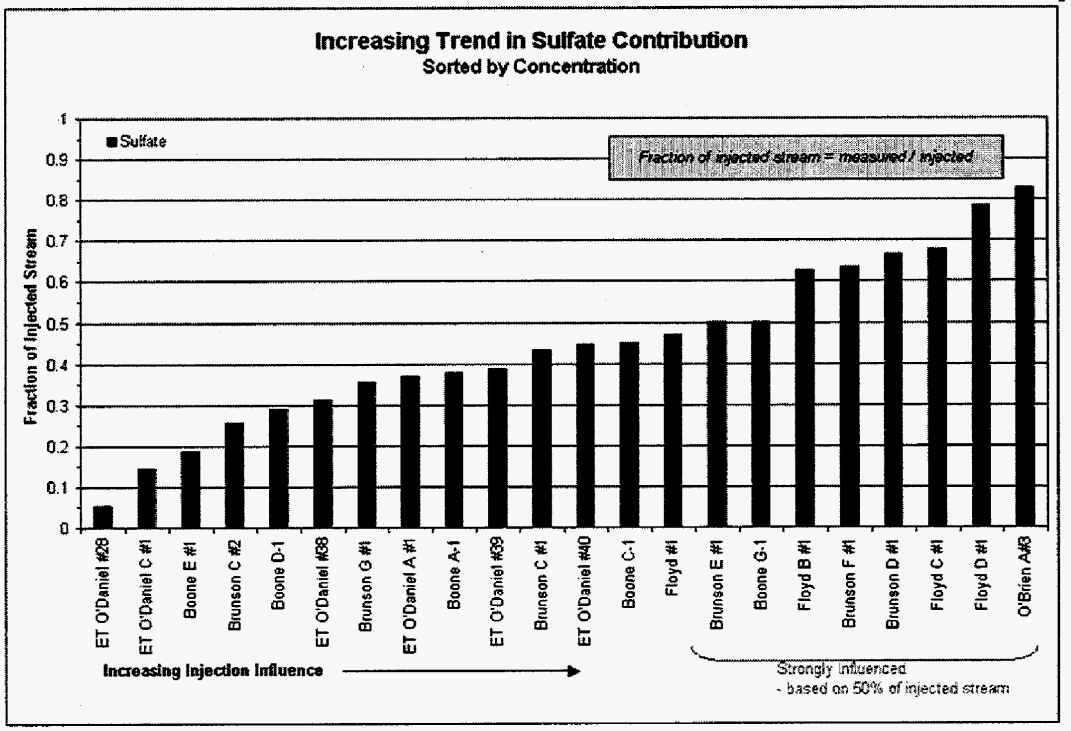

Fig. 2.14 – Fraction of Injected Stream Influencing Production Wells Based on Sulfate Sampled.

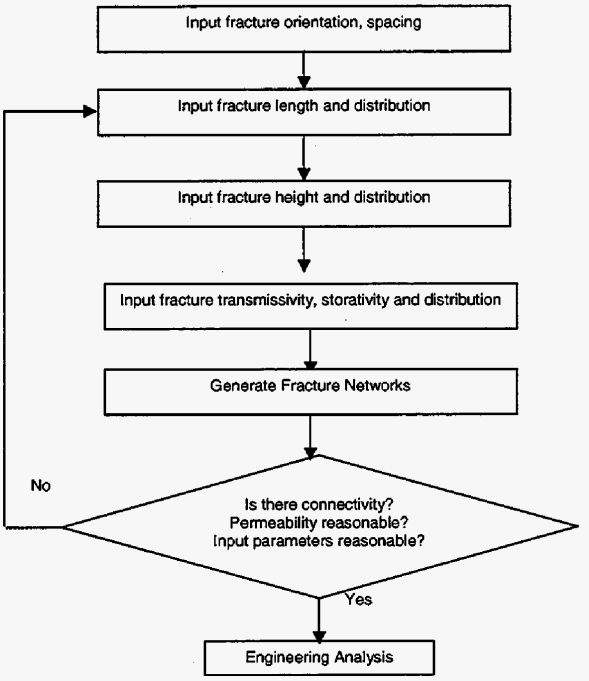

Fig. 2.15 – Steps Involved in Development of a DFN Model

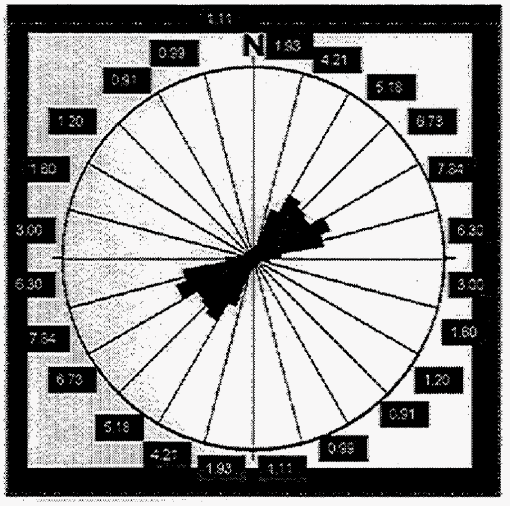

Fig. 2.16 – Calculation of Directional Permeability Using FRACMAN for Average Length = 100 ft, Height = 2ft, Transmissivity = 2 10^{-6} m^2/s (Using Fracture Orientations from 5U). Note k_{max}/k_{min} = 8.60.

Table 2.1 – Fracture characteristics and permeability contrast, Spraberry Trend area field.

	Fracture Trend	Ratio Permeabilities[b]	Avg. Deviation Calculated vs. Measured Pressures	Equivalent Permeability[a] (m/d f/t)
Midkiff Area				
Humble Water Flood	N50°E	144		
Pressure analysis (17 Wells)	N43°E	100 to 1000	78.4	443
North Driver Area				
Atlantic Water Flood[c]	N42°E	--		
Pressure Analysis (21 Wells)	N36°E	9	53.3	406
Pembrook Area				
Gas Injection test	N48°E	--		
Pressure Analysis (16 Wells)	N62°E	49	60.6	446
Aldwell Area				
Radioactive Gas Tracer	N53°E	approximately 16	--	
Driver Area				
Pressure Analysis				
55-Well Composite	N56°E	13	31.6	888
14-Well Davenport A Lease	N76°E	36	24.7	1130
15-Well Davenport B Lease	N52°E	6	28.4	965
13-Well X. B.Cox and J.C. Bryans Leases	N76°E	36	15.2	1020
12-Well C.J. Cox and T.X.L. Leases	N36°E	7	14.7	481

a. $h\sqrt{k_x ky}$

b. Ratio of permeability along major fracture trend to permeability perpendicular to fracture trend

c. Orientation determined by general pattern of reduction of gas-oil ratio and water breakthrough

Table 2.2 – Results of Sensitivity Runs; Effect of Different Fracture Aperture and Fracture Height (Using Fracture Orientations from 5U)

	Mean fracture height = 5 ft *Mean transmissivity = 0.40 10^{-7} m^2/s*		
Mean Fracture Length	10 ft	100 ft	500 ft
k_x *(md)*	0	0.22	0.50
k_y *(md)*	0	0.14	0.39
k_z *(md)*	0	0.01	0.13
	Mean fracture height = 5 ft Mean transmissivity = 1.00 10^{-5} m^2/s		
Mean Fracture Length	10 ft	100 ft	500 ft
k_x *(md)*	0	5.40	12.48
k_y *(md)*	0	3.47	9.63
k_z *(md)*	0	0.37	3.37
	Mean fracture height = 2 ft Mean transmissivity = 1.00 10^{-5} m^2/s		
Mean Fracture Length	10 ft	100 ft	500 ft
k_x *(md)*	0	3.00	4.47
k_y *(md)*	0	1.98	4.74
k_z *(md)*	0	0.07	0.07

3. Spraberry Reservoir Simulation Model

3.1 Introduction

Waterflooding in the Spraberry Trend Area has always been subject to discussion resulting from ambiguity of performance after waterflooding. In every case of water injection, wells far away from injection wells and located on-trend direction have responded favorably. This behavior did not follow the common waterflooding practice in naturally fractured reservoirs. The practice dictated that all water injection should be aligned along major fracture trends and production wells are located perpendicular to the injection wells (off-trend direction). The reason is to produce oil, which flows in a direction perpendicular to the fractured trend towards a line of production wells, from strongly water-wet rock by force imbibition and to avoid rapid water breakthrough in the production wells.

The behavior of well in the on-trend direction is investigated through the Humble waterflood performance. A five-spot pilot waterflood was initiated in March 1955 in the Midkiff Spraberry Unit. The Humble 80-acre pilot was completely confined with one center production well, Shb-9 and four injection wells, B-2, B-4, B-6 and B-10 as illustrated in Fig. 3.1. During the waterflooding process, extensive data was collected on the center production well as well as on 19 observation wells in the vicinity of the pilot.

The center well responded in a dramatic fashion with the oil production increasing from approximately 50 to 135 B/D. Production continued to increase and reached a maximum of 256 B/D during December 1955. During the time that there is a sharp increase in oil production, a larger pumping unit was installed. The installation of pumping during the water injection clearly obscures the interpretation since the dramatic increase in oil recovery was not by water injection alone. Because of this reason, water injection response on the center production well cannot be used as our waterflood interpretation. Meanwhile, the observation wells located in the vicinity of the pilot area demonstrated a response to water injection. Observation wells located on a northeast-southwest trend received production responses and also had water breakthrough, while wells located perpendicular to this trend demonstrated no response to water injection. To simplify the analysis, it was decided to use only two wells, injection well (Shb-10) and observation well (Shb-8), that demonstrated a good response to water injection with the following assumptions:

- Only two wells were included in the basic model, one is injector (SHB-10) and the other is producer (SHB-8) as shown in Humble Pilot map.
- The production well was located in the same line with injection well (in the on-trend direction).
- The response of oil production rate in the Shb-8 well was only affected by water injection from the Shb-10 well.

The distance between these two wells is 3465.4 ft with number of grid blocks of 25x25x3, which covers about 275 acre. All known reservoir characteristics have been done in the previous work as well as actual production and injection rates were included

in the reservoir model.[1,2] With this flood behavior as criterion for the analysis, the water breakthrough time, ratio of off-trend and on-trend fracture permeability, the proper size of simulation area and effect of fracture orientation on oil recovery were determined.

3.2 Matching Process

Provision was made to allow changes in the value of important variables such as the on-trend and off-trend fracture permeability values and the size of the reservoir model.

Even though the permeability was changed to very high number for both on trend and off trend directions and the grid blocks had been refined at the same size of model area, the water injection rate constraint cannot be maintained during the injection rate period. The water injection rate constraints were changed to the BHP constraints because the boundary created high-pressure build up in that confined area.

To compensate the problem, the reservoir model was increased to 3 times in x and y directions from the original model. The injection rate constraints were still shifted to BHP constraints, but it was only at later injection rate constraints period. Thus, the model was increased to 5 times original reservoir model. The simulation run was able to maintain the water injection rate constraints as shown from the simulation result in Fig. 3.2 and the oil production rate constraints as well (Fig. 3.3).

Figure 3.4 shows that the simulated BHP pressure can be maintained below 3000 psia when using a large simulation area of 6890 acre. This large area is used to take into account very high permeability in the on-trend direction and to avoid a pressure build up because of limited area. The work does not intend to match the observed bottom hole pressure (BHP) because it is a static bottom hole pressure while BHP obtained from the simulation is the flowing bottom hole pressure. However, the observed bottom hole pressure is useful to give a BHP range of values for our simulation result.

Constant production and injection rates were used as simulation constraints during the simulation run. The fracture permeability values in the on-trend and off-trend directions were altered until the best matches were obtained. The fracture permeability values in the on-trend and off-trend directions are determined to be approximately 15000 and 100 md with the ratio of fracture permeability of 150:1. This ratio of fracture permeability is almost similar to the ratio permeability obtained from the previous study.[3,4] Figure 3.5 compares the observed water cut with the water cut obtained from the simulation result. A satisfactory match of water breakthrough time was achieved. From the magnitude of on-trend and off-trend fracture permeability, the values indicate that the permeability is highly anisotropy and the sweep area forms elongated ellipse trending in the major fracture trend.

3.3 Sensitivity Analysis

Because the fracture permeability is high only in y-direction, the grid blocks in the x-direction were optimized. After grid blocks in the x-direction were changed several times by keeping similar grid block in y-direction, we finally obtained at least 50 grid blocks

needed in x- direction. Thus, to properly simulate the two wells that has area of 275-acre we need at least 50 and 125 grid blocks in x- and y- directions, respectively, which covers simulation area of 2756 acre (Fig. 3.6).

The well performances of using 25 x 25 grid blocks are shown in Fig. 3.7. The peak water cut cannot be matched because the bottom hole pressure has reached the pressure limit of 3200 psi, which corresponds to the fracturing pressure. Thus, the simulator automatically reduces the given injection rates to maintain the bottom hole pressure below the fracturing pressure.

The next sensitivity study was conducted on altering fracture permeability. This study was conducted to see the effect of altering this parameter on well performance. Two simulation cases were conducted as follows,
Case 1: Kfx = 10 md and Kfy = 1500 md
Case 2: Kfx = 100 md and Kfy = 20000 md

The well responses were compared to the matched parameter. Herein we called it the base case (Kfx = 100 md and Kfy = 15000 md). The results are presented on Fig. 3.8. The fracture permeabilities in both x- and y- directions (Case 1) are one-tenth the permeability of the base case. Reducing the fracture permeabilities in both directions cause the reservoir to become less permeable causing lower injectivity. Due to lower injectivity, the simulator increases reservoir pressure as well as bottom hole pressure to maintain the constant production rates. However, the reservoir pressure is limited to the fracturing pressure of 3200 psi, therefore, the simulator cuts water injection rate constraints to maintain the pressure bellow the fracture pressure. The result also shows that the water cut response in Case 1 is faster than that in the base case due to lower fracture permeability in x-direction. In Case 2, the permeability in y-direction was changed to higher number (20000 md), and the permeability in x-direction was kept a similar value. The permeability change causes the water cut response is faster than that in the base case. The higher permeability yields faster water cut response in the production well.

Six wells with different orientations were included in the model that had matched parameters to simulate the effect of different fracture orientation on oil recovery during high water injection rate of 1000 STB/D. The six different orientations are 0, 18, 36, 54, 72 and 90 degrees, respectively. All the wells have similar distance to the injection well. The well located at 0 degree is the on-trend well, which is parallel (the same fracture line) to the injection well. Meanwhile the well located at 90 degree is the off-trend well, which is perpendicular to the injection well. The wells were produced with constant flowing pressure of 2000 psi for 15 years. The simulation results are presented in Fig. 3.9.

After injecting water for 2 years, the on-trend well had the highest cumulative oil production, because this well had the fastest response to water injection (co-current). However, this well simultaneously produces a high water production rate that significantly reduces the oil production rate. The wells located at 18 and 36 degrees have favored of slowing water production rate in both counter-current and co-current

imbibitions. Therefore, the cumulative oil productions from those wells are much higher than that produced from the on-trend well after 2 years producing time. Even though the wells are located at higher than 36 degrees from the fracture trend, they have favored both counter-current and co-current imbibitions. However, the response on water injection rate takes very long time. The off-trend well has the same cumulative production as the on-trend wells at about 13^{th} year. The long time response of production wells due to water injection remains uneconomic in the life span of waterflood project.

3.4 Conclusions

1. Because of high permeability in the on-trend direction, the size of the simulation area must be large enough to avoid a pressure buildup in the confined area.
2. The fracture permeability values in the on-trend and off-trend directions of 15000 and 100 md, respectively, indicate that the reservoir permeability is highly anisotropy.
3. It is recommended to place the production wells between 0 and 36 degrees relative to fracture trend to have efficient waterflood response.

3.5 References

1. Schechter, D.S., McDonald, P., Sheffield, T., Baker, R.O.: "Integration of Laboratory and Field Data for Development of CO2 pilot in the Naturally Fractured Spraberry Trend," paper SPE 36657 presented at the 1996 SPE Annual Technical Conference and Exhibition, Denver, Colorado, 6-9 October.
2. Putra, E. and Schechter, D.S.: "Reservoir Simulation of Waterflood Pilot in Naturally Fractured Spraberry Trend Area," paper SPE 54336 presented at the 1999 SPE Asia Pacific Oil and Gas Conference and Exhibition, Jakarta, Indonesia, 20-22 April.
3. Barfield, E.C., Jordan, J.K., and Moore, W.D.: "An Analysis of Large-Scale Flooding in the Fractured Spraberry Trend Area Reservoir," *JPT* (1959), Vol.11, No. 4, p.15-19.
4. Elkins, L.F., and Skov, A.M.: "Determination of Fracture Orientation from Pressure Interference," *Trans.* AIME (1960), Vol. 219, p.301-304.

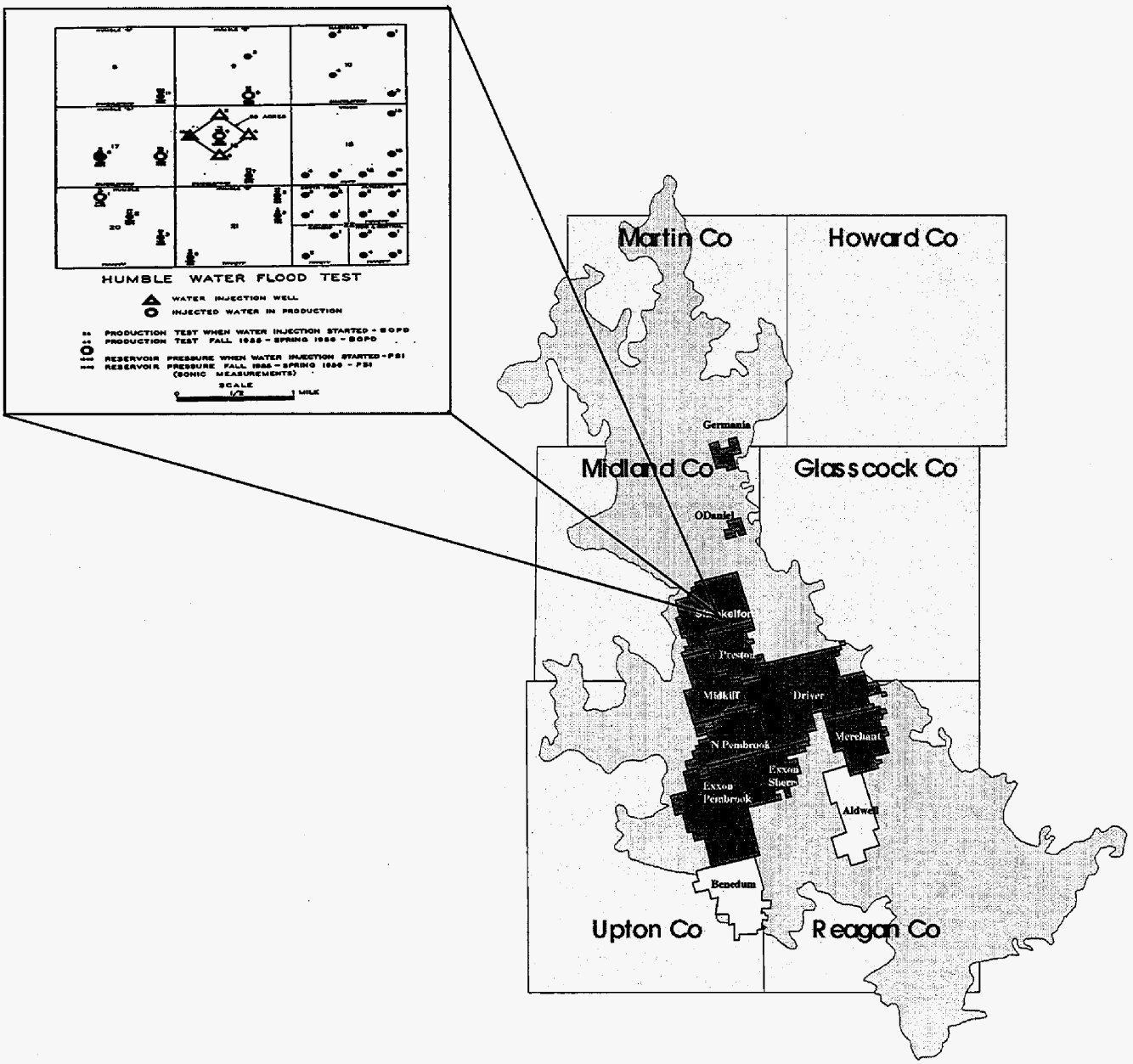

Fig. 3.1 – The Spraberry map shows the location of the Humble waterflood pilot.

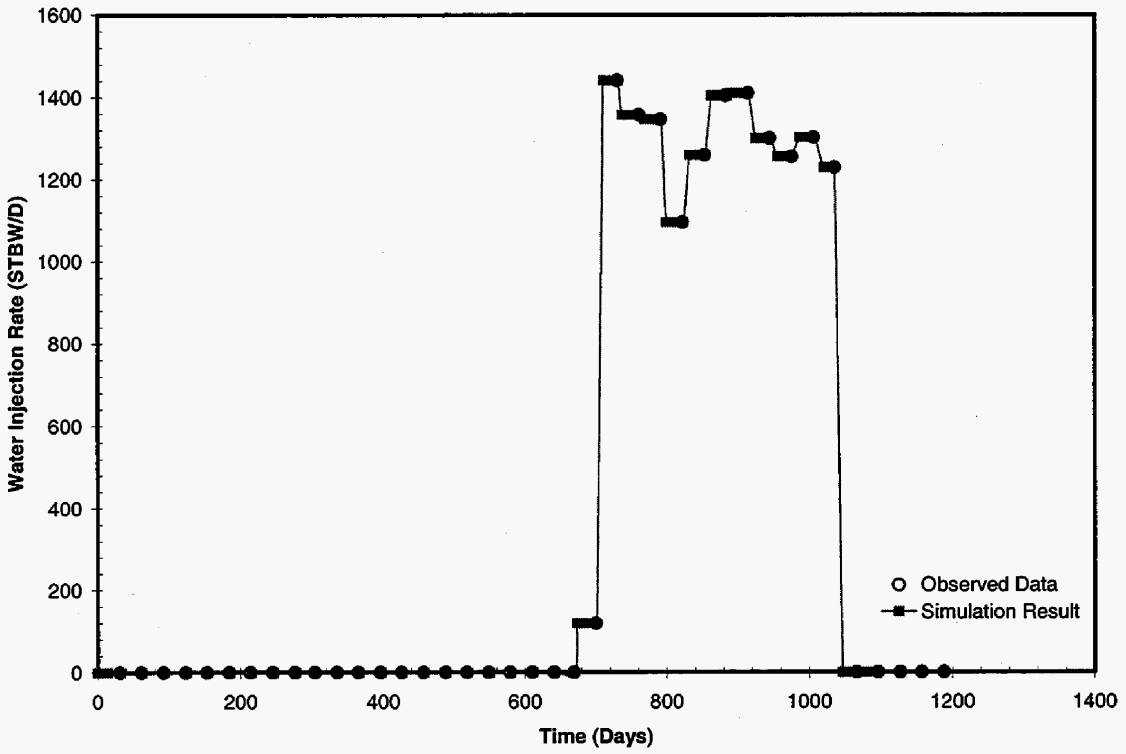

Fig. 3.2 – Comparison between observed water injection rate and simulation result.

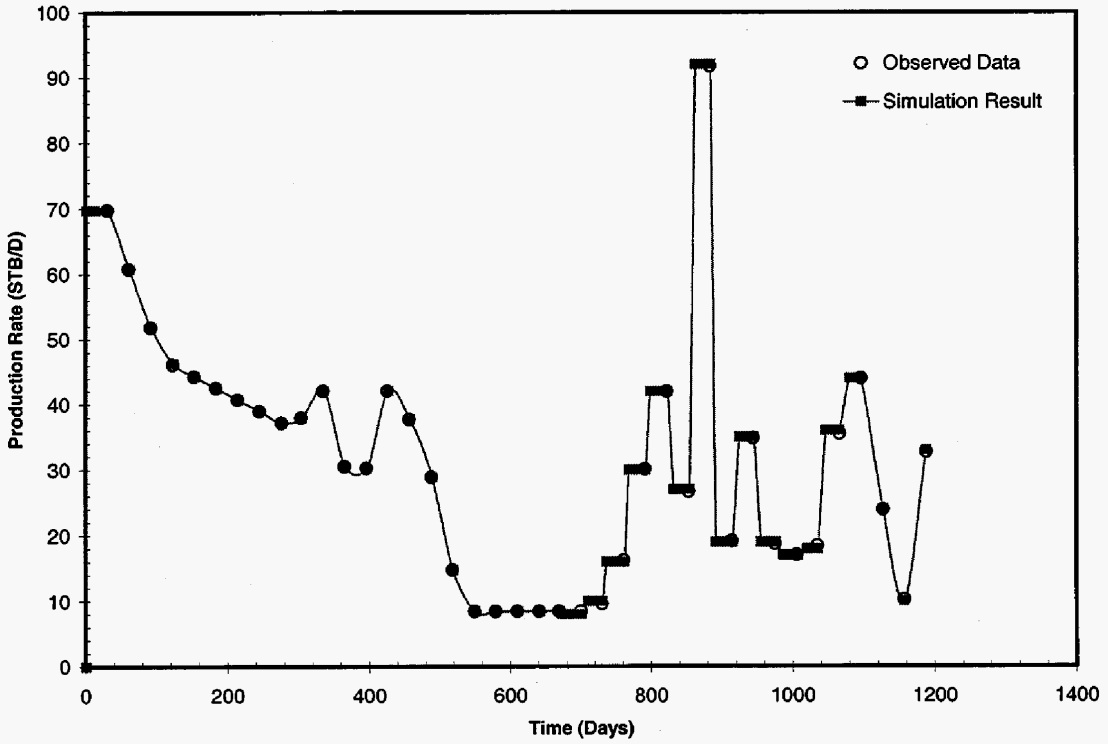

Fig. 3.3 – Comparison between observed oil production rate and simulation result.

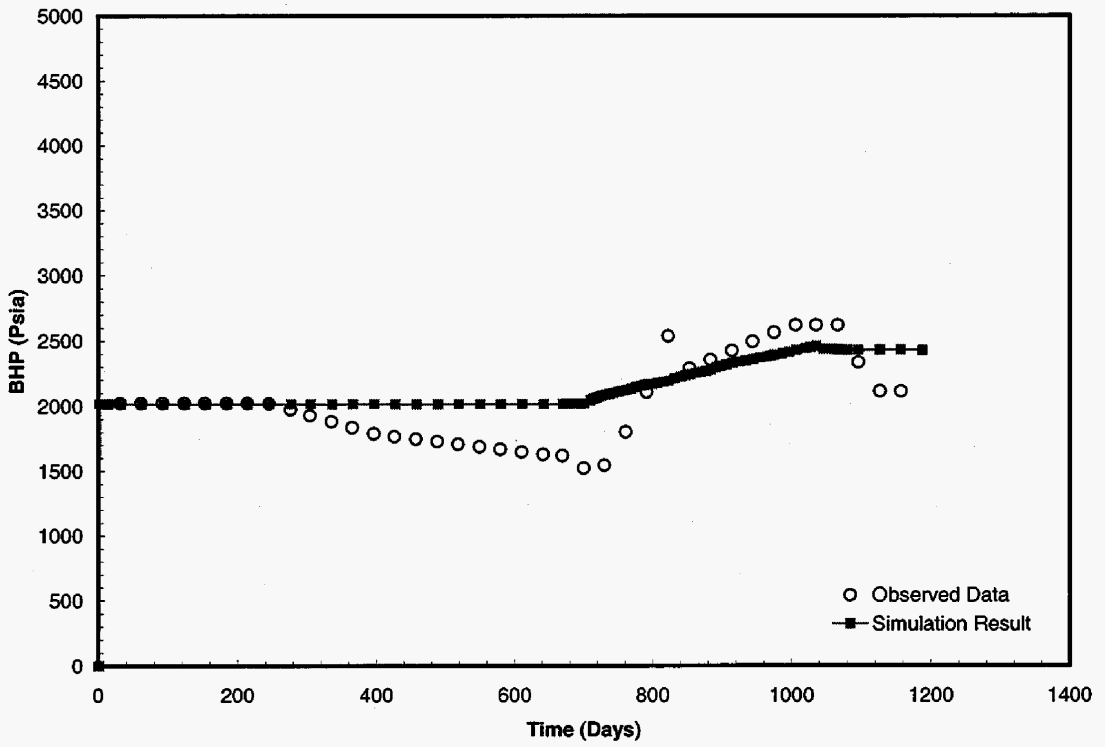

Fig. 3.4 – Comparison between observed bottom hole pressure (BHP) and simulation result.

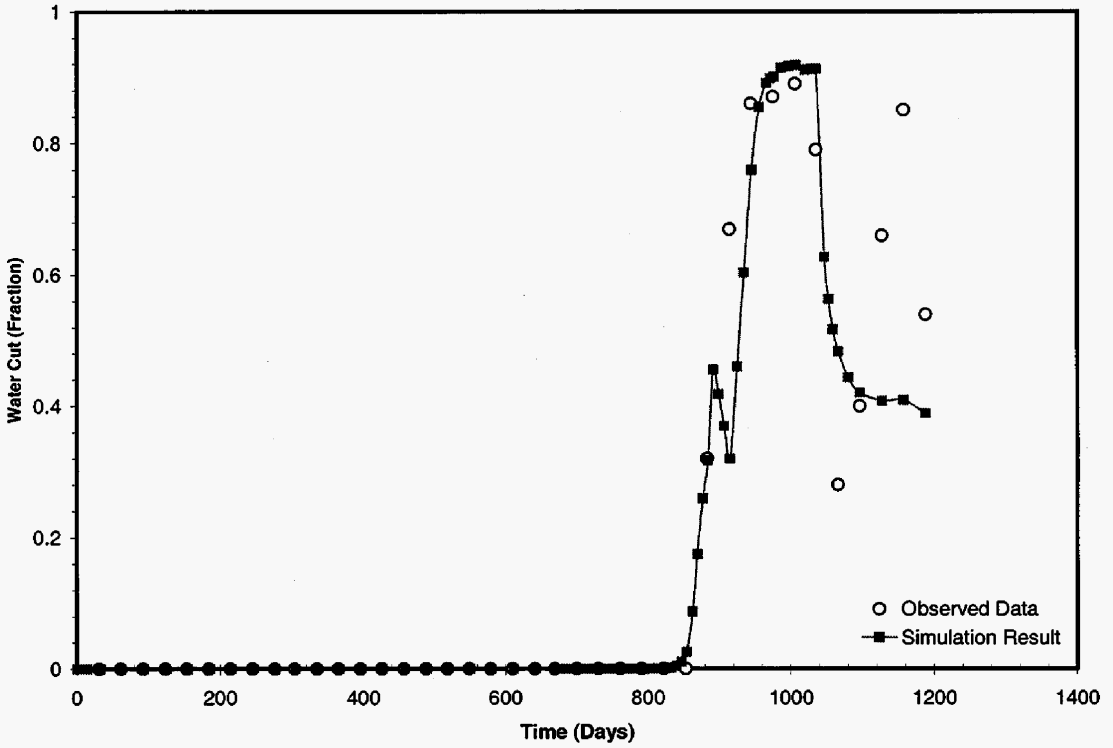

Fig. 3.5 – Match between observed water cut and simulation result.

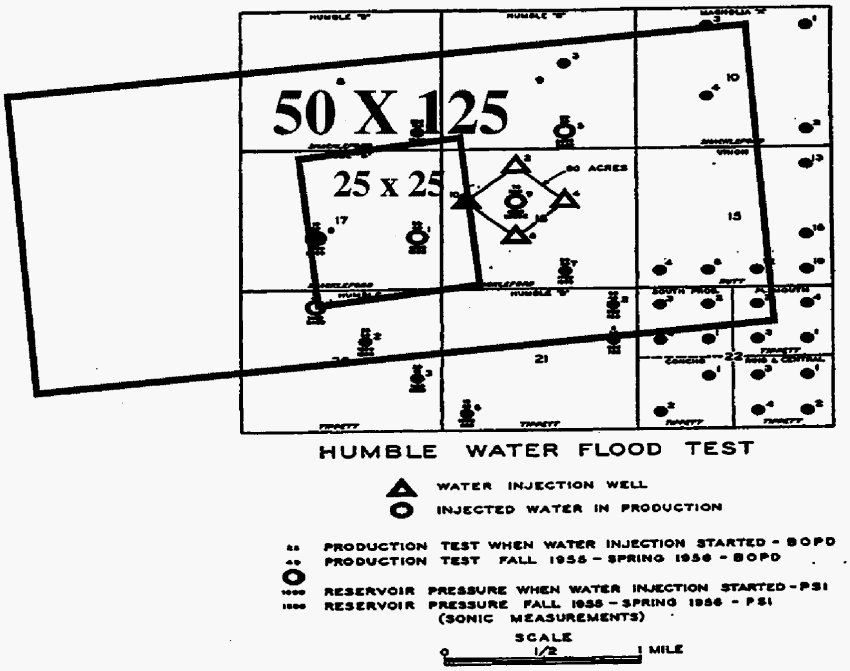

Fig. 3.6 – Effect of reservoir size on simulating two wells in Humble waterflood pilot.

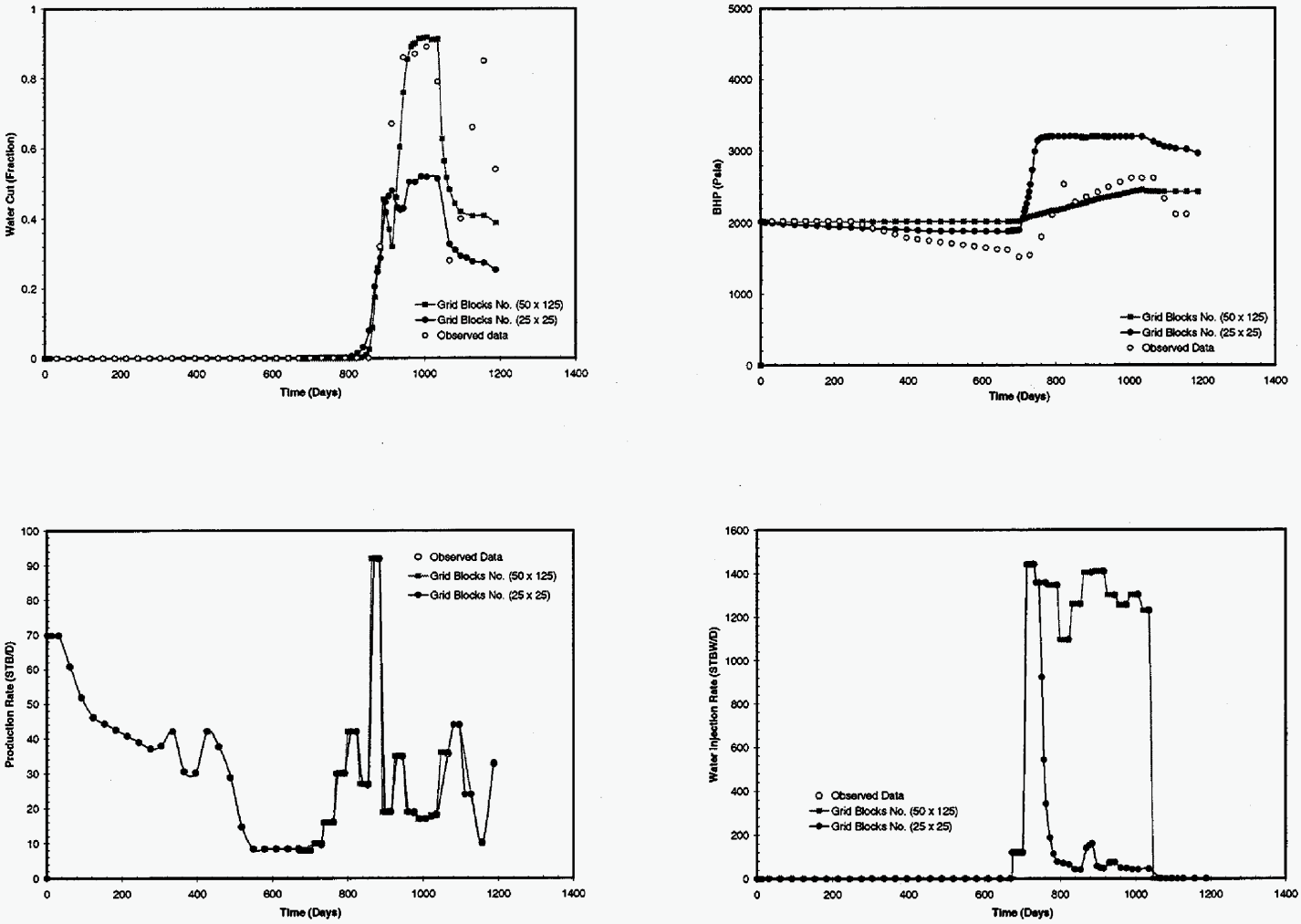

Fig. 3.7 – Effect of reservoir size on well performance during high water injection rate.

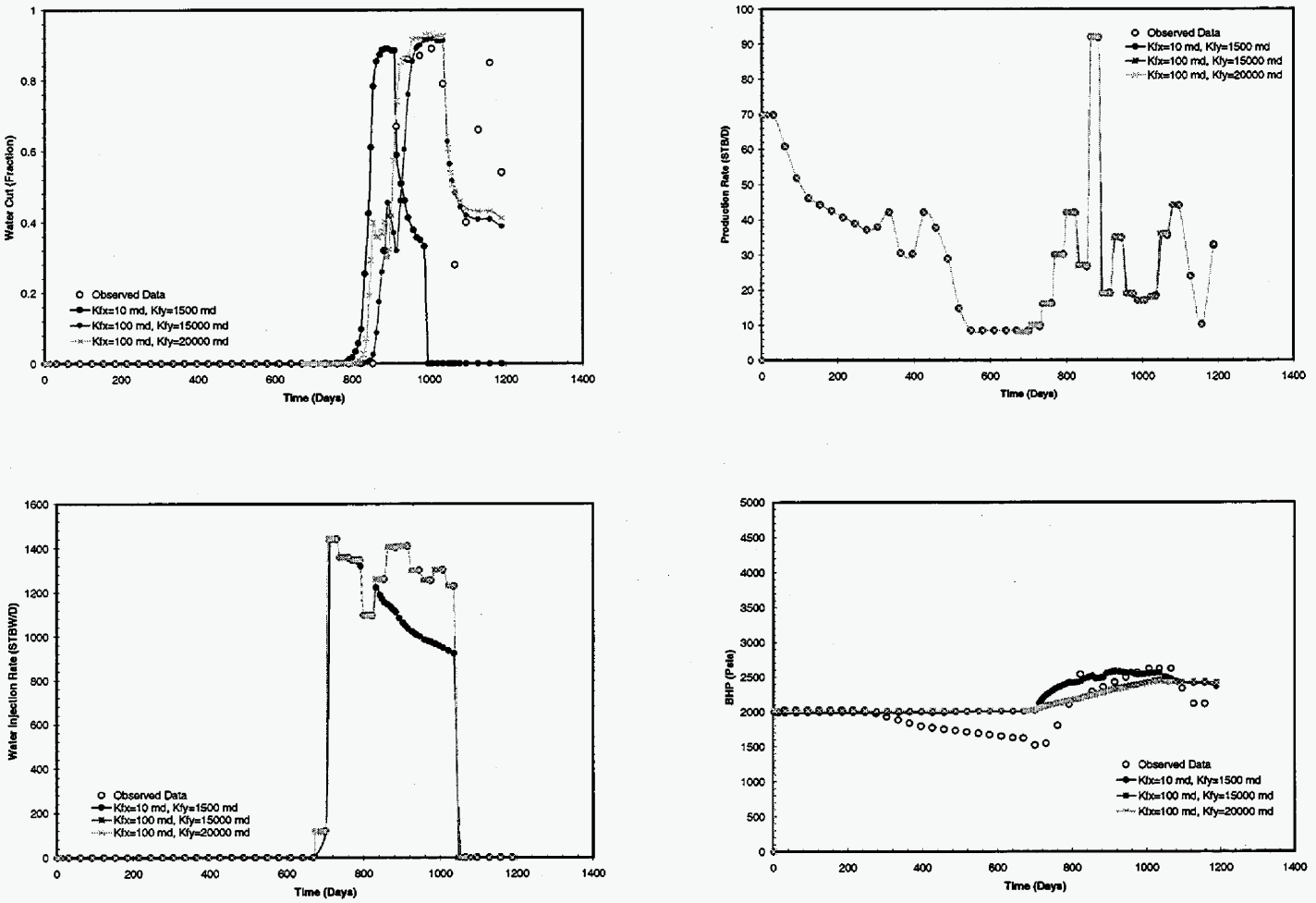

Fig. 3.8 - Effect of fracture permeability on well performance during high water injection rate.

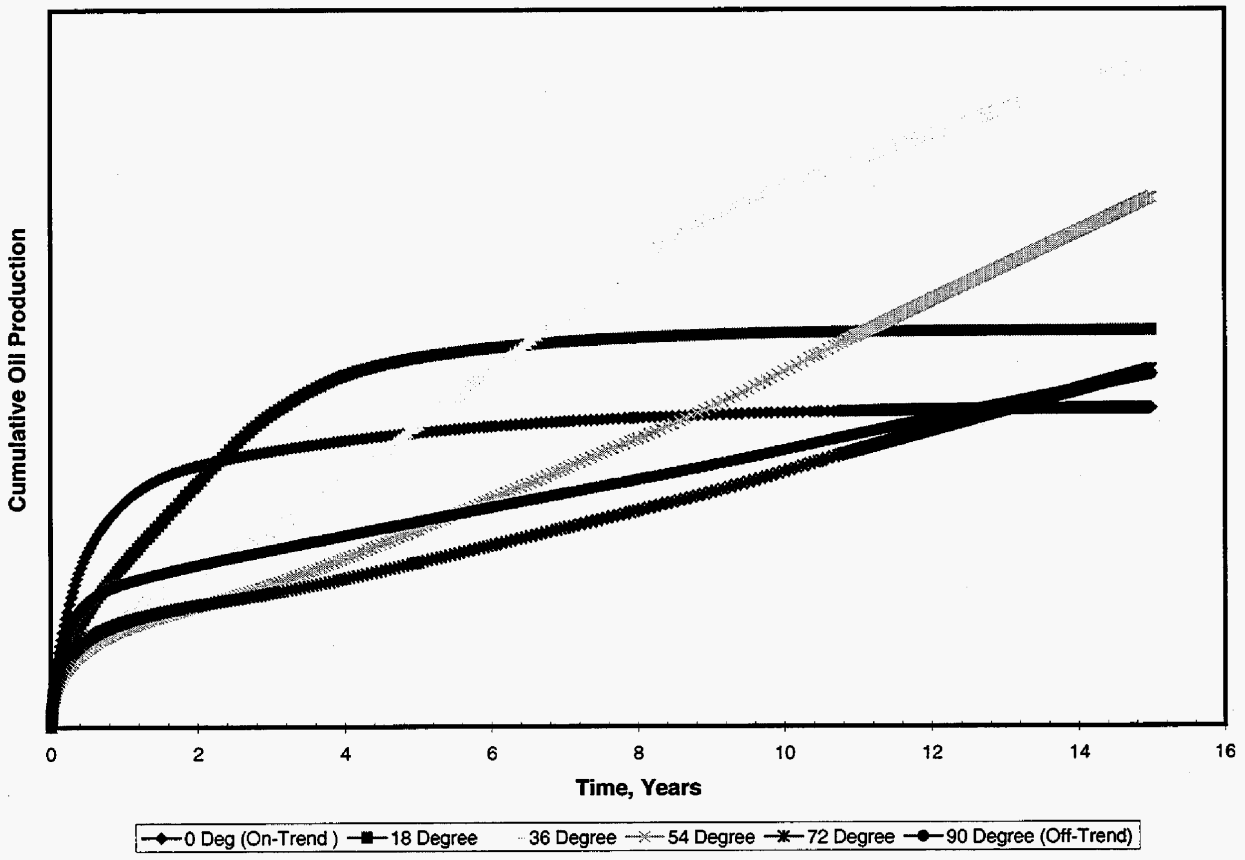

Fig. 3.9 - Effect of different well orientation on oil recovery during high water injection rate.

4. Simulation of Tracer Response in E.T O'Daniel Pilot Area

4.1 Introduction

Six water phase inter-well tracers were injected into the six ring fence wells of the E. T. O'Daniel Lease in the middle of Aug. 2000. The injection schedule is shown in Table 4.1. Analysis was performed on the collected water samples from the twenty-nine producing wells in the O'Daniel Tracer Program. The result of the tracer program is presented in Fig. 4.1. The analysis indicates that tracer has arrived at twenty-seven of the twenty-nine producing wells. The result shows that there are four tracer concentrations near or exceeding 100,000 ppt in observation wells due to tracer injection, which are:

1. WIW #47 to Brunson D-1
2. WIW #46 to Brunson D-1
3. WIW #48 to O'Daniel A-1
4. WIW #45 to Pilot Well #38

The remaining wells have only shown weak tracer response or the tracer wave is just beginning to arrive at the well. In the three wells with high peak tracer concentration, tracer shows up in a few days after tracer injection. Tracer breakthrough in this short time is usually indicative of communication in the reservoir via isolated natural fractures or extremely high permeability, thin intervals. The breakthrough time and the peak concentration are presented in Table 4.2. From the tracer test analysis it is observed that the wells mentioned above have a very high velocity of tracer transport, which is presented in Table 4.3. These wells, which are very far from the injection wells, are subject to very fast breakthrough because of this extremely high tracer velocity. So it is assumed that there is a very high permeability path between each pairs of injection and production wells.

4.2 Analyzing the Tracer Response

A simple two well simulation model is chosen to analyze the tracer test. First an optimum number of grid blocks were selected by performing a grid sensitivity analysis. Then the sensitivity analysis was performed to obtain the ranges where the match might exist. The results found during a previous simulation (the Humble Pilot simulation) were used as a basis to start the sensitivity analysis.[1] The process of matching the simulation results with the observed data began after getting a good understanding of the model with the help of sensitivity results.

It is observed that there are several peak concentrations in the inter-well tracer response between the injection well WIW#47 and the production well O'Daniel D-1. Fig. 4.2a shows a typical tracer response curve. The observed data of WIW#47 to O'Daniel D-1 is shown in Fig. 4.2b. With this simulation model only the first peak of Fig. 4.2b was matched because different simulation models are necessary to match the second and all other successive peaks in the observed data. It is assumed that all the successive peaks are

due to the contribution of tracer from the secondary fracture trend i.e. from different fracture sets.

4.3 Simulation Model

The behavior of naturally fractured reservoirs is considerably different from conventional reservoirs. This difference arises from the existence of two interconnecting paths for fluid flow having totally different properties, which communicate with each other. The tracer test was performed and analyzed to understand the fracture system of the naturally fractured Spraberry Trend Area. To simplify the analysis a two well model was chosen with one injection well (O'Daniel#47) and one observation well (Brunson D-1). The two wells have a very good inter-well tracer response indicative of a continuous fracture path. The model is shown in Fig. 4.3.

The distance between these two wells is 3200 ft. The size of the model is 100x100x3 grid, which covers some 602 acre area. Of these three layers only the first and the third layers are pay layers. The model is assumed to have dual porosity behavior. The size of each grid block is 51.2 ft. The rock, fluid properties and reservoir characteristic data were taken from the Humble pilot. Actual injection rate, tracer concentration and the duration of tracer injection were used in this simplified model. Finally a model of 100x100 grid size was chosen with 3 layers.

4.3.1 Sensitivity Analysis

The 602 acre model has 5120 ft in both x and y directions. Grid block sensitivity was performed in this area with 55x55, 100x100 and 150x150 grid sizes. For a fixed orientation and a given on-trend and off-trend permeability, it is observed that a model with 100x100 grid gives a similar response to a model with 150x150 grid as shown in Fig. 4.4. So, to optimize the simulation run time the model with 100x100 grid was utilized for history matching the tracer test.

The grid orientation effect on the tracer response was analyzed by varying the on-trend and off-trend permeability for different orientations. When the grid is oriented at 33°, which makes the injection well in the on-trend direction towards the production well, there is no significant effect of the off-trend permeability (K_x) on the tracer response from the production well. Tracer response from this on-trend production well will be very much affected if the on-trend permeability (K_y) is varied. An increase in K_y gives a faster breakthrough (Fig. 4.5) and higher peak concentration (Fig. 4.6). If the grid is rotated so that the production well D-1 becomes 43° off-trend from the injection well O'Daniel#47, then the off-trend permeability K_x should have a significant effect on the tracer response. For the off-trend well, an increase in K_x gives a faster breakthrough (Fig. 4.7) and a higher peak concentration (Fig. 4.8). The production well in the off-trend direction (43° for this case) will also be affected by the on-trend permeability. This is observed in Fig. 4.5, where an increase in K_y gives a faster breakthrough. When K_y is increased, unlike the on-trend well, the off trend well experiences a decrease in the peak tracer concentration (Fig. 4.6). When K_y is increased, much tracer goes to the on-trend direction relative off-

trend. This will reduce the amount of tracer reaching the off-trend production well. If the production well is located further from the off-trend direction then the tracer breakthrough is delayed and the concentration becomes very small.

4.3.2 Matching

After performing the sensitivity analysis the reservoir parameters, such as on-trend, off-trend permeability and fracture orientation, were identified. The effect of these parameters on the tracer performance (breakthrough time and peak concentration) gives us guidance towards the matching process.

The variables used for the matching process are: 1) on-trend, off-trend permeability and 2) fracture orientation. During the simulation runs, tracer was injected into the O'Daniel#47 at a constant rate, with a tracer concentration of 158.9 ppm for 11.67 hours. Different simulation runs were performed for various orientations starting from the on-trend to farther off-trend directions. The permeability values in the on-trend and off-trend directions were changed for each orientation to match the observed data. In the best-fit match, the on-trend and off-trend permeability were found to be 15000 md and 84 md. This result is very close to that of the Humble Pilot simulation[1] where the permeability was 15000 and 100 md in the on-trend and off-trend directions respectively. The comparison between the observed data and simulation result is shown in Fig. 4.9. A very satisfactory match was found for the breakthrough time, the peak concentration and the width of the tracer performance plot.

Furthermore, the best match for fracture orientation was N43°E which is the average fracture orientation measured for horizontal core taken in the O'Daniel area.[2,3] Thus, the tracer results confirm the NE-SW fracture set in the 1U pay zone is responsible for tracer breakthrough in the Brunson D-1.

4.5 Conclusions

1. The fracture permeability values in the on-trend and off-trend directions were found to be 15000 and 84 md respectively. This result confirms the reservoir permeability is highly anisotropy.
2. The on-trend and off-trend permeability obtained in this study is very close to the values obtained for a history match of water in the Humble Pilot simulation[1] where the result was 15000 and 100 md in the on-trend and off-trend directions respectively.
3. A finite difference, dual porosity simulation indicates the primary fracture orientation is N43°E similar with the average orientation obtained from natural fracture counts in horizontal core acquired in a near-by well.[2,3]
4. The off-trend permeability has no significant effect on tracer response in production wells that are located along the on-trend fracture orientation.
5. Increasing the permeability in the simulation for on-trend orientation will reduce the tracer concentration in the off-trend production wells.

4.6 References

1. Schechter, D.S: "Advanced Reservoir Characterization and Evaluation of CO2 Gravity Drainage in the Naturally Fractured Spraberry Trend Area," First Quarterly Technical Progress Report, 2001 (DOE Contract No.: DE-FC22-95BC14942).
2. Schechter, D.S., Putra, E., Baker, R.O, Knight, W.H., McDonald, W.P., and Leonard, P.: "CO_2 Pilot Design and Water Injection Performance in the Naturally Fractured Spraberry Trend Area, West Texas," Paper SPE 71605 will be presented at the 2001 SPE Annual Technical Conference and Exhibition, New Orleans, Louisiana, 30 September–3 October.
3. McDonald, P., Lorenz, J. C., Sizemore, C., Schechter, D.S., and Sheffield, T.: "Fracture Characterization Based on Oriented Horizontal Core From the Spraberry Trend Reservoir: A Case Study" paper SPE 38664 presented at the 1997 Annual Technical Conference and Exhibition, San Antonio, Tx, 5-8 October.

Table 4.1 - Schedule of Tracer Injection.

Injection Well	Tracer Material	Date of Injection	Duration of Injection (hours)	Injection Concentration (ppm)
ET O'Daniel #37	3-FBA	8/15/00	9.88	178.2
ET O'Daniel #47	4-TFMBA	8/15/00	11.67	158.9
ET O'Daniel #45	4-FBA	8/16/00	9.35	188.4
ET O'Daniel #46	3-TFMBA	8/16/00	10.25	171.8
ET O'Daniel #25	2-FBA	8/17/00	9.03	194.9
ET O'Daniel #48	2345-Tetra FBA	8/17/00	9.02	200.9

Table 4.2 - Summary of Result for the Four High Interwell Responses.

Well Name	Breakthrough Time (Days)	Peak Concentration (ppt)
WIW#47 to Brunson D-1	1	171000
WIW#46 to Brunson D-1	3	164000
WIW#48 to O'Daniel A-1	3	180000
WIW#45 to Pilot Well#38	4	83200

Table 4.3 - Tracer Breakthrough Velocity for Injector Producer pairs.

Well Name	Breakthrough Velocity (ft/day)
WIW#47 to Brunson D-1	1559
WIW#46 to Brunson D-1	1103
WIW#48 to O'Daniel A-1	1843
WIW#45 to Pilot Well#38	642

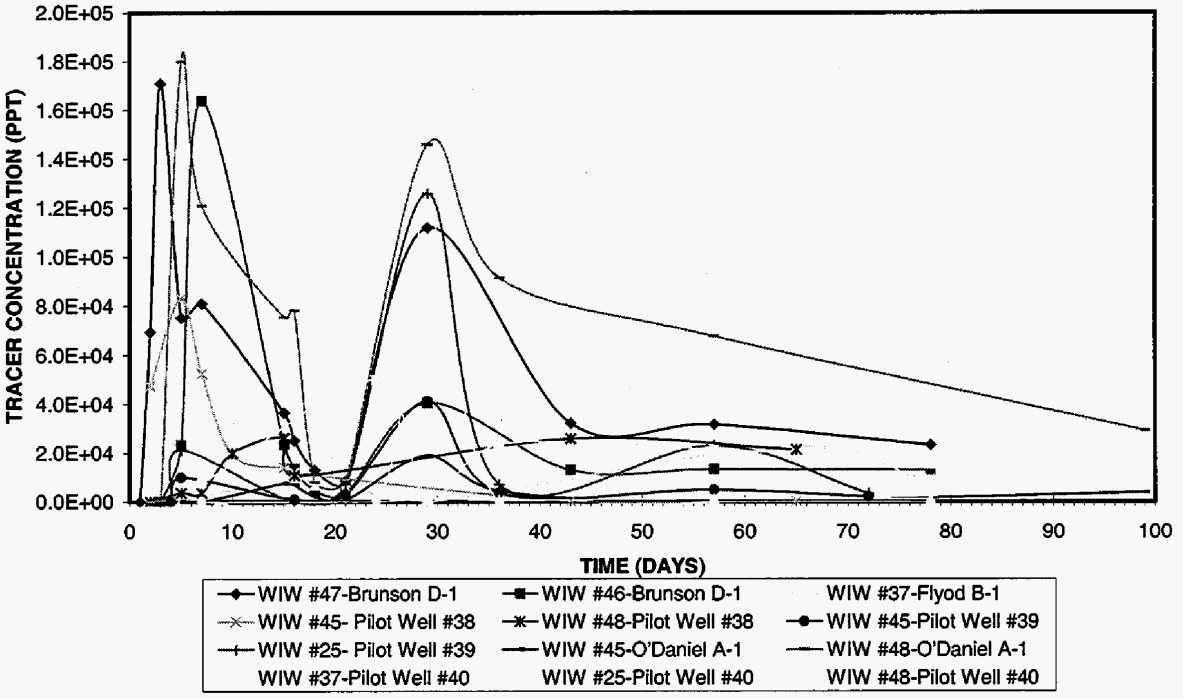

Fig. 4.1 - Response of Surrounding Wells on Tracer Injection at E.T O'Daniel Pilot Area.

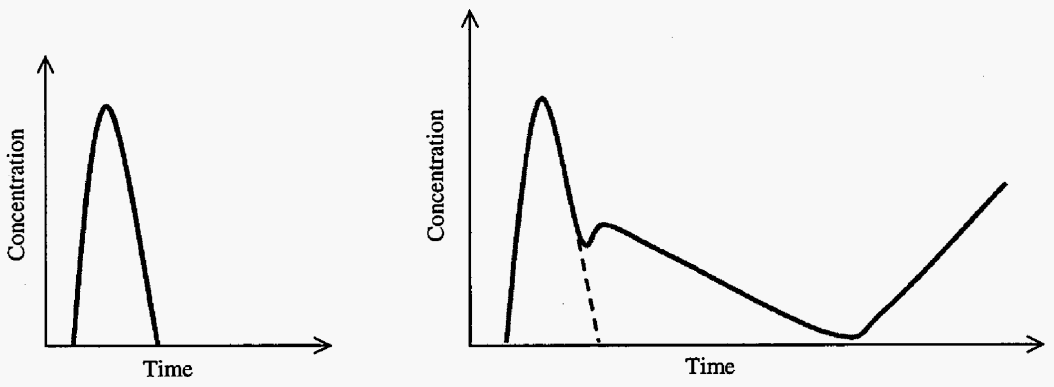

a) Typical Response

b) The Shape of Actual Response From WIW#47 to O'Daniel D-1

Fig. 4.2 - Typical and Actual Tracer Responses.

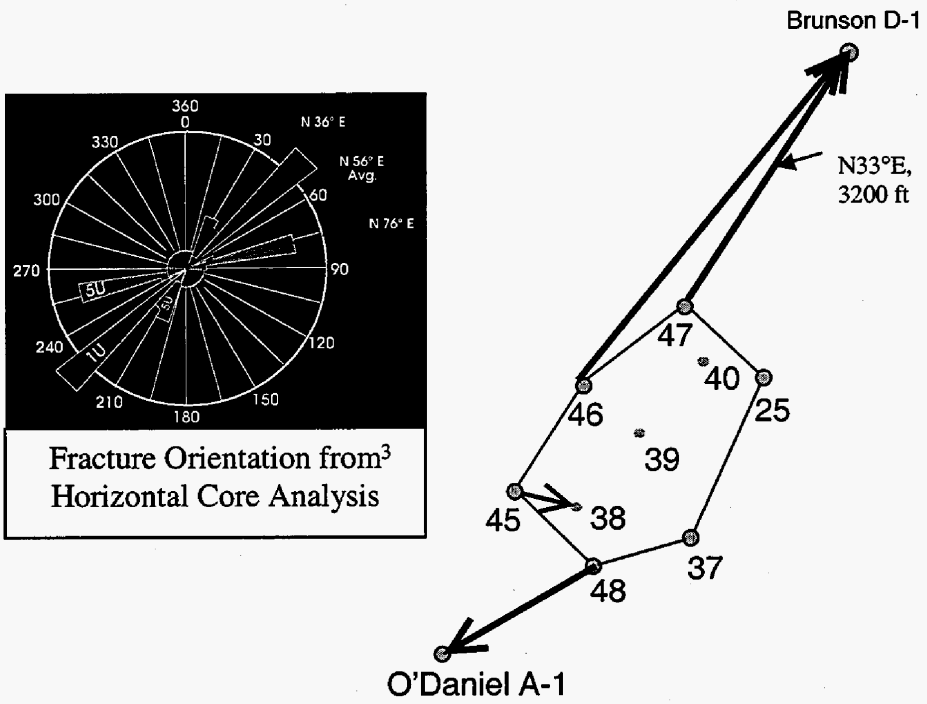

Fig. 4.3 - Schematic of Fracture Orientation as a Result of Tracer Injection.

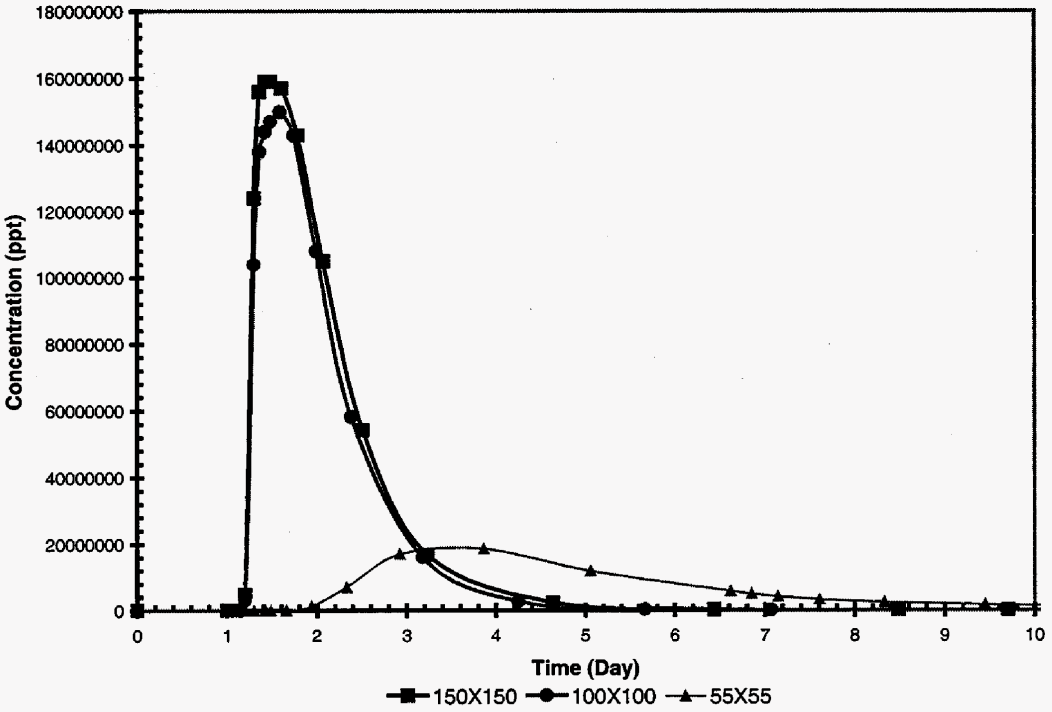

Fig. 4.4 - Effect of Grid Size in 35° Orientation With Kx/Ky = 100/15000 (WIW#47-D1).

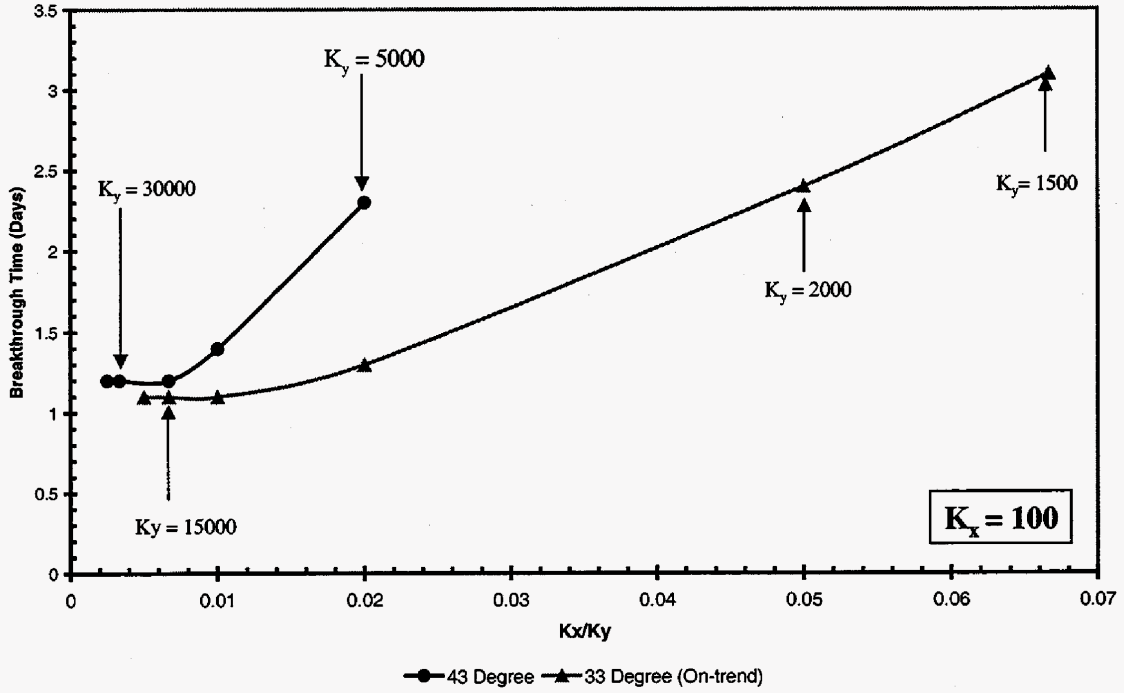

Fig. 4.5 - Effect of On-trend Permeability (K_y) on Breakthrough Time.

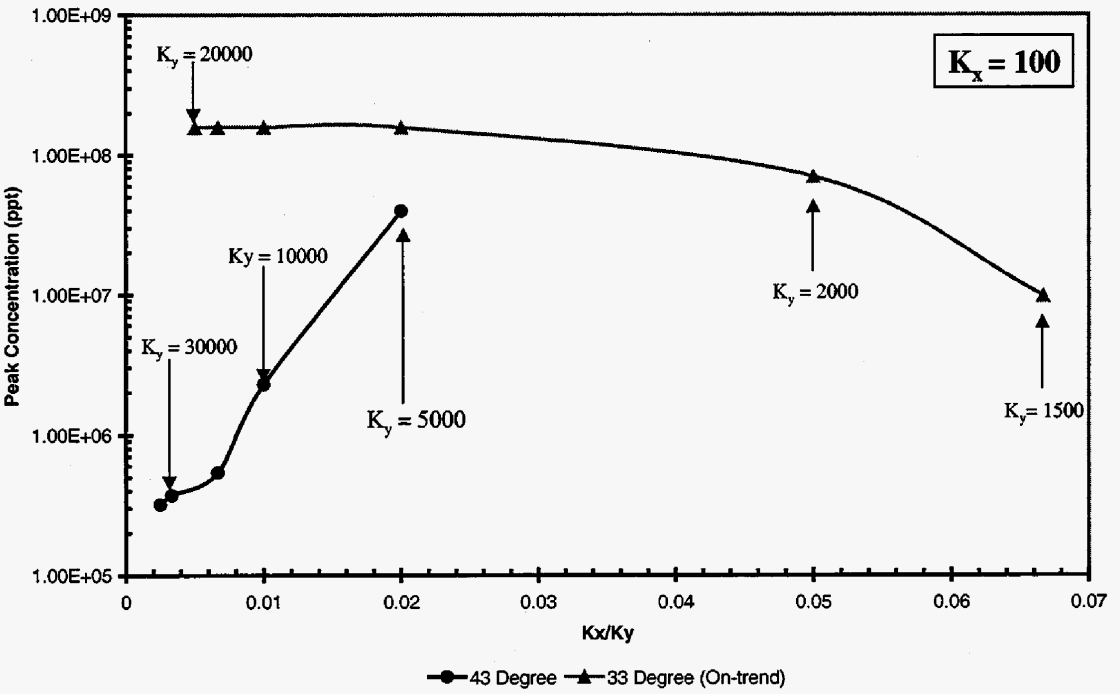

Fig. 4.6 - Effect of On-trend Permeability (K_y) on Peak Concentration.

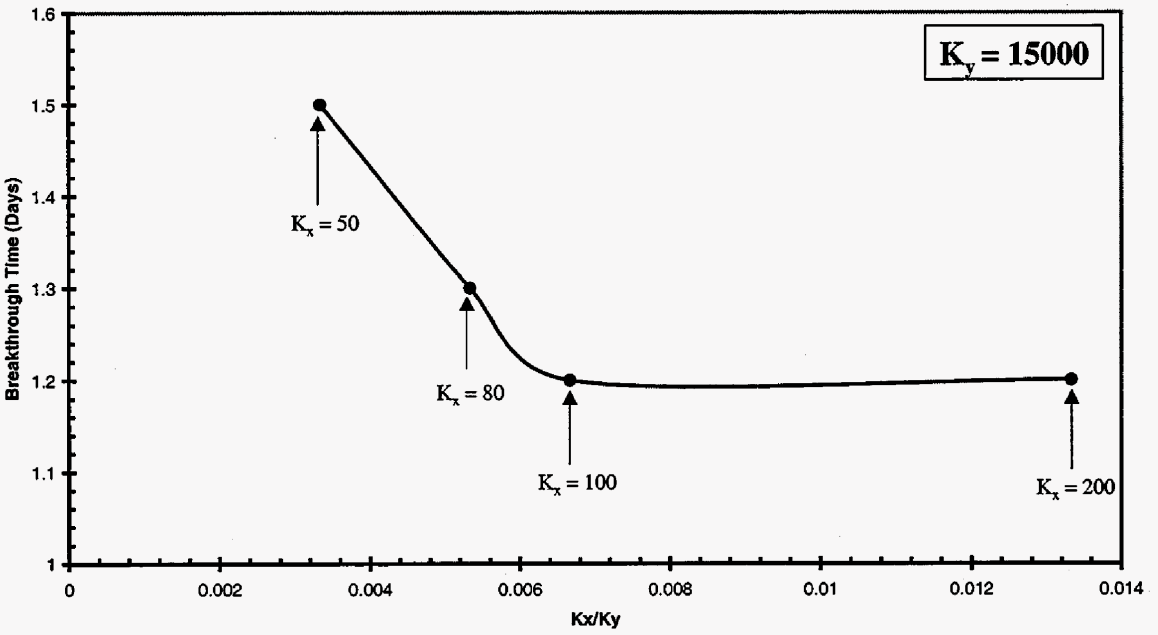

Fig. 4.7 - Effect of Off-trend Permeability (K_x) on Breakthrough Time for 43°Orientation.

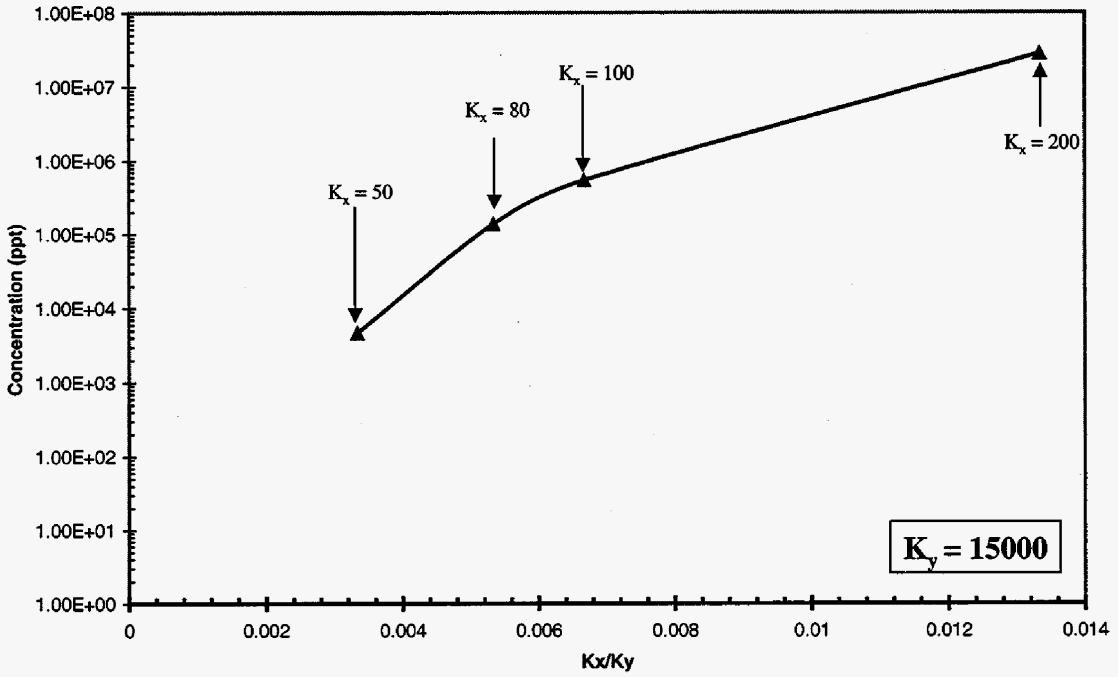

Fig. 4.8 - Effect of Off-trend Permeability (K_x) on Peak Concentration for 43° Orientation.

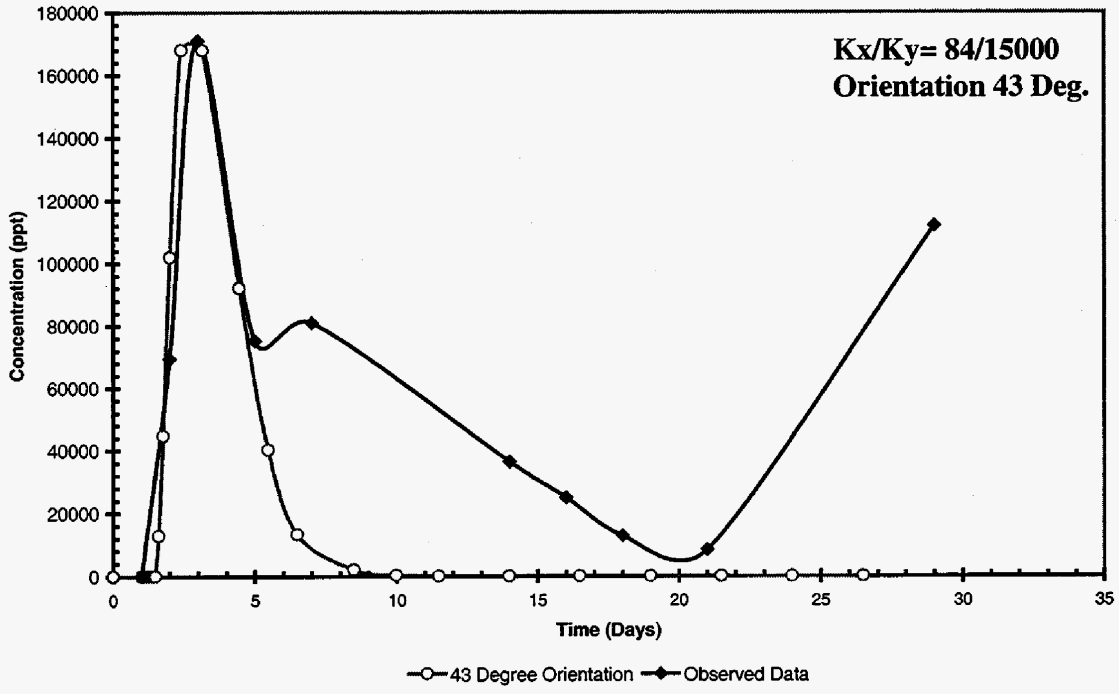

Fig. 4.9 - History match Result.

5. Analysis of Logging Observation Wells (LOW) in E.T O'Daniel Pilot

5.1 Introduction

This report discusses the progress of the CO_2 pilot project through the interpretation of logs from the observation wells in the Spraberry CO_2 flood pilot. A background of the Spraberry reservoir and the events leading to the initiation of CO_2 flood has been presented elsewhere.[1-5] The purpose is to monitor the movement of CO_2 and saturation changes of oil, water and gas in the upper Spraberry interval of E.T O'Daniel wells by utilizing logs from two observation wells.

To date six logging runs have been conducted at regular intervals (Table.5.2). Schlumberger™ has conducted all the logging for the Spraberry Unit CO_2 Flood pilot. A review of logging tools used to evaluate reservoir fluid movements is presented below:

Compensated Neutron Log (CNL)
This tool is used to measure the change in the initial free gas saturation during waterflooding and change in CO_2 saturation during and after CO_2 flooding. This log responds primarily to hydrogen present in the oil and brine. Although natural gas contains hydrogen, the hydrogen density in gas is very small compared with oil or brine; thus the tool responds weakly to hydrocarbon gas. A decrease in compensated neutron porosity between logging runs indicates an increase in gas porosity, either hydrocarbon gas or CO_2. The Schlumberger CNL tool was used primarily for taking compensated neutron logs.

High Definition Induction log (HDIL)
The array type HDIL subsurface instrument is a high-resolution instrument used to measure the resistivity of the formation. This instrument investigates at median formation depths of 10, 20, 30, 60, 90 and 120 inches, which significantly improves the definition of the invasion profile. Identical readings of 90 inch and 120 inch depth measurements provide direct indication of R_t.

When combined with porosity measurements, a saturation image over the same formation volume can be presented. A higher value of resistivity indicates the presence of hydrocarbons or CO_2.

Natural Gamma Spectrometry tool (NGT)
The Natural Gamma Tool is used to measure the natural gamma ray radiation of the formation from the three most common components of the naturally occurring radiation: potassium, thorium, and uranium. The presence of potassium indicates presence of shale.

To analyze the log curves the following procedure was followed:
1. The LAS files of each logging run from both the observation-wells (#49 and#50) for different run times were obtained.

2. For our case, natural gamma ray, neutron porosity and resistivity data was required. Hence only this information was sought from the LAS files.
3. All the data was modified in such a way that the start and end depths of the logging interval are the same.
4. The modified LAS file was imported to GEOGRAPHIX and the suite of log curves was obtained by using PRIZM.

Our preliminary analysis includes two log tracks, compensated neutron log and the array induction log.

5.2 Logging Observation Well #49

Fig 5.1 shows two log tracks, the neutron porosity log and the array induction log. These two curves have been obtained from the two logging runs carried out on Jan 31st 2001(base log) and March 16th 2001. The change in neutron porosity is evident in all the layers and the decreasing trend indicates the presence of hydrocarbon gas or CO_2.The change in resistivity is more pronounced in the 2U, 3U and 4U layers as shown. But in 1U and 5U there is not much of change in the resistivity values even though there is a marked changed in porosity. This might be due to inadequate movement of CO_2 in these layers as compared to 2U, 3U and 4U. It can also be noted that there is excellent vertical conformance of the CO_2 flood as evidenced in the neutron log suppression.

Fig. 5.2 depicts the change in resistivity and neutron porosity in August as compared to January logging run. The neutron porosity shows a decreasing trend hinting the possibility of CO_2. The resistivity does not decrease in layers 1U and 5U hinting no movement of CO_2 in these layers but there is a definite change in saturations in the other layers as seen by the change in resistivity. Again it is clearly evident of movement of CO_2 in the all layers.

5.3 Logging Observation Well #50

In the case of Well 50 the base log is taken as the March 16th 2001 logging run and in Fig 5.3 this log is being compared with the log taken on June 12th. The trends in both resistivity and porosity logs are not very convincing to show a definite movement or presence of CO_2.The gamma ray also shows a shift. Unlike Well 49, the non-pay zones do not show convincing decrease in neutron porosity to warrant the presence of CO_2.

Fig 5.4 shows the log tracks from the March 16th and August 18th logging runs. Even here the resistivity and porosity logs do not show a definite change to warrant the presence or movement of CO_2. The gamma ray also shows a decreasing shift.

The observation made from the logs of this well is very inconclusive and more investigation has to be carried out. Some of the reasons for such anomalous readings might be attributed to:

1. High Logging Speed

2. Inconsistent CNL reading
3. Inaccurate data during the February logging run in Well 50
4. Very few logging runs

To facilitate an accurate interpretation and decrease uncertainty the following recommendations can be made:

1. Maintain a lower logging speed
2. Make two logging passes at this speed.
3. Use other tools such as MWD neutron, Dual Porosity to get a better and more consistent estimate of porosity

5.4 Conclusions

The observations made from the logs of the two observation wells are contrary and more investigation has to be carried out to draw a firm conclusion. However, the following preliminary conclusions can be made based on presence results:

1. Comparison between the NPHI values from LOW #49 before and after injection of CO_2 confirms that there are decrease in compensated neutron density (NPHI) and increase in resistivity logs at different depths hinting the presence of a hydrocarbon gas or CO_2.
2. Even though CO_2 is going into all the layers as indicated in LOW #49 by the changes in resistivity and density logs, but those changes are not seen in LOW#50.

5.5 References

1. Schechter, D.S, Banik, B.S.: "Intergration of Petrophysical and Geological Data with Open Hole Logs for Identification of the Naturally Fractured Spraberry Pay Zones," paper SPE 38913 presented at the 1997 Annual Technical Conference and Exhibition held at San Antonio, TX, October 5-8.
2. Guidroz, M.G.: "E.T.O'Daniel Project-A Successful Spraberry Flood," paper SPE 1791 presented at the 1967 Permian Basin Oil and Gas Recovery Conference, Midland, TX, July 18.
3. Li H., Putra E., Schechter, D.S. Grigg, B.R.: "Experimental Investigation of CO_2 Gravity Drainage in a Fractured System," paper SPE 64510 presented at the 2000 Asia Pacific Oil and Gas Conference and Exhibition held at Brisbane, Australia, October 16-18.
4. Baxter, W.A, Harvey, P.A.: "Log Monitoring at the Midale CO_2 Flood Pilot" Internal report on CO_2 flood at the Midale Unit, Texas A&M University.
5. WZI Inc.: Design and Operating Policy E.T. O'Daniel Pilot CO_2 Flood, report prepared for Pioneer Natural Resources Company (Feb 2001), Texas A&M University.

Table 5.1 - Well Inventory

Type of Well	O'Daniel Well I.D No	Number of wells
Water Injector	#45,#46,#47,#25,#37,#48	6
CO_2 Injector	#41,#43,#44,#43	4
Producer	#38,#39,#40	3
Observer	#49,#50	2
Total		15

Table 5.2 - Logging Runs Conducted

Logging Runs	Type of Logs		Date Conducted
	Well#49	Well#50	
1	AHT, CNL, ILD, GR, ILM, MSFL, SPHI, DT	DT, GR, IDPH, ILD, ILM, IMPH, SFLU, SFHI	Jan 31 2001
2	AIT, GR, NPHI	AIT, GR, NPHI	Feb15 2001
3	AIT, GR, NPHI	AIT, BS, GR	Feb18 2001
4	AIT, GR, NPHI	AIT, GR, NPHI	Mar16 2001
5	AIT, GR, NPHI	AIT, GR, NPHI	Apr 16 2001
6	AIT, GR, NPHI	AIT, GR, NPHI	Jun 12 2001
7	AIT, GR, NPHI	AIT, GR, NPHI	Aug 18 2001

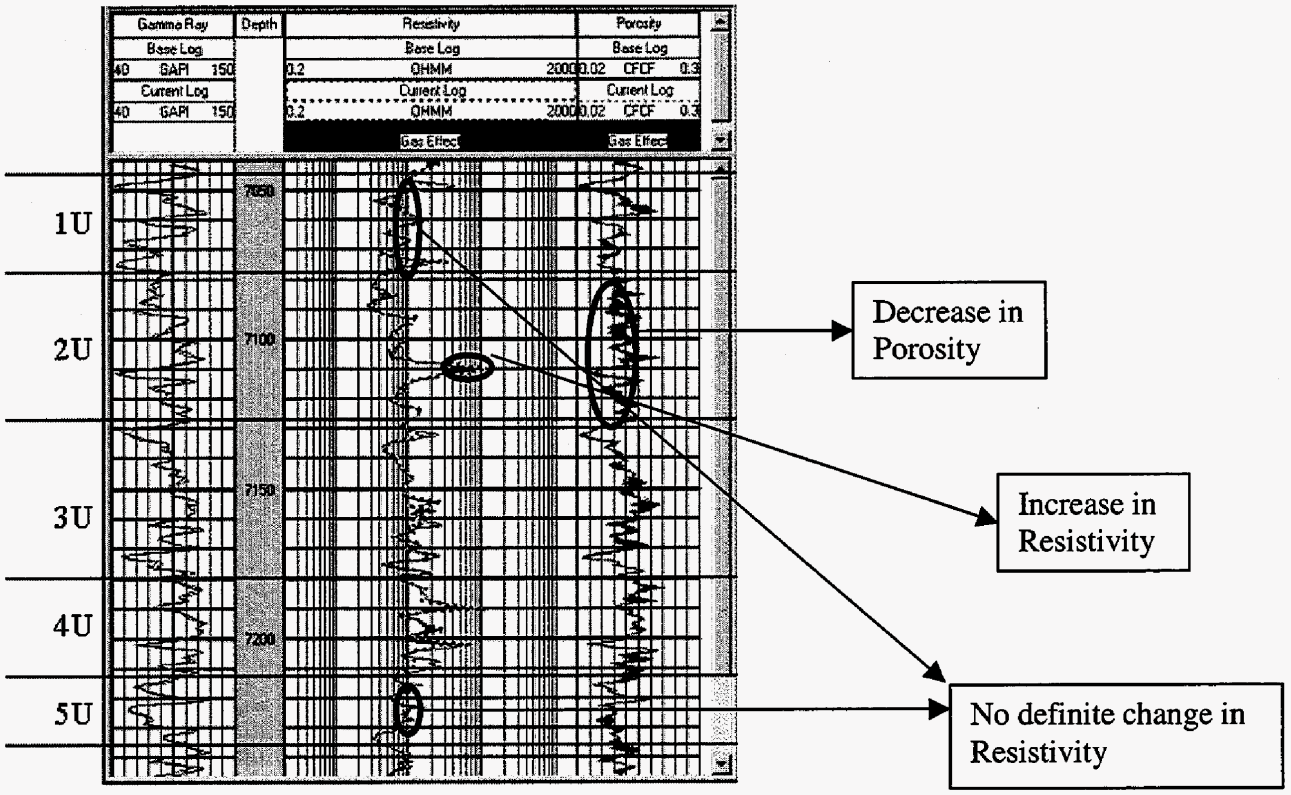

Fig. 5.1 - Neutron Porosity and Resistivity Profile of Well 49 (Jan-Mar)

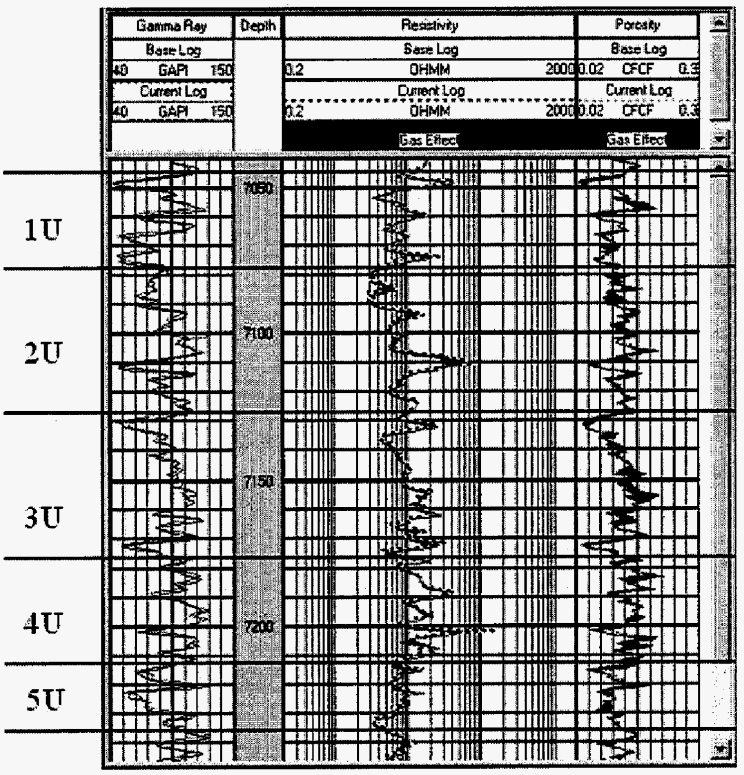

Fig. 5.2 - Neutron Porosity and Resistivity Profile of Well 49 (Jan-Aug)

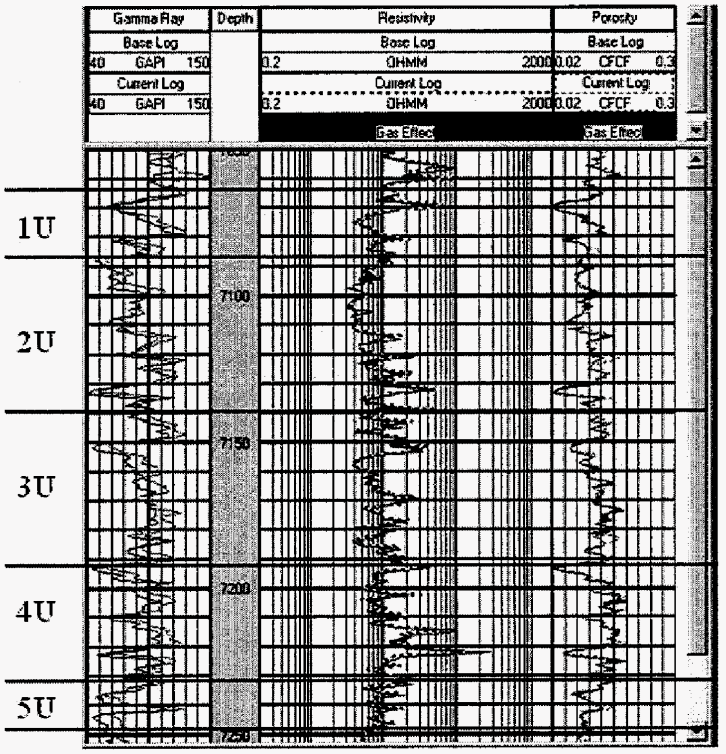

Fig. 5.3 - Neutron Porosity and Resistivity Profile of Well 50 (Mar-Jun)

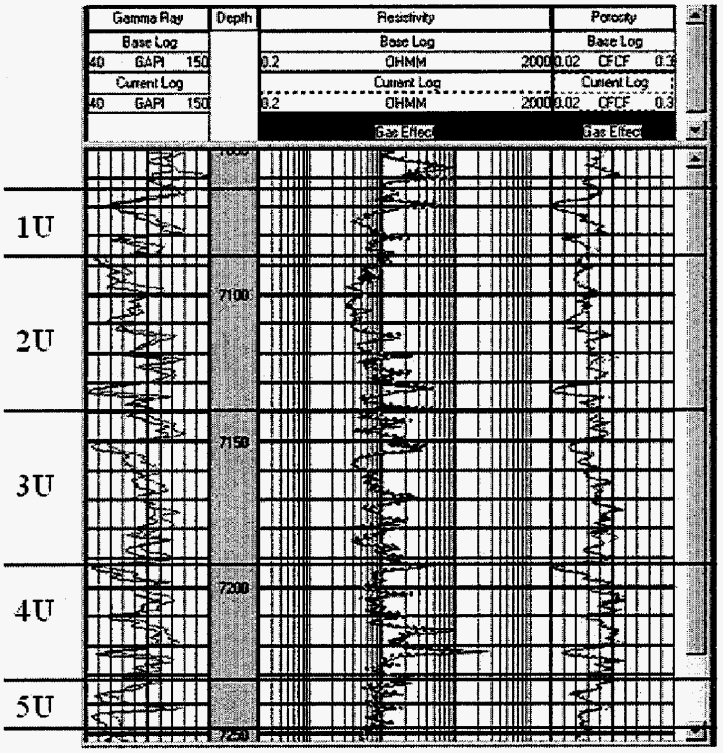

Fig. 5.4 - Neutron Porosity and Resistivity Profile of Well 50 (Mar-Aug)

III. FIELD DEMONSTRATION STATUS

After remedial action was taken on cement problems in one of the logging observation wells, on Monday on February 26th, 2001 CO_2 was officially injected into the Spraberry formation.

During CO_2 injection into the pilot area, the injection rate in each of the six confined water injection wells was reduced from 280 to 245 BWPD to compensate for the target 200 RVB/D of CO_2 injection. A few minor glitches have been encountered such as the turbine meters for CO_2 getting clogged with debris. After injecting 2.5 days, the interior producers (O'Daniel wells #38, #39, and #40) experienced CO_2 breakthrough. We believe that although breakthrough of CO_2 to the interior producers is liable to be a problem the situation was aggravated tremendously when the CO_2 meters froze up the evening of Tuesday, Feb 28th and the control valves sensing that flow rates had dropped below target rates. The automated system reads this as a decrease in the target injection rate and the system compensates by opening valves automatically, so more CO_2 has been injected than planned during the first two days. Each CO_2 injection well has experienced some unique problems during start-up but no problems that have required serious remedial action.

To date there is still no immediate oil response observed in the interior production wells as well as other wells away from the pilot area. We believe that the oil production rate at exterior wells will start responding to CO_2 injection when the volume of CO_2 injection is comparable to water injection volume (about 250,000 bbls) as indicated previously during waterflooding course (Fig. 1). Fig. 2 shows that the amount of CO_2 injected is still very small compared to the volume of water injected.

The battery monitoring the four wells closest to the pilot shows that the interior producers (wells #38, #39 and #40) experience increased percentages of CO_2 after about 3 weeks of CO_2 injection. Surprisingly, CO_2 produced at well "A" #1 (in Fig. 3) directly along the NE-SW fracture orientation has observed moderate CO_2 break-through. The line of production wells experiencing high CO_2 fraction are perpendicular to the natural fracture trend and the CO_2 injection wells. The interior wells have produced 80-100% gas composition of CO_2 and the well "A" #1 has produced 20-60% of the CO_2. While the total oil production rate is steadily between 20 to 40 bbls/d.

Based on 3DSL simulation,[1] Baker concluded that eliminating CO_2 injection increases the oil production and decreases CO_2 production. He then recommended to shut-in all of the CO_2 injectors for a period of three weeks (7/20/2001-8/21/2001) to quantify the effect of CO_2 injection at interior production wells. During the shut in of CO_2 injectors, the gas produced in all observed production wells (interior and exterior wells) dramatically decreases. But the oil production remains producing with the same rate (Fig. 4). It means that CO_2 injection may not efficiently sweep the oil to the production wells. The poor CO_2 sweep efficiency may because of the direct cross fractures that exist between injectors to producers that had been created during high step injection rate[2] and interference tests.[2]

After the CO_2 was started again, the interior production wells immediately produced 100% of CO_2, which also indicated poor sweep efficiency. However, a better sweep efficiency was shown in the exterior well (Well "A" #1) as indicated by low gas produced after starting CO_2 injection.

The amount of gas that has been produced from observation wells is small compared to the amount of CO_2 that has been injected as indicated in Fig. 5. Number 1 indicates the amount of CO_2 that has been produced, while number 2 indicates the amount of CO_2 remaining in the reservoir. It means that there is a considerable amount of CO_2 (about 60.5 %) remaining in the reservoir that we expect could mobilize oil to the production wells. Accordingly, the water that has been produced from interior wells since initiation of CO_2 injection is about 19% of the total water that has been injected through the confined six injection wells (Fig. 6). Before CO_2 injection commenced, water injection significantly improved oil recovery especially on the wells along the natural fracture trend 2,000 to 5,000 feet from the pilot area. To distinguish the oil response due to CO_2 injection, two watered-out wells (Brunson D-1 and O'Daniel A-1) will be observed as potential key wells.

The fact that large volumes of CO_2 are being retained in the reservoir as observed during water injection and a relatively small total volume of CO_2 has been injected on a HCPV basis warrants continuation of CO_2 injection.

References

1. Baker, R.: Recommendation Regarding CO_2 Flooding, Internal Memo (June 21, 2001).
2. Schechter, D.S., Putra, E., Baker, R.O., Knight, W.H., McDonald, W.P., Leonard, P., and Rounding, C.: "CO_2 Pilot Design and Water Injection Performance in the Naturally Fractured Spraberry Trend Area, West Texas," paper SPE 71605 will be presented at the 2001 SPE Annual Technical Conference and Exhibition, New Orleans, LA, 30 Sep.-3 Oct.

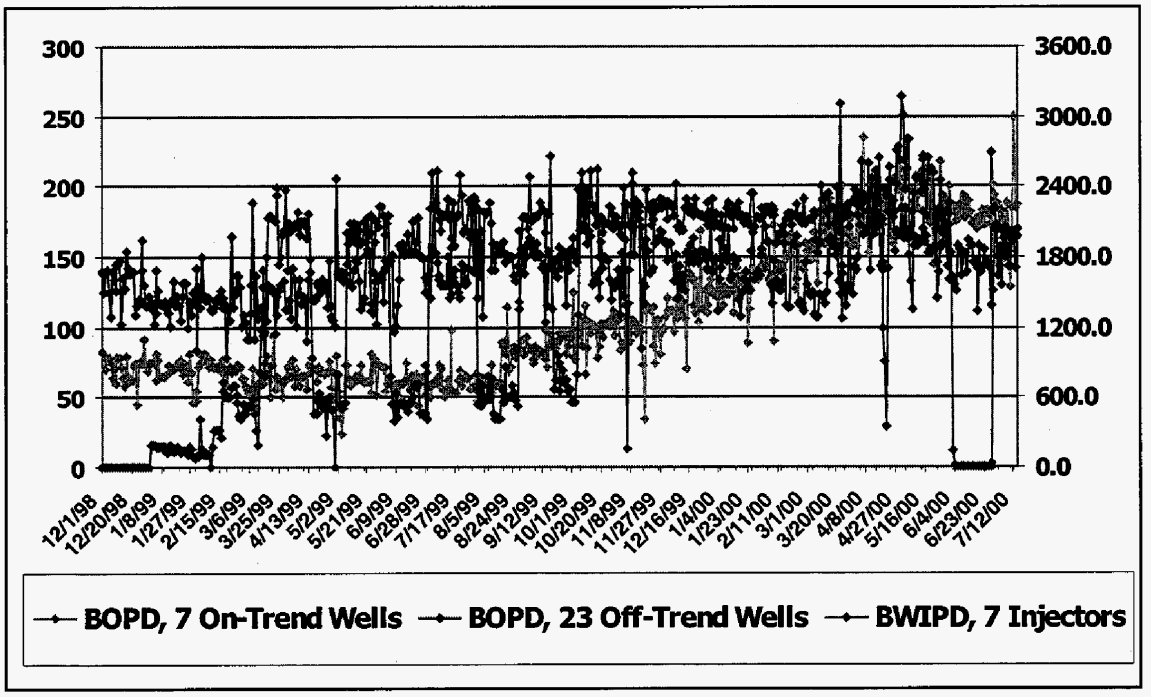

Fig. 1.1 – Oil response during water injection in the off-trend and on-trend wells. Note: A total of 250,000 bbls water was injected to produce a dramatic oil respond in on-trend wells.

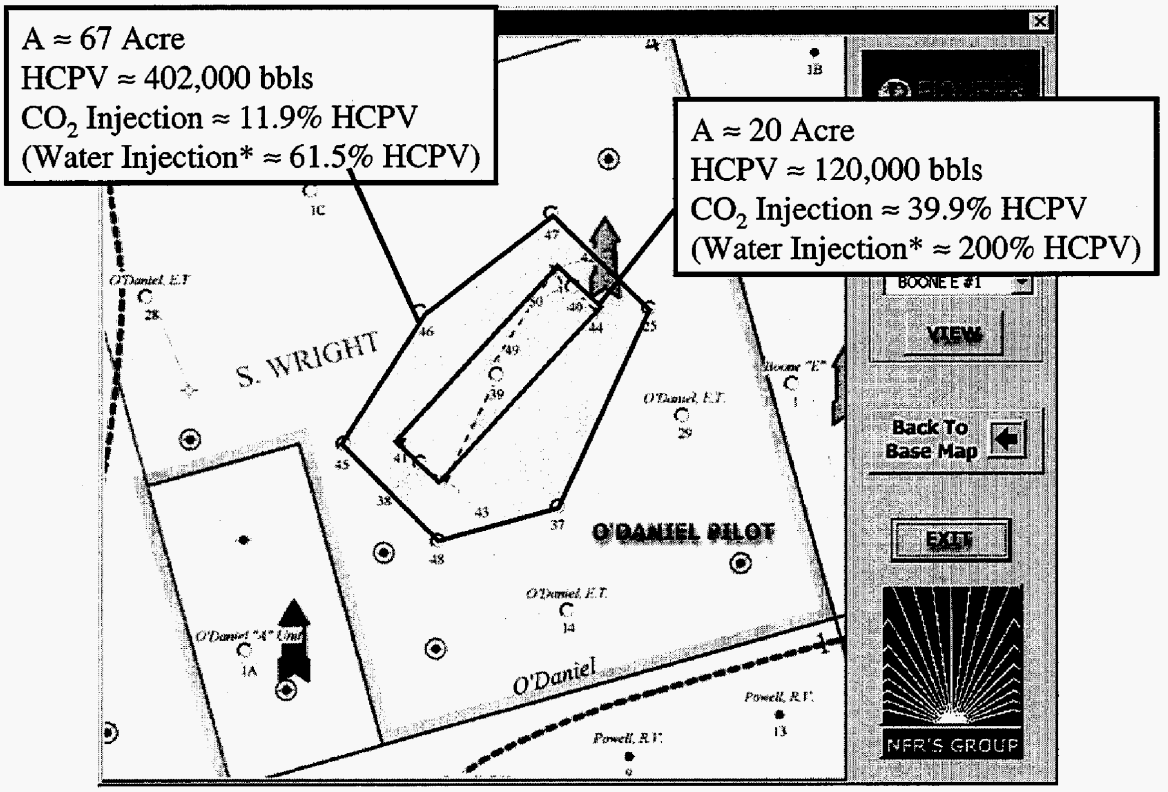

Assuming HCVP = 6000 bbls/acre
360 Mcf is equal to 200 bbls/d (at 2500 psi)
Days of injection = 63 days (Feb 26-May 1, 2001)

Fig. 1.2 – A comparison between water and CO_2 injection volumes in different area sizes. Note: the volume of CO_2 is converted to volume of water.

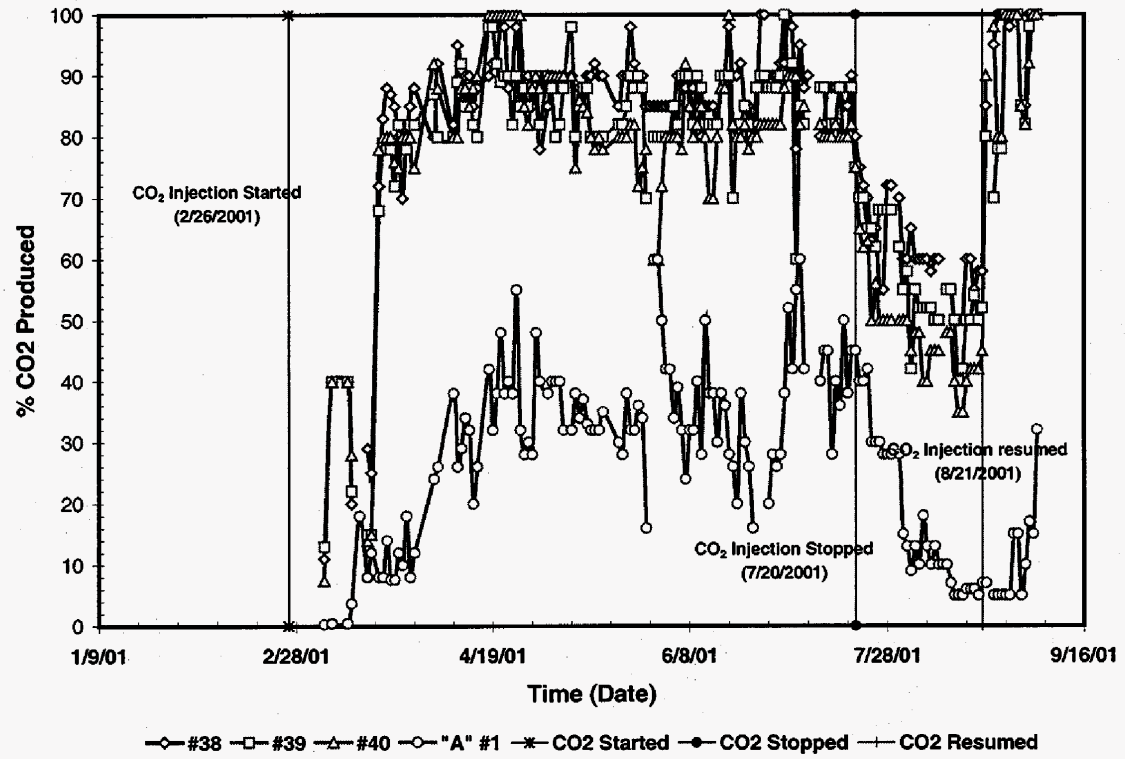

Fig. 1.3 - Percentage of CO_2 produced at four wells closest to the CO_2 injectors.

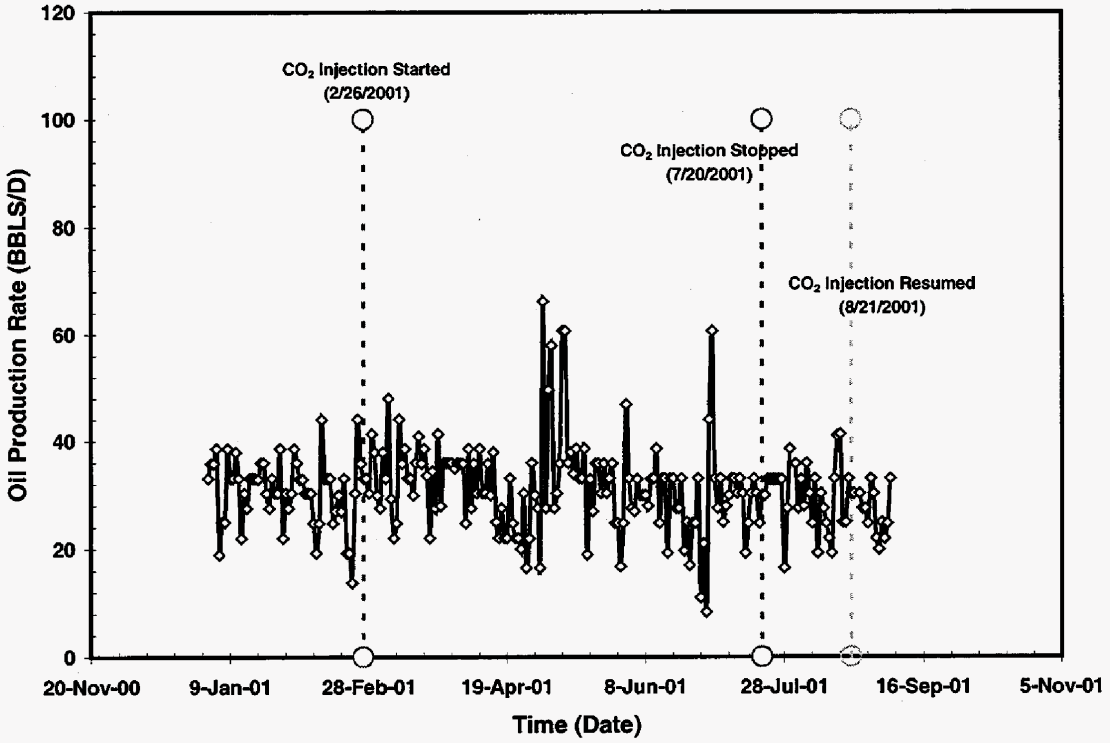

Fig. 1.4 – Total oil production rate at four observation wells.

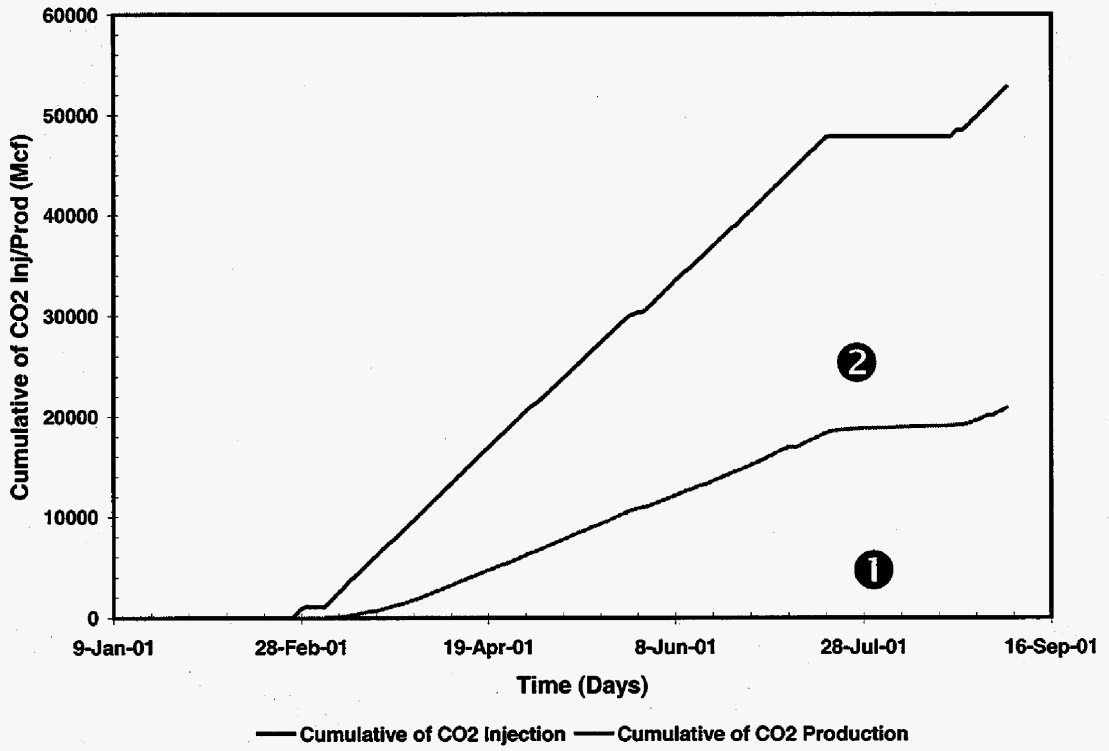

Fig. 1.5 - Comparison between cumulative CO_2 injection and CO_2 production.

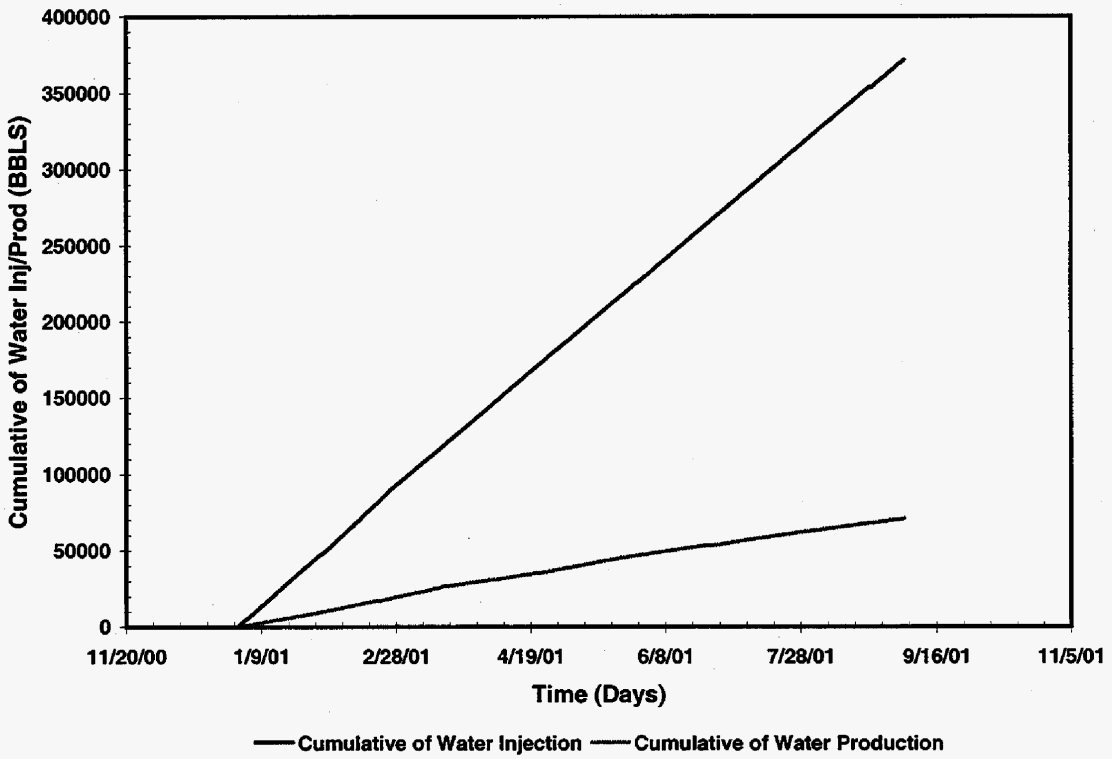

Fig. 1.6 - Comparison between cumulative water injection and water production.

E.T O'Daniel Database

During this period, we also developed a database to provide some information on a well-by-well basis particularly for the E.T. O' Daniel pilot area. This database contains information such as daily and monthly production rate, well bore schematics and well log information. The objectives are to obtain the information quickly by clicking the well and to manage the abundant data on each well to monitor the progress and development of the CO_2 pilot. This user-friendly program was written using visual basic application (**VBA**). The example of E.T O' Daniel Database is presented as follows and the entire program is available at: http://pumpjack.tamu.edu/faculty/schechter/baervan/homepage.html

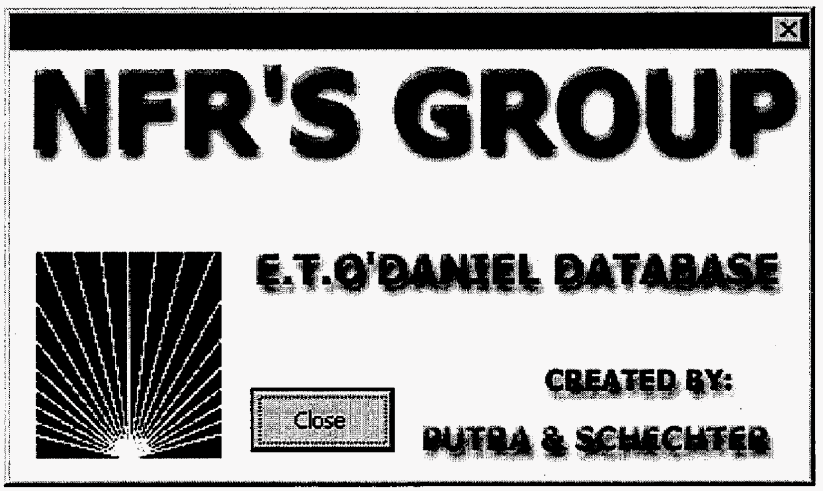

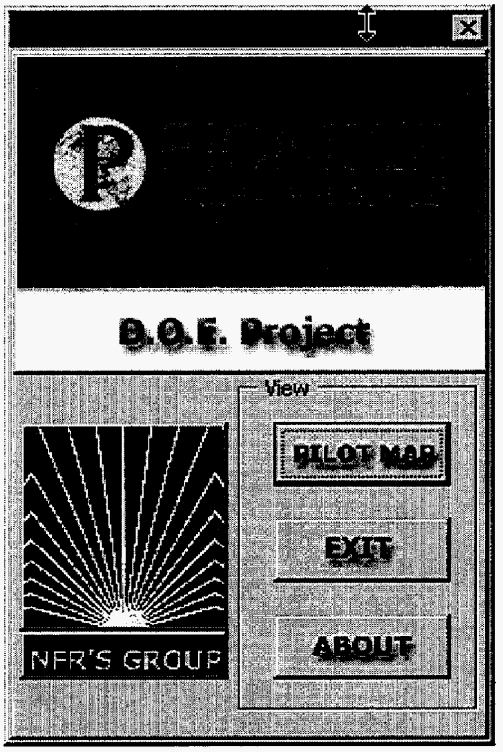
D.O.E. Project
View
PILOT MAP
EXIT
ABOUT
NFR'S GROUP

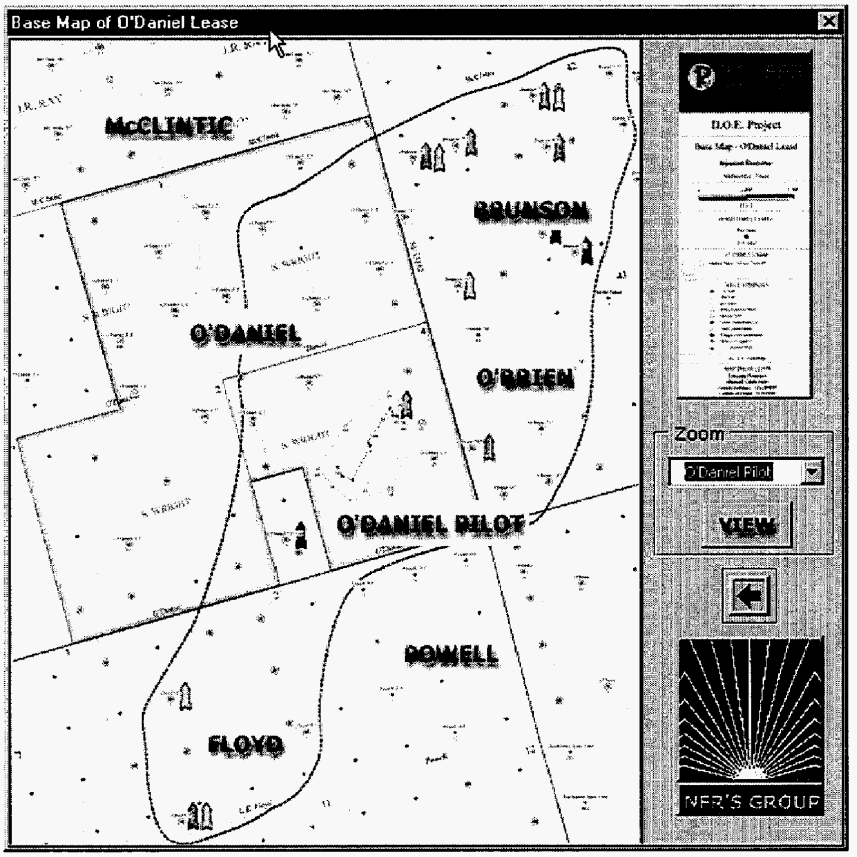
Base Map of O'Daniel Lease
McCLINTIC
BRUNSON
O'DANIEL
O'BRIEN
O'DANIEL PILOT
POWELL
FLOYD
D.O.E. Project
Zoom
O'Daniel Pilot
VIEW
NFR'S GROUP

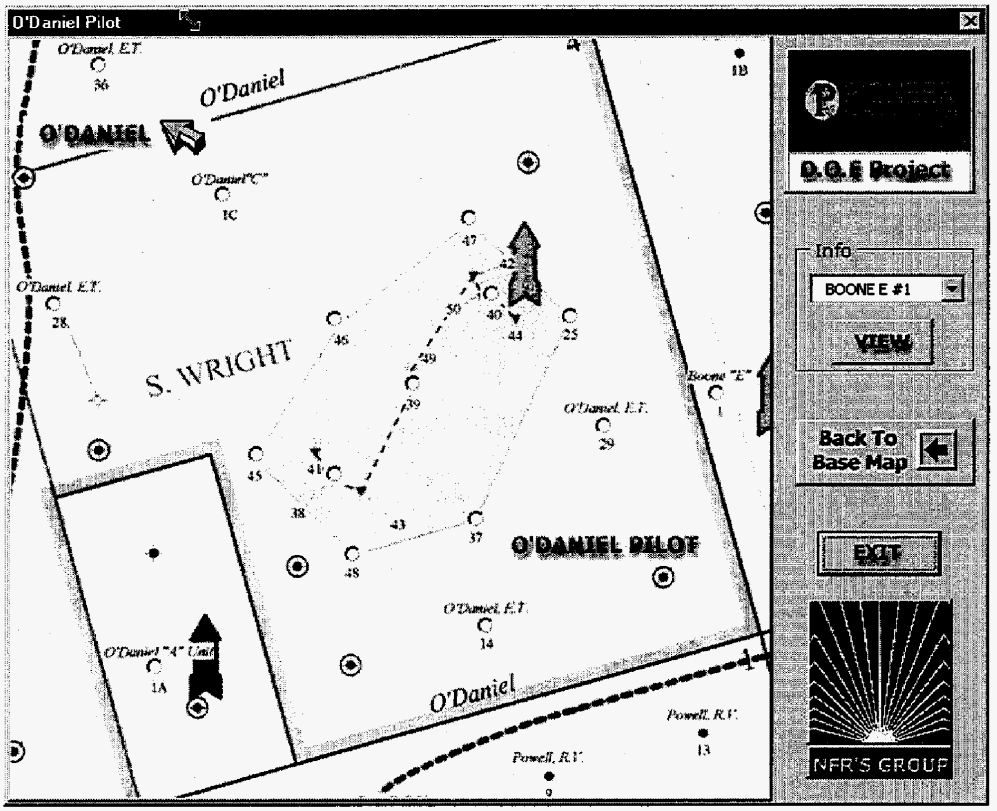
O'Daniel Pilot
O'Daniel E.T.
36
O'Daniel
O'DANIEL
O'Daniel"C"
1C
O'Daniel E.T.
28
S. WRIGHT
46
47
42
50
40
44
25
49
39
Boone "E"
1
O'Daniel E.T.
29
45
41
38
43
37
O'DANIEL PILOT
48
O'Daniel E.T.
14
O'Daniel "A" Unit
1A
O'Daniel
Powell, R.V.
13
Powell, R.V.
9
1B
D.O.E Project
Info
BOONE E #1
VIEW
Back To Base Map
EXIT
NFR'S GROUP


Microsoft Excel - DBaseODaniel2.xls
File Edit View Insert Format Tools Data Window Help
NFR'S GROUP
E.T.O'DANIEL DATABASE
E T ODANIEL #48WIW
PRODUCTION
Daily
Monthly
O'DANIEL PILOT LOGS
Log Information
WellBore Schematics
D.O.E. Project
Retrieve Info
Wellbore Schematics
VIEW
BACK TO BASE MAP
NFR'S GROUP
IndexInfo

Microsoft Excel - UpdateDataTest.xls

File Edit View Insert Format Tools Data Window Help

DAILY PRODUCTION
O'DANIEL PILOT AREA

D.O.E Project

Name: E T ODANIEL #38 — Choose : E T ODANIEL #48WIW

	Data			
Date	Oil Production	Water Production	Gas Production	Total Fluid (BTFPD)
1/1/99	0	150.591	0	150.591
1/2/99	0	151.771	0	151.771
1/3/99	0	151.368	0	151.368
1/4/99	0	164.167	0	164.167
1/5/99	0	141.97	0	141.97
1/6/99	0	166.043	0	166.043
1/7/99	0	142.85	0	142.85
1/8/99	0	142.712	0	142.712
1/9/99	0	142.712	0	142.712
1/10/99	0	142.712	0	142.712
1/11/99	0	193.249	0	193.249
1/12/99	0	136.254	0	136.254
1/13/99	0	145.36	0	145.36
1/14/99	0	152.078	0	152.078
1/15/99	0	152.078	0	152.078
1/16/99	0	152.078	0	152.078
1/17/99	0	152.078	0	152.078
1/18/99	0	169.134	0	169.134
1/19/99	0	119.028	0	119.028
1/20/99	0	148.08	0	148.08
1/21/99	0	105.867	0	105.867
1/22/99	0	105.867	0	105.867
1/23/99	0	105.867	0	105.867
1/24/99	0	105.867	0	105.867

Daily Production Graph | Table

Microsoft Excel - UpdateDataTest.xls

File Edit View Insert Format Tools Chart Window Help

E. T. O'DANIEL DOE PROJECT
PRODUCTION RATE
E T ODANIEL #38

D.O.E Project

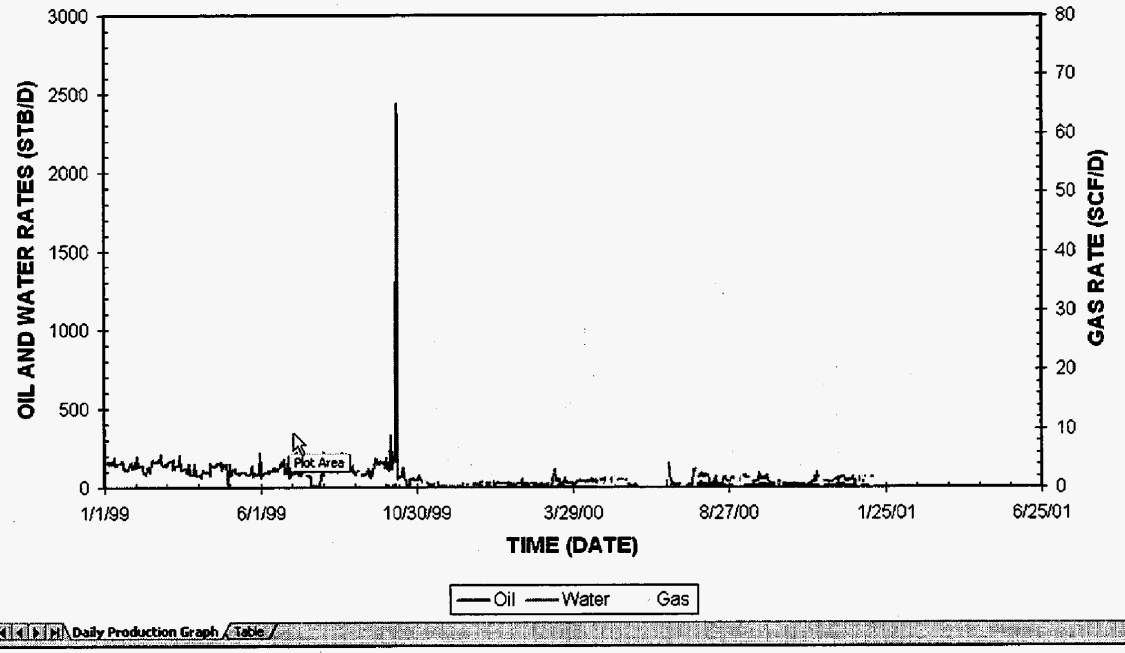

Daily Production Graph | Table

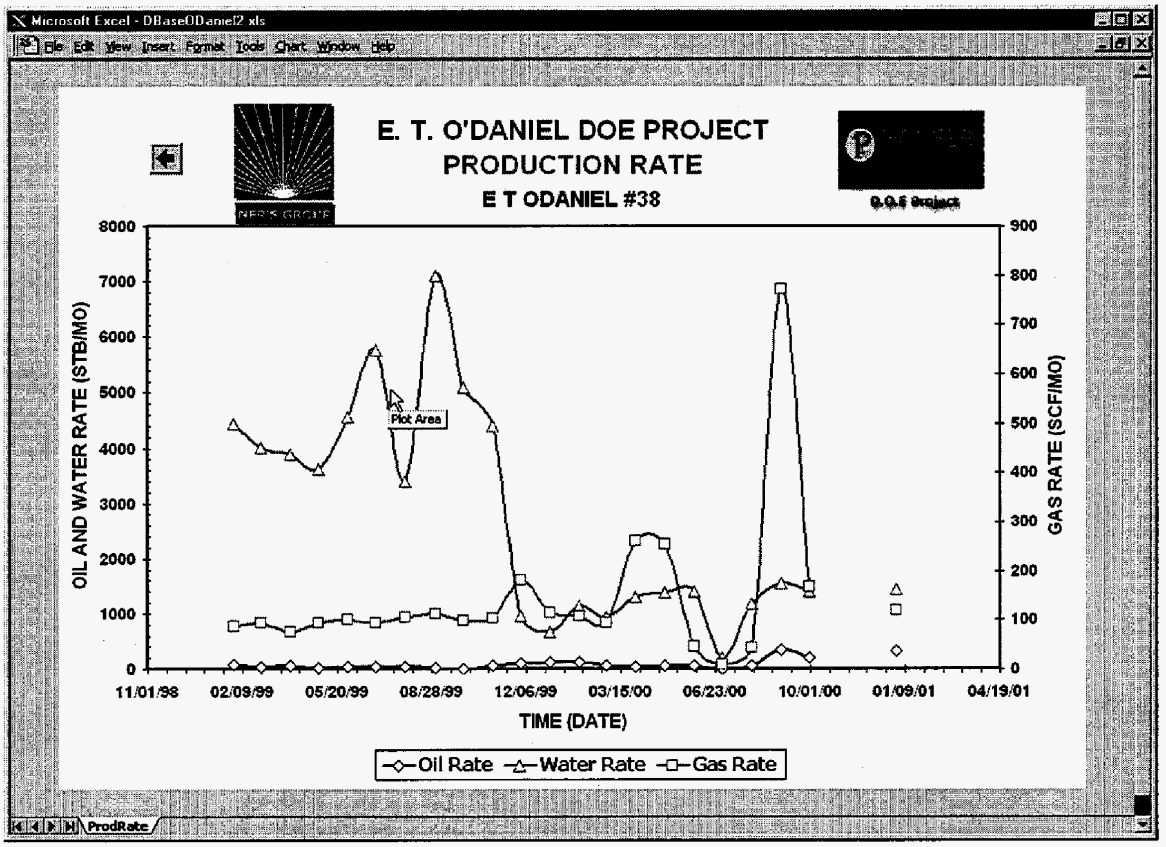
Microsoft Excel - DBaseODaniel2.xls
File Edit View Insert Format Tools Chart Window Help
E. T. O'DANIEL DOE PROJECT
PRODUCTION RATE
E T ODANIEL #38
NER'S GROUP
D.O.E Project
OIL AND WATER RATE (STB/MO)
GAS RATE (SCF/MO)
8000
7000
6000
5000
4000
3000
2000
1000
0
900
800
700
600
500
400
300
200
100
0
Plot Area
11/01/98
02/09/99
05/20/99
08/28/99
12/06/99
03/15/00
06/23/00
10/01/00
01/09/01
04/19/01
TIME (DATE)
Oil Rate
Water Rate
Gas Rate
ProdRate

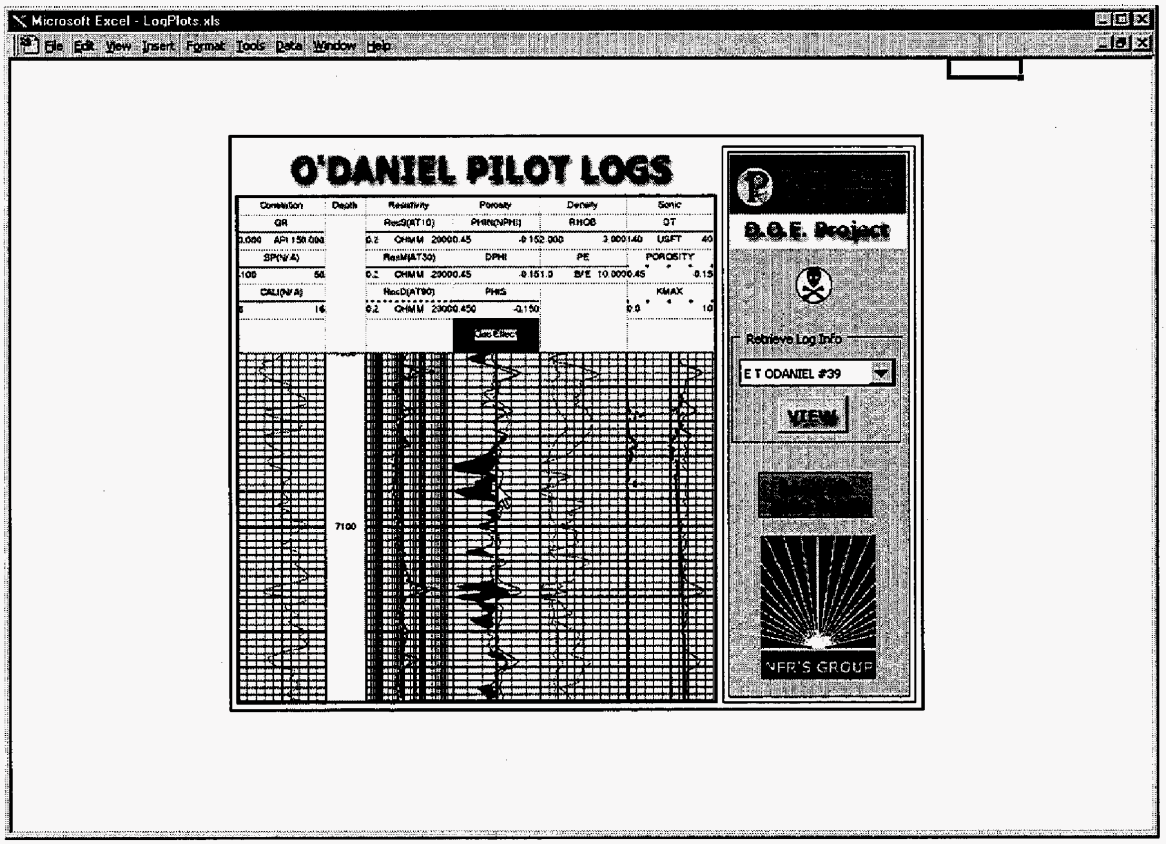
Microsoft Excel - LogPlots.xls
File Edit View Insert Format Tools Data Window Help
O'DANIEL PILOT LOGS
Correlation
Depth
Resistivity
Porosity
Density
Sonic
GR
RHOB
DT
SP(MV)
DPHI
PE
POROSITY
CAL(INCH)
PHIS
KMAX
7100
D.O.E. Project
Retrieve Log Info
E T ODANIEL #39
VIEW
NER'S GROUP

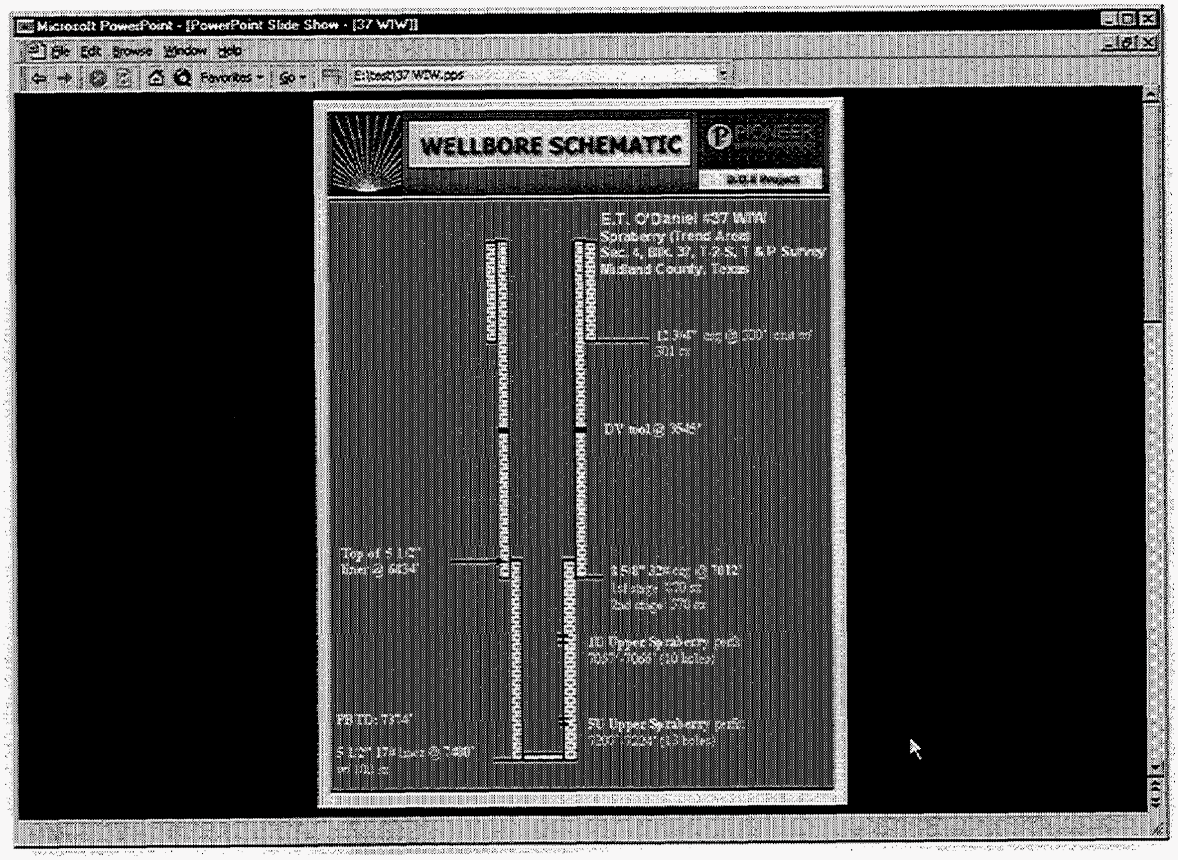
Microsoft PowerPoint - [PowerPoint Slide Show - [37 WIW]]
File Edit Browse Window Help
Favorites Go
E:\test\37 WIW.pps
WELLBORE SCHEMATIC
PIONEER
E.T. O'Daniel #37 WIW
Spraberry (Trend Area)
Midland County, Texas
DV tool @ 3545'
PB TD: 7774'